COPY 2

NASA CR-66015

PRELIMINARY DESIGN AND TEST OF HIGH ENTHALPY DEVICE

by Ira Nathan, Martin Novack and Manuel Recarey

Prepared under Contract No. NAS1-3909 by
General Applied Science Laboratories, Inc.
Merrick and Stewart Avenues
Westbury, L.I., New York

for

NATIONAL AERONAUTICS AND SPACE ADMINISTRATION

COPY

NASA CR-66015

PRELIMINARY DESIGN AND TEST OF HIGH ENTHALPY DEVICE

by Ira Nathan, Martin Novack and Manuel Recarey

Prepared under Contract No. NAS1-3909 by
General Applied Science Laboratories, Inc.
Merrick and Stewart Avenues
Westbury, L.I., New York

for

NATIONAL AERONAUTICS AND SPACE ADMINISTRATION

ABSTRACT

15233

A study has been made of the feasibility of adding kinetic energy to the supersonic exhaust of a shock tunnel by reversing the flow direction with a high speed piston. A critical element of the concept, the 180° turning passage, has been studied experimentally to determine the quality of the flow and pressure recovery of the reversed stream. A scheme of the overall facility design is presented with approaches to individual problem areas indicated.

Author

TABLE OF CONTENTS

LIST OF TABLES

LIST OF FIGURES

I. INTRODUCTION

The performance requirements of facilities for ground testing are traditionally dictated by the theoretical concepts and advanced designs under investigation by aerodynamicists. Such facilities have increased in capability as more advanced configurations have been studied, as new reentry vehicles and high performance power-plants have been developed. It has often been necessary to accept compromises in the simulation of flight conditions to enable tests to be performed. Such compromises have involved model scaling, separate testing of system components, short test times, and reduced energy and temperature levels; however, now that a new range of higher performance configurations are under consideration compromises are no longer allowable in temperature and energy. The importance of heat transfer processes with true energy and pressure conditions has increased with the interest in anti-ICBM missiles and maneuverable re-entry bodies. Engineers are interested in the changes in aerodynamic performance wrought by real gas effects. With the development of supersonic combustion, the chemistry of energy release, reaction rates and non-equilibrium flow phenomena at realistic temperatures and pressures have become prime processes of interest. In the interest of higher performance ground test facilities, GASL has considered alternate ways of providing a better simulation of high speed environment.

Present facilities provide high enthalpy levels for short test times through shock tunnels and other impulse type devices such as the "hot shot" tunnel, which uses electrical discharge. In the latter type facility materials have tended to limit stagnation conditions. In steady state of plasma-type facilities the ability to apply high pressures is limited by the increased losses of the plasma jet at elevated pressure. Even in these latest type facilities static pressures and temperatures are low.

The facility under consideration in this report proposes to produce high temperatures and pressures through a theoretically simple kinematic energy addition device. We shall hereafter refer to this device as the PGA or Piston Gas Accelerator. In the PGA the high stagnation conditions are truly never seen by elements of the PGA until the test chamber is reached and the model is exposed to the full stagnation conditions.

The practical implementation of the PGA requires answers to certain problems in fluid mechanics and structural design. The aerodynamic efficiency of the total system depends on the efficiencies of components which have not heretofore been tested under conditions as exist in the PGA. Design of flow passages poses problems of sealing and removal of flow barriers within the system. Thus, the purpose of the present study has been to examine these problems to experimentally define realizable efficiencies and to indicate the method of sealing and removing barriers in a preliminary design.

The current effort has been bases on adpating the GASL shock tunnel or its equivalent to the PGA energy-addition system. Early estimates of the performance potential of the PGA has been predicted on very high energy and pressure inputs generated by an advanced performance shock tunnel. However, we feel that a lower performance which would be produced through our own shock tunnel is a large step in advancement of test conditions and could be produced much sooner than if a complete facility were to be built including the input and the energy additive stages.

This final report presents

- a review of themethods and principle of operation of the PGA
- a projection of what could be done in a new facility
- a projection of what can be done in the GASL installation
- a general scheme for erection of the facility
- the test results of a program in which a critical component has been examined
- a preliminary design of several key components
- a projection of costs to develop the facility
- a tentative schedule for procurement and erection of the facility

II. THEORY OF OPERATION OF THE HIGH ENTHALPY DEVICE

The basic principle of the GASL Piston Gas Accelerator for high energy air is the acceleration of air which is at an initially high velocity and temperature. Thus, the total system requires two stages, the first stage being a high energy air source and the second stage being the accelerator. The performance of the total system is improved as the energy level of the first stage is increased. Consider that for a fixed incremental velocity, the total enthalpy (which is proportional to the square of the final velocity) is much greater if the initial velocity is greater.

The process can be described as follows: discharge air from a shock tube is expanded isentropically through a nozzle and is introduced into a second stage which contains a moving piston. This second stage, which is the piston gas accelerator (PGA), accelerates the high velocity air and thus increases its total kinetic energy. If repeated passes through the PGA are made, the number of increments to the total kinetic energy can be increased. The highest velocity air is subsequently discharged from the PGA through a test nozzle to reach the desired test section conditions. A schematic diagram of the overall system is shown in Figure 1.

The kinematic principle of operation of the PGA can be simply described by considering a single pass system as shown in Figure 2. A piston incorporating an internal flow passage is propelled to the left at an absolute velocity U by gas pressure acting on its

base. The internal passage of this piston consists of a flow duct which changes direction of the air by 180°. Air from the shock tube is directed toward the moving piston with an absolute velocity to the right V_1 so that the air velocity relative to the piston is $W_1 = U+V_1$. For simplicity of presentation it is assumed that relative velocity of the air leaving the piston equals the relative velocity entering, ($W_1=-W_2$) so that pressure losses are felt in both static and stagnation pressures. Thus, for a 180° turn the absolute velocity of the air leaving the piston becomes W_2+U, or $V_1 + 2U$.

The system considered in detail in this report features a piston having two turning passages displaced 90° from each other. Sketches indicating the flow through the PGA are shown in Figure 3. Air from the shock tube enters the PGA at A at a velocity of V_1 and is directed toward a moving piston traveling at a velocity U. Air is turned 180° by the first piston passage so that the absolute velocity leaving the first turn ofthe piston becomes V_1+2U. The air is then directed toward a stator or fixed turning vane and re-enters the piston through the second turning passage at B, thereby being turned a second 180° to produce a final absolute velocity $V_3 = V_1+4U$. Additional passages could have been added to further increase the final air velocity. The air at this final velocity is then passed through an expansion nozzle to attain the static pressure and temperature desired in the test section.

To efficiently use the limited time interval of steady state discharge from the shock tunnel source, optimization schemes were studied wherein inlet, fixed turning passage, and discharge stations were staggered in various combinations. Figures 4a and 4b indicate the apparent increase in test time which can be realized by displacing the turning passage and discharge port. However, as the piston passes the inlet port andcuts off the flow, an expansion wave is propagated into the flow as indicated by the dotted line in Figures 4a and 4b. The pressure and velocity behind the expansion wave is altered and the uniform-flow test time is shortened. Figure 4c shows the flow kinematics of unstaggered ports and turbing passage. This arrangement provides the longest useful test time. On each of these figures the shock tunnel discharge has been assumed to flow for 5 milliseconds at 10,000 ft/sec and the piston has moved at 3,000 ft/sec. The diagram shows how the 5 millisecond flow time is reduced by the ratio of initial to final velocities. There is an additional loss in testing time of less than 1 millisecond from the unsteady flow of the initial expansion to the 10,000 ft/sec through the throat of the shock tube. An additional loss will also be created by the non-steady flow at the discharge port, at which point a final adjustment of flow is made to the test conditions.

The thermodynamic cycle of this device is described by Figure 5 which shows the cycle on a Mollier diagram. Air discharged at a total temperature and pressure as indicated at Point A, is

expanded isentropically to one atmosphere, at point B. An increment in total enthalpy (the increase in kinetic energy of the gas created by the 12,000 fps velocity increase provided by the piston gas accelerator) would isentropically synthesize a total temperature and pressure, as shown at Point C. However, in the process there is a pressure loss and entropy increase to the same total enthalpy but a new total pressure, along the dotted line to Point D. The gas at condition D is isentropically expanded to $300^{o}K$, as shown at Point E.

III. THEORETICAL CAPABILITY

Figure 6 shows the performance envelope of altitudes and velocities that can be attained with shock tunnel total temperatures between approximately 2500°K and 8500°K and pressures between 1000 atmospheres and 6000 atmospheres. A pressure recovery of 1/8 for the total accelerator cycle has been assumed and a piston velocity of 3000 ft/sec has been assumed to produce a total velocity increment of 12,000 ft/sec in a double pass circuit. Figure 6 also indicates the incident shock Mach numbers which would be required to produce this envelope of testing conditions; shock Mach number is an equivalent measure of the stagnation temperature requirements for the shock tunnel facility. For tailored interface operation, incident shock Mach numbers between 6 and 9.5 are possible with the driver containing either cold hydrogen gas, helium with hydrogen-oxygen mixtures added, or heated hydrogen at a temperature of 1200° Rankine.

IV. CAPABILITY OF PGA WITH GASL SHOCK TUBE

Figure 7 shows the envelope of flight conditions which can be reproduced in a test chamber after the PGA has accelerated a shock tube discharge of 100 to 300 atmospheres. A pressure recovery of 1/8, and a velocity increment of 12,000 ft/sec have been assumed. Lines of constant stagnation temperature of input gas are also given on this figure. The arbitrary recovery of 1/8 is based on a 50% loss in each of the three successive turns of the PGA. However, even if this recovery were substantially poorer the performance of this facility remains high. Note the equivalent pressure-altitudes between 30,000 ft and 240,000 ft. The stagnation pressure corresponding to Point I on Figure 7 is 250,000 atmospheres and the pressure corresponding to Point II is 500,000 atmospheres but the static pressure in the PGA remains on the order of 1 atmosphere. If each turn developed a 25% recovery, the stagnation pressures would be respectively 30,000 and 60,000 atmospheres. Total enthalpies of Points I and II are approximately 5300 BTU/pound and stagnation enthalpies of III and IV are approximately 11,400 BTU/lb. Higher initial temperatures (as Points III and IV with initial stagnation temperatures of 5000^{o}K) produce low test section pressures because of the expansion required to match the 300^{o}K static test section temperature. No currently existing facility can match these energies and pressures with running times on the order of milliseconds.

The range of shock tunnel conditions herein described are easily produced and duplicated in GASL shock tunnel through application of the double diaphragm technique on firing a driver mixture of helium hydrogen and oxygen. The tunnel has been designed for a pressure of 2000 atmospheres, but the reproducibility of pressures and temperatures (through combustion firing of the driver) is less dependable at the higher pressure levels. The double diaphragm technique provides discharge for nearly 20 milliseconds whereas combustion firing at high pressures furnishes 5 milliseconds.

If the results of the preliminary test program (see Section VII.) represent the best possible performance of each component of the facility, the over-all pressure ratio would be the product of a 50% recovery in each of 3 turning passages, a 50% recovery in each of 4 ducts, and 50% recovery in both the entry and the discharge ports. The total recovery would thus be .002 instead of .125. However, the losses in the entry port from a poorly fabricated passage can be reduced; the losses in the constant area duct which results from the non-uniform entering flow can be similarly reduced. With good design the combined entry port, discharge port and constant area duct losses should not be more than 50% in total. A realizable facility pressure ratio thus becomes .06 and the envelope of Figure 7 shifts as shown by the dotted line.

V. APPLICATION OF PGA TO GASL FACILITY

The PGA consists of a combustion chamber to furnish the accelerating force to the piston, an acceleration cylinder through which the piston attains its test velocity, a testing section into which the test gas is ducted and in which its kinetic energy is increased, a test chamber into which the gas is ducted for the actual test, and a deceleration cylinder in which the piston is stopped.

To incorporate a piston gas accelerator with the GASL shock tube facility the following arrangement is envisioned: A second driven tube would be mounted to the present driver as shown in Figure 8. This driven tube would discharge into the test section passage of the piston gas accelerator as shown. The piston would be accelerated through a 60' length of cylinder driven by the products of combustion of a helium-hydrogen oxygen mixture. The trajectory of the piston, which has been determined by the methods of Ref. 8 is shown in Figure 9 for an assumed $\gamma = 1.5$ and speed of sound, $a_o =$ 6000 fps. At the end of the 60' the piston would be moving at a velocity of 3000 ft/second after an initial acceleration of 4000 g's which during the trajectory would have dropped to a level of approximately 2000 g's. The maximum driving pressure to produce this acceleration would be 2200 psi at the initiation of the test cycle.

Immediately before entering the test section the piston would pass a discharge port and the accelerator tube would be vented to reduce the driving pressure behind the piston. In this manner a constant velocity "stroke" would be maintained during the test cycle. The length of test section is defined by the piston velocity and the time during which high temperature, high pressure air is delivered from the shock tube. Thus, if a 20 millisecond discharge could be delivered by the GASL shock tunnel to a 3000 fps piston, a sixty foot test section would be required. If the tunnel only delivered 5 milliseconds, a 15 ft. section would be required.

At the end of the test section of the PGA are located the entry, turning passage and exit of the test section; the exit would in turn duct directly into a test chamber, as shown in Figure 8. Following the test section of the PGA an additional 60 ft. length has been allowed for deceleration of the piston. Such deceleration would be accomplished by combustion of a mixture of air and hydrogen contained behind a diaphragm. The combustion would be so coordinated as to produce a pressure after combustion of 600 psi as the piston reaches the entry to the deceleration cylinder. With such a pressure impeding the piston motion the deceleration could be complete within less than 60 ft without the build up of pressure through reflection of the compression waves at the downstream end of the deceleration cylinder. The trajectory during such a deceleration is shown in Figure 10. If these reflections were also accepted the piston would decelerate even faster. To protect the cylinder against excessive

pressures during the deceleration a system of blow-off valves or blow-out patches could be incorporated into the end of the cylinder.

Because the test conditions will vary, the test cylinder length should be amenable to changes for different operating times. Although the performance potential with combustion operation of the GASL shock tunnel is very high as indicated by Points III & IV on Figure 7, the available test time of 5 milliseconds of discharge from the shock tunnel is reduced (for example at Point IV) to $\frac{10880}{22880}$ x 5 or 2.4 milliseconds.

On the other hand, cold tests such as at Point II of Figure 7, have an available shock tunnel discharge of 20 milliseconds which is reduced to $\frac{4240}{16240}$ x 20 or 5.2 milliseconds. The facility as envisioned would produce either test conditions if the test section lengths were properly adjusted.

VI. AERODYNAMIC DESIGN

The 180° turning passage which will be incorporated in the accelerator piston is designed to take advantage of supersonic vortex flow in which all streamlines are concentric circles with constant velocity along each streamline. The velocity of each streamline varies inversely with the radial distance from a common center. The design effort requires only the initial establishment of vortex flow, after which the turning passage can be rotated through as many degrees of turning as required for the particular design. If viscous effects could be discounted, the flow could continue to be turned through any angle with no change in the velocity of each streamline. The basic design problem is to establish the transition surfaces prior to the region of vortical flow whereby the entering flow, which is assumed to be uniform, is compressed by one wall and expanded by the other wall to establish the vortex profile across the turning passage.

The methods used in development of the turning passage for this project are essentially those methods listed in Reference 2. However, in the present analysis, we have discarded the ideal gas ($\gamma = 1.4$) assumption made in the referenced report because of the high temperature of gases that were expected to be used in the flow, and have applied real gas equilibrium properties. In addition, the present turning passage is designed for higher Mach numbers, and for larger turning angles than were used in the referenced report.

The method of design for the transition arc is as follows: Along one radial line (see Figure 11) a vortical velocity distribution is assumed. This velocity distribution should bracket the desired entering Mach number for uniform flow; that is, the Mach number (M_i) on the inside of the turning passage should be above the uniform flow Mach number and on the outside of the passage it(M_o) should be below this Mach number. The total variation should not be too great in order to minimize the amount of compression or expansion by the transition arc. There is an element of trade-off involved, however, in the choice of velocity distribution. To enable development of a passage in which the cross-section flow area is large compared to the total cross-section, the Mach variation is greatest and the contraction area ratio is also greatest. If however, small variation in Mach number is desired, the flow area becomes a small portion of the total projected piston frontal area. Thus, in Figure 12, w/W varies with M_i/M_o.

As shown in Figure 11, the Mach number distribution assumed varies from Mach 2.8 at the outside to Mach 4.14 at the inside of the turn. The design then proceeds in reverse by defining the number of degrees of expansion (30.1^o) required to raise the lower Mach number to the initial free stream value (M=4) and the amount of compression (2.4^o) to drop the higher Mach number to the free stream value. Inasmuch as a different amount of turning is required on each surface, the vortical flow will continue on the inner surface

for the difference (27.7^{o}) required to reach a common Mach number as is shown in Figure 11. When the initial point on each of the walls for the start of vortical flow has been established then the characteristic network upstream is developed which contains the vortical flow distribution (area abc). Thereafter, waves of compression or expansion are projected from the final Mach lines as indicated (in area dbc and eba) to define the flow direction at the wall which will produce the two families of waves which develop the known characteristic network. Streamlines traced through these waves define the transition arcs. After each of the transition arcs has been developed a uniform flow should result at the farthest upstream station.

The number of total degrees of rotation from the incoming flow to the point of established vortical flow (30.1^{o}) should be subtracted from 90^{o} and the vortical flow should continue downstream for the balance of 59.9^{o}. The flow passage thus developed is repeated in mirror image from the 90^{o} point onward so that the full 180^{o} passage is developed. At the downstream termination of vortical flow the compression-expansion procedure would be reversed, that is, the outer wall would now be producing an expansion from the vortical flow to raise the Mach number to the free stream value and the inner wall would be compressing or decelerating the flow to the same value. The coordinates of the 180^{o} passage as defined in Figure 12 are given in Table I. Figure 13 shows a photograph of the turning section.

To develop the characteristic network with equilibrium real gas properties a table of such properties was developed. From an assumed total temperature and pressure (5240°K and 320 atmospheres) of the discharge conditions of the combustion-driven shock tube, a total enthalpy and entropy value were determined on a Mollier Chart (Ref. 3). The static enthalpy, static temperature and pressure, speed of sound and Mach number were determined for a range of assumed velocities. By the method recommended in Reference 4 as indicated below, the Prandtl-Meyer turning angle vs. Mach number variation was determined.

$$N = \tfrac{1}{2} \int_{F_1}^{F_2} \left(\frac{2F}{a^2} - 1 \right)^{\frac{1}{2}} \frac{dF}{F}$$

Where:

a is the local speed of sound

$F = \frac{u^2}{2}$, n is the local gas velocity

N is the Prandtl-Meyer turning angle

Therefore:

$$N = \tfrac{1}{2} \int_{u_1^2/2}^{u_2^2/2} (M^2-1)^{\frac{1}{2}} \frac{du^2}{u^2}$$

where:

$M = \frac{u}{a}$, Mach Number and $\frac{du^2}{u^2} \approx \frac{2\left(u_n^2 - u_{n-1}^2\right)}{u_n^2 + u_{n-1}^2}$

Figure 14 shows N versus M and Figure 15 shows u versus M for the stagnation conditions which have been chosen.

In addition to design of the 180° turning passage, it was intended in this project to provide a design for the entry turn through which gas would be introduced into the piston gas accelerator. The test apparatus was therefore designed to provide acceleration and flow turning from the shock tunnel throat into a constant area duct before entering the 180° turning passage. A schematic diagram of the testing circuit is shown in Figure 16. The initial expansion to the nominal Mach 4 flow was accomplished by symmetric two-dimensional nozzle to Mach 3.4 based on the same turning angle - Mach number dependence of Figure 14, and a subsequent 14° turning passage based on Prandtl-Meyer one-wave flow to develop the final Mach number M = 4. The basic characteristic system is indicated in Figure 17.

An approximate scale drawing of the initial turning passage is shown in Figure 18 and the coordinates of this system are listed in Table II. The coordinates have been corrected for boundary layer displacement thickness by the method of Reference 5. The side walls have a constant width of 2.15 inches and the contoured walls include a correction for the boundary layer of the side walls.

The assumption of equilibrium flow through the nozzle was examined. Reference 6 indicates that relaxation times defined by shock tube experiments are 15 times as long as those which have

been measured in an expansion nozzle. We assumed the relaxation time of Figure 19, shown in the reference from shock tube results, which is shown to be conservative. Consider that a gas particle requires approximately 235 microseconds to travel from the throat to the Mach 4 station with the pressure varying from 180 to 1 atmosphere and the temperature from 4780^{o}K to 2050^{o}K. Corresponding relaxation times are .03 microseconds at Mach 1 and 150 microseconds at Mach 4. The two-dimensional nozzle geometry requires a very short length for the symmetric expansion and a much greater length for the turn. Equilibrium flow thus appears to be a safe assumption.

VII. TEST PROGRAM AND RESULTS

Although a theoretically valid scheme has been conceived, analyzed and designed, the performance of the piston gas accelerator requires a satisfactory recovery in the 180° turning passage. The analysis has assumed a 50% recovery within any one turning passage. However, no previous experimental work has furnished results which justify such an assumption in the present configuration. It was therefore required that a test program be conducted to indicate the feasibility of turning supersonic flow through 180° with reasonable recoveries. In addition, since the design of the initial entry into the test section cylinder was a part of the contract work statement, the experimental program was devised so that the entry could also be experimentally investigated.

The test program has been conceived as three distinct series of tests, to determine the flow at the following stations:

A) the end of the initial entry passage, which accelerates and turns the initial flow

B) the end of a constant-area duct

C) the discharge from the 180° turning passage,

as shown in the schematic test set-up of Figure 16.

The tests, hereafter described, are outlined in Table III.

Program A) Because the discharge of each element effects the performance of all subsequent elements, the test program initially examined the discharge of the 14^{o} initial entry passage, the first element. The results, which were reported in Reference 7, are shown in Figures 20 and 21. They indicate that the initial expansion and turning passage does not provide uniform flow as hoped for, under the double diaphragm test conditions of test N1 through N5.

The difference in pressure profiles of tests N1, N2 and tests N3, N4, and N5 cannot be attributed to instrumentation or upstream stagnation conditions. It must therefore be assumed that some internal contour change, caused by hot gas erosion or scoring by diaphragm particles, altered the flow.

Static pressures on the upper and lower walls were measured and the variation was assumed linear across the passage to evaluate Mach number variation for test N5 as shown in Figure 22 . To improve the flow a boundary layer bleed slot was machined in the upper wall, but test N7 showed no significant effect. (see Figure 23.) A subsequent test, N11 was run with a combustion driver and high pressure-temperature conditions to determine whether the non-uniform flow was caused by off-design stagnation conditions. This test provided incomplete results (Figure 24) but it still indicated different pressures on the upper and lower walls.

Conclusions for Program (A):

The difference in static pressures measured on the upper and lower walls in tests N5, N7 and N11 indicates that errors inherent in the design or fabrication of the duct were sufficient to produce

a Mach number and pressure gradient across the duct. The only static pressure determined in the early tests N-5 and N-7 were wall static pressures. If a linear variation is assumed as shown in Figure 23 and 24, the Mach number distribution is computed as shown. The mass-averaged pressure recoveries from shock tunnel stagnation conditions are computed respectively at .46 and .75. It is believed that the poor flow leaving the 14^{o} turning passage was caused by

a) the alteration of the nozzle contour caused by the shrinkage of the throat insert during assembly welding. Although considerable handwork was performed to correct the contour, it did not match the design shape and may have initiated the disturbances which caused the non-uniform flow.

b) the different boundary layer structures on the upper and lower walls caused by the different curvatures. In design, an equal displacement thickness correction was applied to both walls.

c) the viscous effects of a high aspect ratio throat. An axisymmetric nozzle before turning might eliminate this problem.

Program B) Although the flow leaving the 14^{o} turn passage was not uniform it was decided to test downstream because

a) in the full facility, thePGA would probably be required to operate on flow which was non-uniform.

b) the test program was primarily concerned with the 180° turning passage; the constant area duct and turning passage were added as secondary considerations.

The second group of tests surveyed the discharge of flow at the end of a seven-foot constant area duct. The seven-foot length was chosen because the flow in the PGA device would be through a constant area duct with length varying from zero up to and as much as 60 feet by virtue of the moving piston. Seven feet was a convenient length for the GASL facility. The effect of the constant area duct tested is thus only qualitative; a zero length duct would obviously make no change on the discharge of the 14° turning passage. A splitter plate was incorporated at the upstream end of the constant area duct to remove some of the boundary layer to improve the flow. However, this splitter plate was not very effective as shown in Figure 25. At the downstream end of the constant area duct a modest expansion was then incorporated for the last 1½ feet, as shown in Figure 26, in the hope that such expansion would provide a larger core of uniform flow. In earlier tests Mach numbers were deduced on the assumption of a linear static pressure distribution. However, the use of cone surface pressures more accurately reflects the static pressure variation across each station of interest. Surveys were made of the pilot pressure at the end of the constant area duct and of

the cone surface pressure to allow the computation of Mach number distribution across the duct. Mach number and stagnation pressures have been based on Figure 27 which applies to the probe used. The cone pressure rake was adapted from the pitot pressure rake as shown in Figure 28. The flow from the expansion section on the constant area duct continued to maintain a fully-developed pipe-flow profile, as shown in Figure 29 (pitot pressure). Figure 30 (cone pressure), and Figure 31 (Mach number and stagnation pressure).

Conclusions for Program (B):

The Mach number distribution measured at the end of the constant area duct is moderately reduced from the values computed at the entry as can be seen by comparing Figures 31 and 23. It would appear that the flow disturbances originating in the first turn or entry continue in the constant area duct and cause a modest redistribution of the flow to a more symmetric one but at lower Mach numbers with a substantial pressure loss. Based on the assumed linear static pressure distribution at the entry to the constant area duct, the pressure recovery in the duct is .53 based on test N-5 or .33 based on N-7.

Program C) The first attempts to pass air through the 180° turning duct as it was originally designed was unsuccessful. The flow unstarted as evidenced by a pressure trace on the wall of the passage (Figure 32) and by the pitot pressure measured at the end of the duct (Figure 33). Wall static pressure within the 180°

turn were very high on the inside wall as shown in Figure 34. The flow configuration was assumed analagous to the sketch at the bottom of Figure 32 which was consistent with all data taken.

Possible causes of the failure to start are:

- the design was based on a hot gas whereas test conditions were cold
- the actual entering flow was non-uniform, whereas a uniform flow had been presumed
- the minimum area in the duct was less than the area required for swallowing a shock during starting

To increase the minimum area of the 180° turning duct, the entire inner wall was translated forward ½ inch, i.e., the passage width in the symmetry plane was increased by ½ inch as shown in Figure 35. The pitot pressures and cone pressures of Figures 36 and 37 defined the Mach number and stagnation pressures of Figure 38. In addition, wall surface pressures were measured during these tests and the results are shown in Figure 35 and can be compared with the wall pressures in Figure 34 of the unstarted duct. Note that the pressure rise of the inner wall of the modified turn is less severe.

Because starting of the turning passage was accomplished by

½ inch translation of the inner wall, it was translated 3/8 inch further to see if flow could be further improved. The cone and pitot pressures are shown in Figures 39 and 40, and the calculated Mach numbers and stagnation pressures are on Figure 41. The wall pressures are shown in Figure 42. It is apparent from these pressures that a more uniform flow was discharged from the first 180° duct with the smaller enlargement.

A mass-averaged computation of the recovery through the 180° duct indicates that the first configuration with an opening of one half inch developed pressure recovery of 51%. The second configuration with a larger variation in pressure across the passage provided a recovery of 58%, but it was felt that the lower recovery with higher uniformity was preferable.

The mass-averaged recovery, η was defined as follows:

$$\eta = \frac{\left(\sum_i \Delta W_i P_{t_i} / \sum_i \Delta W_i \right)_{out}}{\left(\sum_J \Delta W_J P_{t_J} / \sum_J \Delta W_J \right)_{in}}$$

where: $\Delta W_i = \rho_i V_i \Delta A_i$

ΔW_i, Incremental mass flow through

ΔA_i, incremental area

ρ_i, density in area A_i

V_i, velocity through area, A_i

ρ_i and V_i are functions of Mach number, total pressure, and total temperature. The total temperature was assumed constant at the shock tunnel supply value. Conservation of mass was satisfied in the numerical data reduction when $\sum_i \Delta W_i$ checked $\sum_j \Delta W_j$ within 5% for Modification I and within 9% for Modification II.

Conclusions of Program (C)

The 180° turning duct when modified provided a good pressure ratio. Inasmuch as the flow was most affected by the long compression surface of the outer wall, and the gas near the inner wall was of lower density, it is believed that translating the inner wall did not violate the theoretical design too seriously. The main effect of this translation was to improperly cancel the compressions of the outer wall as shown by the wall static pressures. The 180° turning passage does reverse the direction of supersonic flow with reasonable pressure recovery.

VIII. PRELIMINARY MECHANICAL DESIGN OF THE PISTON GAS ACCELERATOR

A. Introduction

A preliminary mechanical design of the piston gas accelerator is presented in this section, which permits achievement of the desired piston velocity of 3000 ft/sec with an initial acceleration of the order of 4000 g's. In addition, the piston gas accelerator (PGA) can be constructed by ordinary fabrication techniques using common materials operating within their safe design limits.

B. Principle and Description

The piston gas accelerator will operate in accordance with the scheme described previously in Section II. We must first accelerate the piston at 4000 g's to a velocity of 3000 ft/sec. in a 60 foot long acceleration cylinder. Since the space within the acceleration cylinder in front of the moving piston is evacuated, there is no requirement that there by any partition between the inlet and outlet vanes of the piston until the piston reaches the test section cylinder. However, in the test section cylinder we must prevent the entering test gas from bypassing the turning passages and thereby preventing proper gas acceleration. This must be accomplished by some method of partitioning which isolates each of the passages from one another while the piston is within the test section.

We have considered two approaches in detail to the solution of this problem, and these are illustrated in Figures 43 and 44. One is to allow a cylindrical partition finger to travel with and be positioned forward of the piston as shown in Figure 43. Longitudinal

seals are positioned on the external finger surface to prevent bypass flow between passageways until the piston has passed the gas entry and exit port locations. Disposable curved diaphragms which can be readily sheared by the piston are located at the ports in each of the four passageways to permit shock tunnel gas to:

- enter the test section and be directed toward the moving oncoming piston
- discharge to the stationary turning vane after being accelerated through the first-stage piston turning vanes
- reenter the second test section passageway (in a plane perpendicular to the first test section) leading towards the oncoming second stage piston turning passage
- and finally, exhaust through a discharge nozzle to a test chamber.

These functions of the diaphragms are accomplished within the time interval during which the piston is traveling within the test section. After completing their function, the diaphragms are sheared by the piston as it leaves the test section just prior to entering the deceleration section.

A second design approach is illustrated in Figure 44, with a break-away view shown in Figure 45. Here, instead of a moving partition, there are four stationary partitions in the form of "longitudinal diaphragms" fastened to the open side of each of the passageways within the test section for the entire test gas cylinder length. To serve the same functions explained previously these four diaphragms are curved at the entry and exit port locations.

In comparing these two approaches, we see that the major advantage of the "moving partition finger" approach is that it requires a minimum amount of diaphragm shearing, and this shearing takes place when the test gas has been discharged from the test section. The disadvantages of this approach are that the piston must support and move the long partition forward of itself; the piston structure must be capable of withstanding high stresses resulting from acceleration loads on both itself, and the cummulative effect of the loads on the partition finger. A moving seal is required at each line of contact between finger and wall. The finger must resist column failure from the high acceleration. These factors cause a relatively high piston weight, which in turn requires a high driver pressure for a given acceleration section length. The deceleration cylinder design is further complicated by the space requirements of the finger.

The "Longitudinal diaphragm" approach requires diaphragms sheared for the entire length of piston travel through the test section; however, it has an advantage in permitting significantly lower piston stresses, and there is no length limitation on the test gas section. For a given test section length, a lower piston weight and therefore lower driver pressure and overall cylinder pressure are required. For the particular PGA design evaluated, pressure requirements for the "partition finger" as compared to the "longitudinal diaphragm" approach are reduced from 6000 psi to 2200 psi.

After evaluating both approaches, it was concluded that the "longitudinal diaphragm" design approach should be used. The advantages of designing for, and working with the lower pressures and lower pressure differentials required is significant. The overall cost of the PGA assembly likewise will be significantly lower. Further, shearing of the diaphragm does not impose any serious problems if the method of replacement of the diaphragm is kept simple.

After passing through the test section the piston is brought to rest in a deceleration section having a length of 60 ft. This section does not require diaphragms to separate the flow passages, because the test is terminated when the piston leaves the test section.

C Specific Mechanical Design Objectives

In an effort to achieve satisfactory operation with a minimum of development time,

- common materials
- operation within safe limits of design, and
- simple methods of fabrication

have been used throughout the design. The diaphragm installation has been designed for easy replacement of expended diaphragms and also for easy adjustment to accommodate changes in diaphragm length as experimental test conditions change. The design has also been accomplished with a view towards endurance of components and reproducibility of test results.

D. Component Design Factors

The computational procedures, stress relationships and material properties on which the current preliminary design is based are included in an appendix to this report. A brief description of each component of the PGA follows with a statement of operating conditions and design criteria. The components considered are:

1. Combustion Chamber
2. Piston
3. Acceleration Cylinder & Deceleration Cylinder
4. Test Section Cylinder
5. Diaphragms
6. Bearings
7. Seals
8. Primary Structure

A total facility layout has been shown in Figure 8.

1. Combustion Chamber

The combustion chamber in which the hydrogen-air helium mixture is burned to provide driving force to the piston is a simple pressure vessel. Its 40-foot length will be made in two sections with flanged ends. A wall thickness of 1 inch on an inside diameter of 12 inches provides adequate strength for the maximum pressure of 2200 psi. An ignition system as used in shock tunnel systems will be mounted along the chamber.

2. Piston

Relationships between pressures, accelerations, piston size and weight, lengths of travel and gas properties are given in the appendix. Based on the configuration shown in Figures 45 and 46, and a maximum 4000 g acceleration and deceleration the piston has been designed taking into account the compressive loads during acceleration, tensile loads during deceleration, buckling, and loads resulting from gas pressure within the turning vanes. The turning vane assemblies will be fabricated or welded titanium sheet fastened to an aluminum backplate. The individual ducts are composed of curved plates welded to straight side plates. The side plates extend beyond the gas flow ducts, to transmit acceleration loads to the piston backplate.

During deceleration, the piston assembly is subjected to a tensile load equal to the compressive loading during acceleration. The bolting arrangement which fastens the turning vanes to the back-plate withstand the deceleration of 13,500 lbs on each of 12 ½ inch high-strength bolts.

The stresses in the turning vane walls have been calculated by assuming the duct walls to be simply supported across the 3.9 inch span. Wall thickness of ¼ inch is adequate for pressures of 150 psi. At locations with lower pressures, the wall thickness can be trimmed. The estimated weight of the piston composite described in Figures 45 and 46 is 40 lbs.

3. Acceleration and Deceleration Cylinders

The general outline of the cylinder assembly can be seen in Figures 46 and 47. The acceleration cylinder serves as a pressure vessel to contain the driving gas as it propels the piston, and provides accurately machined surfaces to guide the piston and restrain leakage past the piston. The deceleration cylinder performs similarly, except that the pressure difference across the piston is reversed to reduce the piston velocity. The cylinder is fabricated by inserting and fastening machined inserts into a cylindrical tube to form the cruciform shape required for the piston outline. We conservatively assume only 8 points of contact between the inserts and the cylindrical shell so that the maximum stresses in the shell are the resultant

of the stresses resulting from circumferential tension and a flexural stress from the bending moment due to the assumed 8 point loading. Stresses are in a range where an available carbon steel material in the order of 1 in. thickness can be used. There are a total of 8 similar individual cylinders, each with a length of 15 ft. These are utilized in two groups of 4 cylinders each, for acceleration and deceleration respectively. The cylinders are flanged, and carefully aligned during fabrication and assembly to permit movement of the piston during test operations.

4. Test Section Cylinder

As illustrated in Figures 45 and 47 the test section cylinder is basically similar to the cylinders described above (Figure 46). However it is up to 60 ft. in length and contains provisions at the point of test gas entry to facilitate movement of the test gas in and out of the cruciform-shaped passageways. These provisions are in the form of ducted coverplates which are fastened to the cylindrical surface. The walls of the external ducts are about 1 inch thick. Provisions are made within the cruciform for fastening of the four diaphragms. The diaphragms are inserted into position through the coverplate holes and then clamped into position by means of screws extended through the cylinder shell and bearing upon long sealing bars, extending the length of the cylinder. At the points of test gas entry and exit, an insert is used to fasten the curved portion of the diaphragms in place. For

ease of fabrication, four fifteen-foot sections of test cylinder will be joined by flanges with alignment accurately controlled by reference pins.

5. Diaphragms

The longitudinal diaphragms which provide flow separation are fabricated of a thin gauge metallic sheet with edge reinforcement to facilitate installation. Although many materials are suitable for use, ordinary low carbon steel provides an optimal combination of thermal and strength characteristics. For a 5-mil thick sheet the pressure-induced stresses which depend on the diaphragm curvature can be maintained below the 39,000 psi yield stress at room temperature; the material temperature rise which depends on its specific heat under the most severe operating conditions of time and heat transfer can be kept under $500^{\circ}F$.

Shearing of the diaphragm is accomplished by means of cutting blades located on the leading edge section of the piston turning vanes. For the thickness given, a tear strength in the order of 5 lb force is required for each surface cut, so that shearing of the diaphragm requires only a small force compared to that required to accelerate the piston. The sheared diaphragm is gathered by the piston in a space inside the two turning ducts (See Figure 45.)

6. Bearings

Strip bearings are used to accommodate the high sliding

velocity of the piston within the cruciform channel. The strip bearings are mounted on the piston. A suitable bearing strip assembly is a composite bearing material consisting of a low carbon steel backing into which is sintered a thin porous layer of spherical bronze which is in turn impregnated with teflon and molybdenum disulphide.

The bearing contact area can be adjusted to withstand the friction-generated heat. A two square foot bearing surface with a friction coefficient of .18 and conductivity of 2 BTU/hr-ft-^{o}F will suffer a 200^{o}F temperature gradient across the bearing. However, the material is suitable for operation at over 500^{o}F in either high or low pressure environments.

7. Seals

Seals are required on the rear outer perimeter of the piston to prevent driver combustion gases from entering the evacuated cylinder area. These seals can be adjustable self-energizing bronze strip seals mounted to the piston. A double seal arrangement with a gas accumulator section between the seals to retain combustion gas that may leak past the seals exposed to the combustion gas is made possible by the void volume of the piston between the back plate and the turning passages as shown in Figures 45 and 46.

8. Primary Support Structure

The structural support for the piston gas accelerator must withstand the reaction to the foundation resulting from acceleration and deceleration forces. The support will be a

thrust leg structure as shown in Figure 48 similar to that used for combustion type shock tube wind tunnel facilities. Rubber in compression type dampers are used between the legs and foundation. The legs act as pin connected struts transferring the thrust to the steel bars embedded in concrete as tension and compression members.

E. Conclusions:

Each of the components of the Piston Gas Accelerator is amenable to design by current techniques and fabrication with available materials by simple methods. Notwithstanding the extreme test conditions which are developed, forces and heat loads are not excessive.

IX. PRELIMINARY COST ESTIMATE

A preliminary projection of costs for materials and fabrication of the Piston Gas Accelerator has been prepared. It is based on discussion with suppliers wherein only approximate descriptions of the assemblies were used, and on experience in designing and erecting other facilities on our site as well as for others.

1.	Piston Assembly	$ 6,000
2.	Acceleration and Deceleration Cylinders 8 sections of 15ft. length @ $10,000 ea.	80,000
3.	Test Section Cylinders 4 sections of 15 ft length at $20,000 ea.	80,000
4.	Combustion Cylinders 2 sections of 20 ft length @ 8,000 ea.	16,000
5.	Test chamber and dump tank	21,000
6.	Vacuum System	11,000
7.	Alternate driven shock tube	19,000
8.	Bearings and seals	2,000
9.	Mounting Support Assembly	7,000
		$ 242,000

No costs are included for concrete foundations, supplementary shelter or instrumentation. Gases for acceleration and deceleration, and replaceable diaphragms have been omitted because they are cost items associated with test programs.

X. PRELIMINARY SCHEDULE:

A time schedule to fabricate, assemble and check out the Piston Gas Accelerator has been prepared. It is based on current delivery quotations by suppliers. The total elapsed time from beginning of contract to operable facility might be shortened by tight coordination, but test programs slip from unforeseen contingencies. Therefore, this conservative schedule is presented.

PRELIMINARY SCHEDULE HIGH ENTHALPY DEVICE

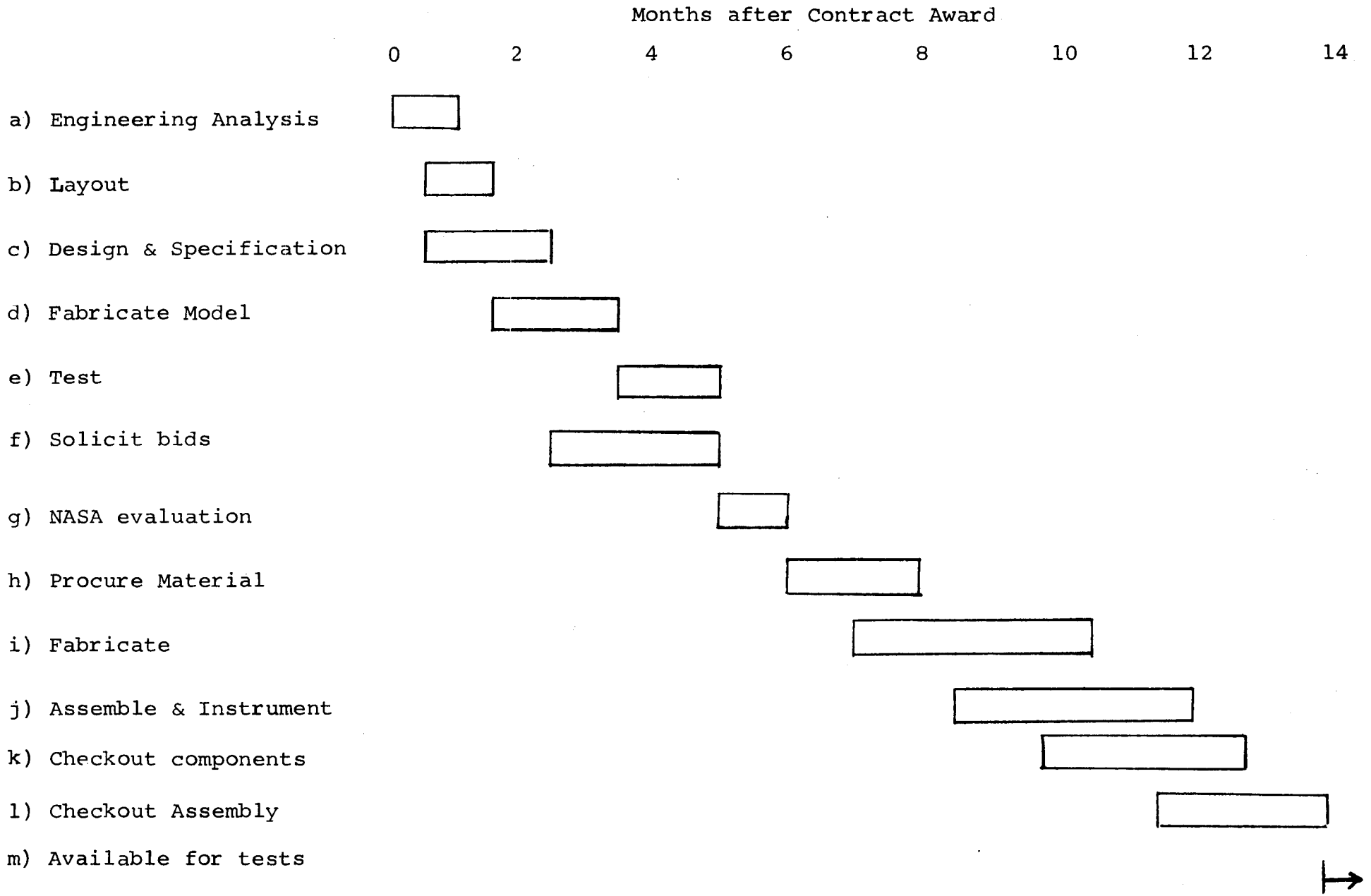

XI. RECOMMENDATIONS

A system has been developed to provide high-enthalpy high-pressure test conditions, a preliminary design has been prepared and one vital component has been tested. It is recommended that to minimize the risks attendant with facility development, that further efforts to build the PGA be separated into two phases. In the first phase a detailed design, shop drawings and specifications shall be produced which are adequate for GASL to solicit firm vendor bids or to make a fixed price proposal. Additional aerodynamic tests of a stationary 2 pass system shall be performed. The results of this first phase -- a complete design, an accurate cost, and a firm schedule - will then provide the basis for a decision to continue with the second phase. The second phase will include all procurement, fabrication, assembly and check out activities necessary to have an operable Piston Gas Accelerator. The first phase, tasks (a) through (f) of the Preliminary Schedule, would require 5½ months. If a month is required to evaluate Phase I and to decide to support Phase II, the facility would be completed within 14 months.

REFERENCES

1. Quarterly Progress Report No.1, June 9, 1964 to August 31, 1964, prepared under Contract NAS1-3909. GASL September 1964.

2. Boxer, Sterrett and Wlordorski, "Application of Supersonic Vortex-Flow Theory of the Design of Supersonic Impulse Compressor - or Turbine Blade Sections" NACA RM L52B06, Langley Aeronautical Laboratory April 24, 1952

3. Mollier Diagram for Equilibrium Air, ARO Inc., March 1964.

4. Feldman, J., Hypersonic Gas Dynamic Charts for Equilibrium Air, AVCO Research Laboratory, January 1957.

5. Ruptash, J., Growth of Boundary Layer in Supersonic Nozzles, Symposium on High Speed Aerodynamics, Summary of Proceedings, National Aeronautical Establishment, Ottowa, Canada.

6. Hurle, Russo, and Hall, Spectroscopic Studies of Vibrational Non-equilibrium in Supersonic Nozzle Flows Journal of Chemical Physics Vol. 40, No. 8, April 1964.

7. Quarterly Progress Report No. 2, September 1 to November 30, 1964, Prepared under Contract NAS1-3909. GASL, December, 1964.

8. Charters, Denardo, and Rossow, Development of Piston-Compressor Type Light-Gas Gun for the Launching of Free Flight Models at High Velocity NACA TN4143, November 1957.

APPENDIX

1) The piston trajectory is developed by the relationships of Reference 8 in which the acceleration is related to the piston properties and gas properties. The basic relationship is:

$$L = \frac{2W_p C^2}{g P_o S (\gamma-1)} \left[\frac{\frac{2}{\gamma+1} - \left(1 - \frac{u_p}{\alpha_o}\right)}{\left(1 - \frac{u_p}{\alpha_o}\right)^{\gamma+1/\gamma-1}} + \frac{\gamma-1}{\gamma+1} \right]$$

where γ = ratio of specific heats $\qquad \alpha_o = \frac{2C}{\gamma-1}$

u_p = piston velocity, ft/sec

C = speed of sound in propellart gas, ft/sec

P_o = initial gas pressure, psi

S = piston area, sq. in.

L = length of travel to attain u_p, ft.

W_p = piston wt, lbs.

g = gravity, 32.2 ft/sec^2

The initial acceleration of the piston

$$a_o = \frac{P_o S g}{W_p} \qquad \text{ft/sec}^2$$

With a helium, hydrogen and air mixture,

$\gamma = 1.5 \qquad C = 6000$ ft/sec

For a 75 sq. in. piston to reach a velocity, u_p, of 3000 ft/sec in a 60 ft length,

$$\frac{P_o}{W_p} = 54.$$ and the initial acceleration,

a_o = 4050 g's. A 40 lb piston requires an inital pressure,

P_o = 2160 psi.

2) The compressive stress, σ, on a uniform structure under acceleration, a, is:

$$\sigma_m = \frac{a}{g} \rho_m \; X \; \text{psi.}$$

where

ρ_m = density of structural material, lbs/in^3

X = length of structure in direction of acceleration, (15 inches for this piston)

therefore the material strength-weight ratio, $\frac{\sigma_m}{\rho_m}$,

must be: $\frac{\sigma_m}{\rho_m} = 4050 \times 15 = 61 \times 10^3$ in.

Typical values are:

Aluminum 2017-T4	396×10^3 in.
Beryllium Copper	437×10^3 in.
410 Stainless Steel	416×10^3 in.
SAE 4340 Alloy steel (heat treated)	528×10^3 in.
Titanium alloy (aged and welded)	1030×10^3 in.

A 15 foot center-body piston would require

$$\frac{\sigma_m}{\rho_m} = 4050 \times 180 = 730 \times 10^3 \text{ in}$$

and a 60-ft center-body could not withstand the compressive stress.

The stress in a piston of titanium alloy whose density is .163 lbs/in is $4050 \times .163 \times 15 = 10{,}000$ psi.

3) The Euler buckling criterion for a column with one end fixed and concentrated load has been applied to the section of the piston gas duct with the lowest moment of inertia

$$F_{cr} = \frac{\pi^2 EI}{4L^2} \quad \text{where}$$

$E = 17 \times 10^6$ lb/in^2 for titanium

$L = 12$ in

min $I = 2.43$ for 1/4 in. wall thickness

$F_{cr} = 707{,}000$ lb

which is well above the total accelerating force:

$F = 4050 \times 40 = 162{,}000$ lbs.

4) The turning vane walls when considered as uniformly-loaded, simply-supported beams develop a maximum flexural stress:

$$f_b = \frac{3}{4} P \left(\frac{\ell}{t}\right)^2$$

where, if p = pressure within turning vane = 150 psi

ℓ = unsupported span = 3.9 in

t = wall thickness = .25 in

f_b = 27,400 psi

Where the walls have lower pressures and some degree of end fixity thinner walls could be used.

5) The combustion cylinder requires satisfaction of hoop stress only:

$$f_t = \frac{P_o\ d}{2\ t}$$

The acceleration cylinder, however, must satisfy the flexural stress of point loading.

$$f_b = \frac{W\ R}{2}\left(\frac{1}{\sin\theta} - \frac{1}{\theta}\right)$$

where W, radial force, $= \frac{\pi\ d\ P_o}{8}$ = 10,175 lb

$2\theta = \frac{2\pi}{8}$ $\qquad \theta$ = .392 rad

R = 6 in d = 12 in

t = 1 in.

$\therefore$ $\quad ft = \frac{2160 \times 12}{2 \times 1}$ = 13,000 psi

$$f_b = \frac{10175 \times 6}{2}\left(\frac{1}{.383} - \frac{1}{.392}\right) = 9150 \text{ psi}$$

$f_t + f_b$ = 22,150 psi

6) The tensile stress in the diaphragm is approximately

$$S_t = \frac{pr}{L}$$

where: S_t = tensile stress (psi)

r = radius of curvature of diaphragm (in)

The bulk temperature rise ($\Delta\,^{\circ}F$) of the diaphragm is:

$$\Delta T = \frac{12\,\dot{q}\,\theta}{\rho\,L\,c_p}$$

where $\dot{q}$ = heat flux ($\frac{\text{Btu}}{\text{sec-ft}^2}$)

θ = time (seconds)

ρ = density (lb/ft^3) = 487 (carbon steel)

L = thickness (inches)

c_p = specific heat ($\text{Btu/lb-}^{\circ}\text{F}$)

= .113 (carbon steel)

For the most severe condition anticipated, we have

$\dot{q}$ = 1,760 Btu/sec-ft^2

θ = 6.15 milliseconds

For L = .005 in

$$\Delta T = \frac{(12)\ (1760)\ (.00615)}{(487)\ (.005)\ (.113)} = 472^{\circ}\ \Delta F$$

For r = 8 inches, p = 14.7 psi.

$$S_t = \frac{14.7(8)}{.005} = 23{,}500 \text{ psi}$$

The final temperature of the steel would be 472 + 70 = 542°F where the yield strength is 30,000 psi, so that our stress value of 23,500 psi would be safe.

TABLE I

Coordinates of 180° Turning Passage

(See Figure 9)

Inner Wall		Outer Wall	
X	± Y	X	± Y
0	3.490	0	5.269
6.056	3.490	1.422	5.208
6.099	3.488	2.204	5.169
6.344	3.486	3.271	5.079
		4.287	4.933
6.197	Origin of Radius	5.023	4.793
	3.487 Radius	5.471	4.695
		5.911	4.574
		6.526	4.381
		7.024	4.214
		7.216	4.162
		7.760	3.891
		8.048	3.745
		8.286	3.609
		6.197	Origin of Radius
			4.170 Radius

TABLE II

Coordinates of First Turning Passage (See Fig. 14)

X	-Y	+Y
0	.067	Same
.055	.070	"
.112	.073	"
.174	.078	"
.236	.084	"
.303	.091	"
.371	.098	"
.444	.108	"
.498	.115	"
.523	.118	"
.619	.132	"
.692	.143	"
.755	.153	"
.826	.164	"
.914	.178	"
1.092	.205	"
1.300	.233	"
1.486	.256	"
1.873	.298	"
2.361	.350	"
2.927	.415	"
3.606	.497	"
3.844	.526	"
4.437	.600	"
4.855	.651	"
6.062	.770	"
7.506	.862	"
9.281	.912	"
9.330	.912	"
9.73	.916	.922
10.38	.923	.969
11.10	.930	1.056
11.99	.940	1.176
13.00	.950	1.356
14.18	.962	1.608
14.98	.974	↑
16.10	.948	⋮
17.78	.856	Straight Wall
19.78	.686	⋮
22.15	.391	⋮
24.94	+.040	↓
27.31	-	4.844
28.16	+.667	
28.35	+.707	

Table III

TEST PROGRAM

Test	Figure #	P_o psia	Rake Measurements See Fig. 16	Comments
N-1	20	2980	1st Sta. pitot	Double Diaphragm tests
N-2	20	2820	1st Sta. pitot	
N-3	21	2880	1st Sta. pitot	
N-4	21	2820	1st Sta. pitot	
N-5	21,22	2750	1st Sta. pitot	and wall static
N-6	25	2820	2nd Sta. pitot	" " "
N-7	23	2950	1st Sta. pitot	
N-8	25	2850	2nd Sta. pitot	
N-9	25	2800	2nd Sta. pitot	
N-11	24	4340	1st Sta. pitot	Combustion test
N-15	29	2930	2nd Sta. pitot	Double diaphragm
N-16	29	2930	2nd Sta. pitot	
N-17	29	3000	2nd Sta. pitot	
N-18	33,34	2960	3rd Sta. pitot	Unmod. 180° duct & wall static
N-19	33,34	3060	3rd Sta. pitot	" " " "
N-20	35,36	3180	3rd Sta. pitot	Mod. I 180° Duct & wall Static
N-22	35,36	3120	3rd Sta. pitot	Mod. I 180° Duct & wall Static
N-24	40,42	3220	3rd Sta. pitot	Mod. II 180° Duct & wall Static
N-25	40,42	3310	3rd Sta. pitot	" " " "
N-26	40,42	3240	3rd Sta. pitot	" " " "
N-27	30	3020	2nd Sta. cone	
N-28	30	3060	2nd Sta. cone	
N-29	39	3030	3rd Sta. cone	Mod. II 180° Duct & wall Static
N-30	39	3000	3rd Sta. cone	" " " "
N-33	37	3030	3rd Sta. cone	Mod. I 180° Duct & wall Static
N-36	37	3070	3rd Sta. cone	Mod. I 180° Duct & wall Static

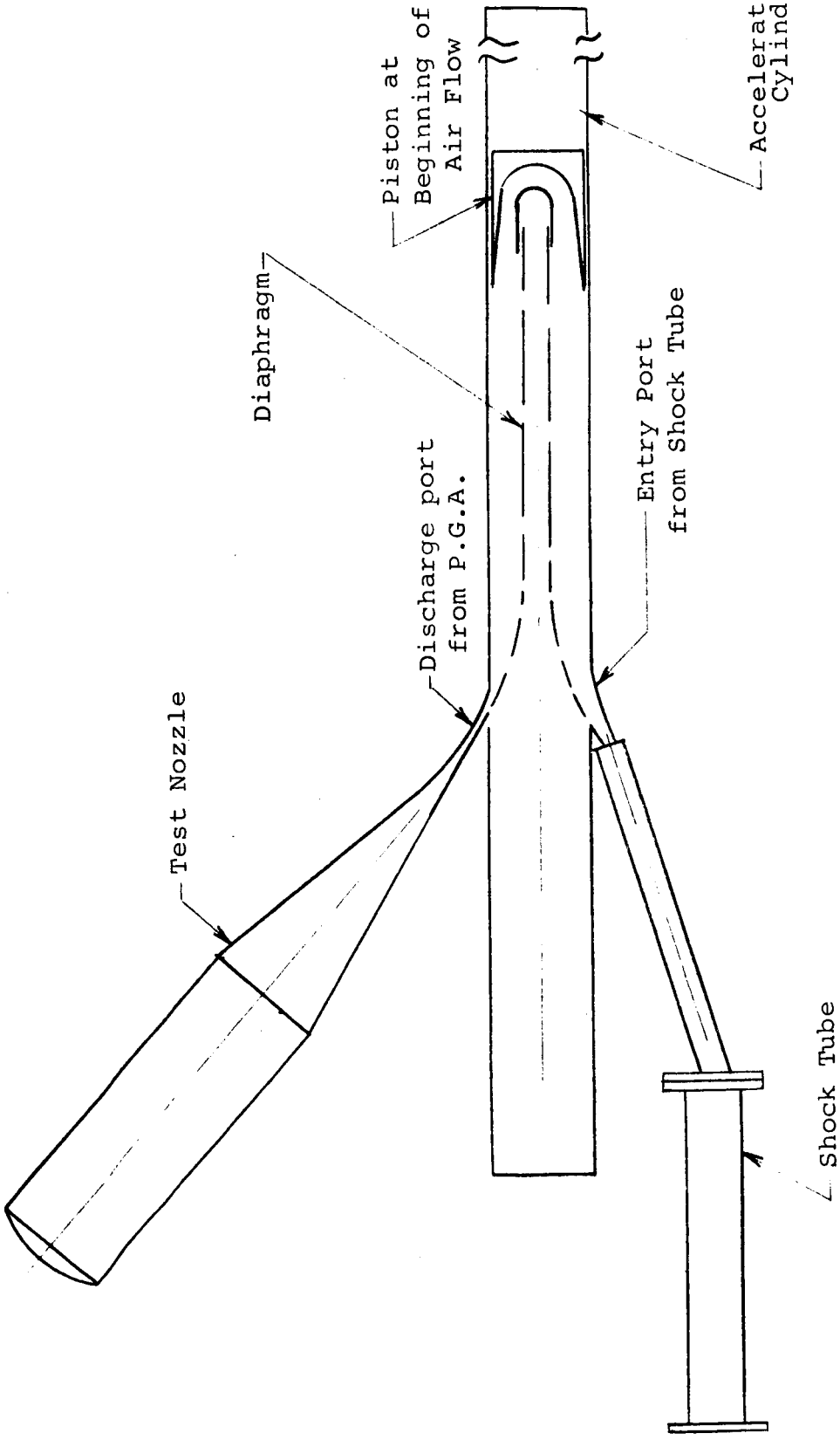

Figure 1 - SCHEMATIC DIAGRAM OF SINGLE PASS SYSTEM

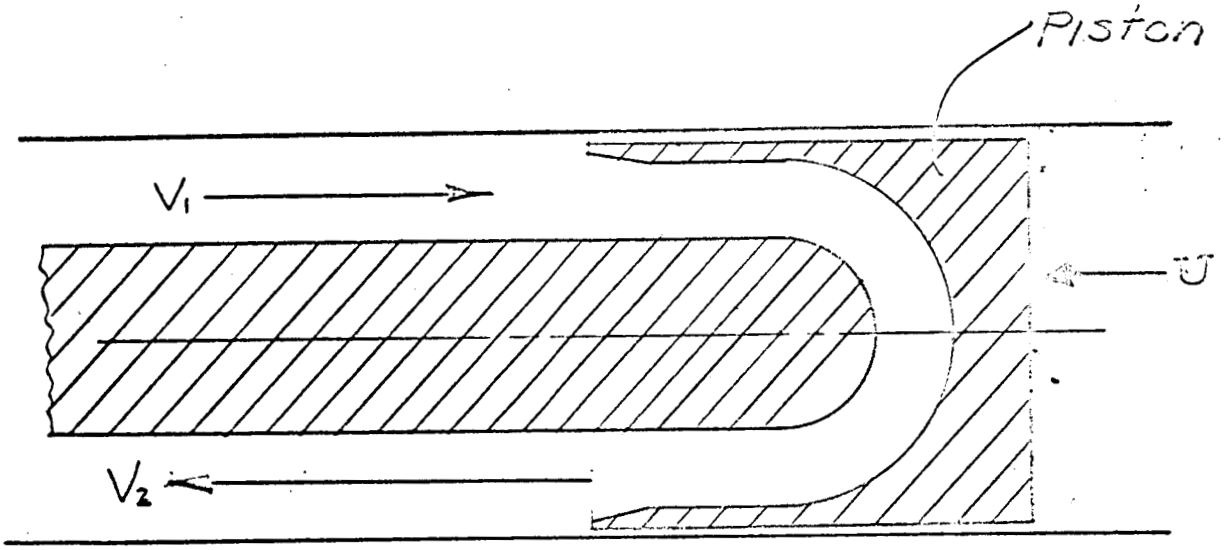

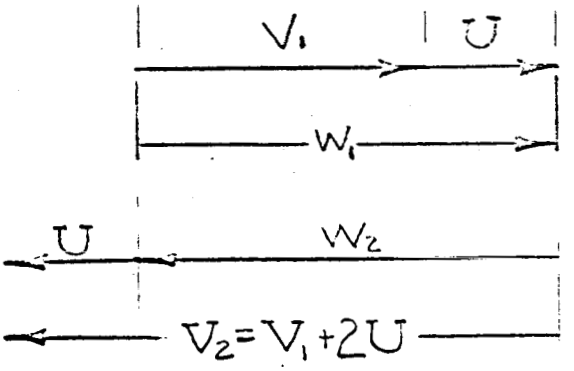

U; velocity of piston
V_1, V_2; absolute velocity of air
W_1, W_2; air velocity relative to piston

FIGURE 2-KINEMATIC OPERATION OF SINGLE PASS PISTON

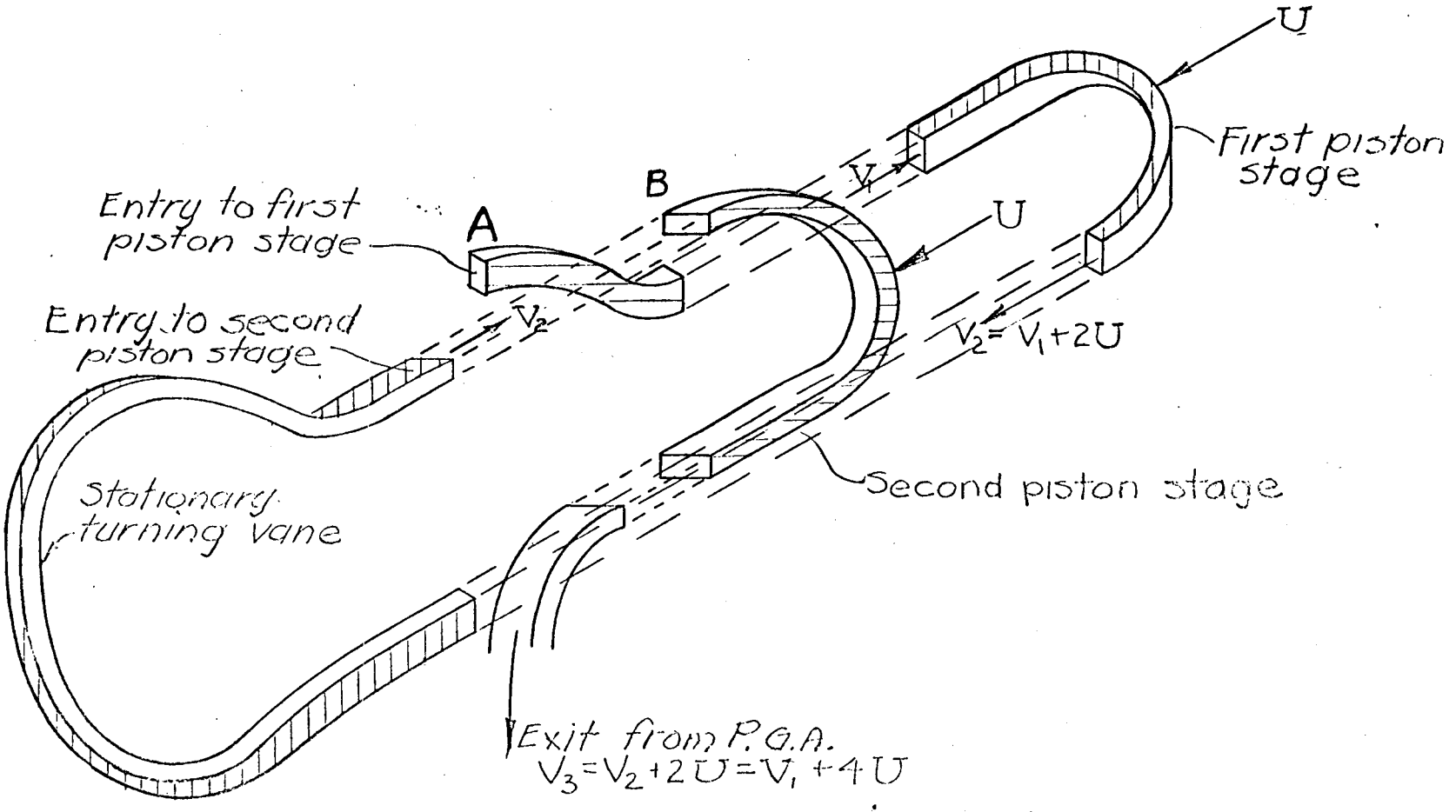

Figure 3 - Diagram of the flow thru a double pass piston

FIGURE 4a KINEMATIC DIAGRAM OF PISTON AND GAS FLOW WITH STAGGERED DISCHARGE PORT

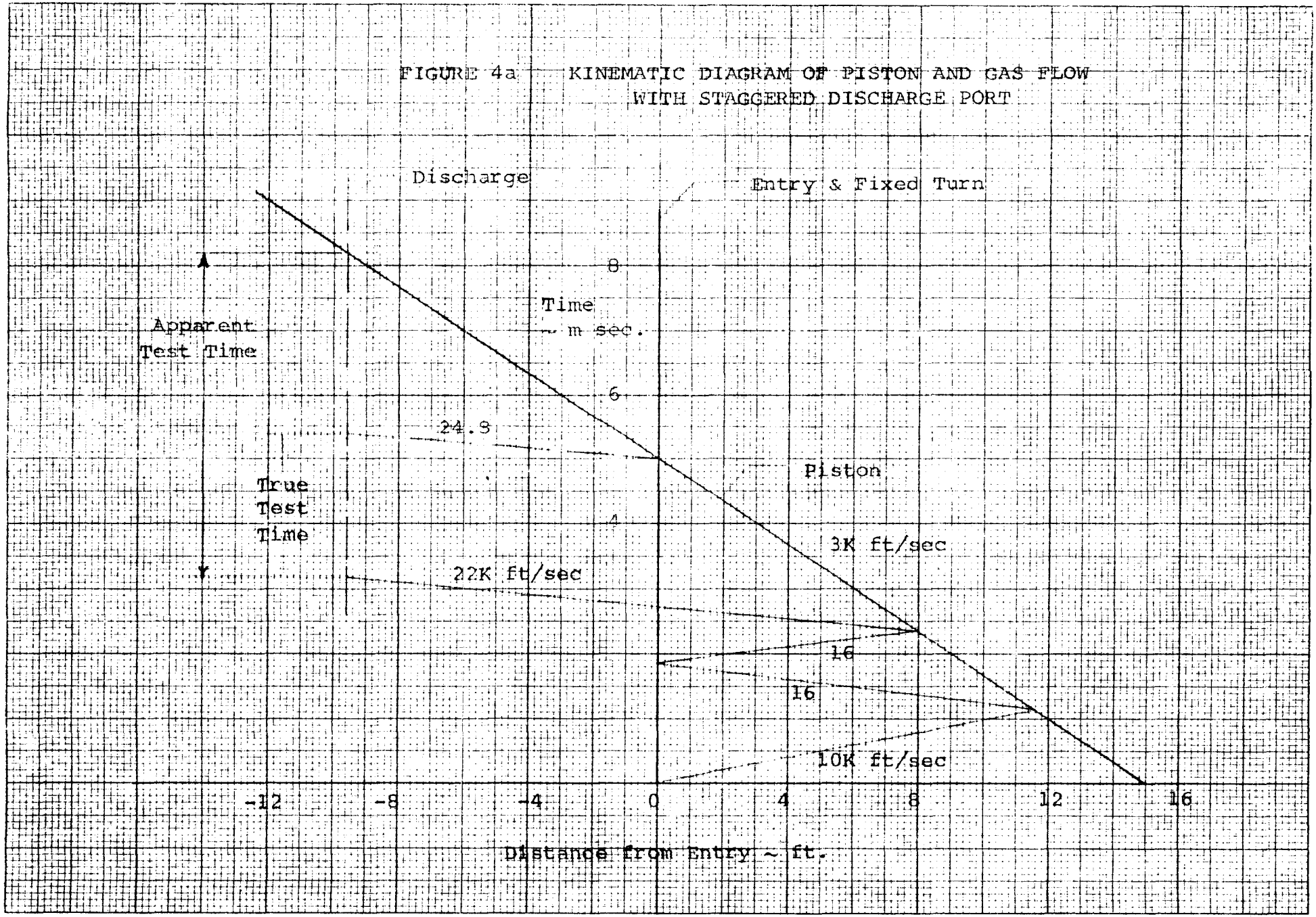

FIGURE 4b KINEMATIC DIAGRAM OF PISTON AND GAS FLOW WITH STAGGERED FIXED TURN AND DISCHARGE PORT

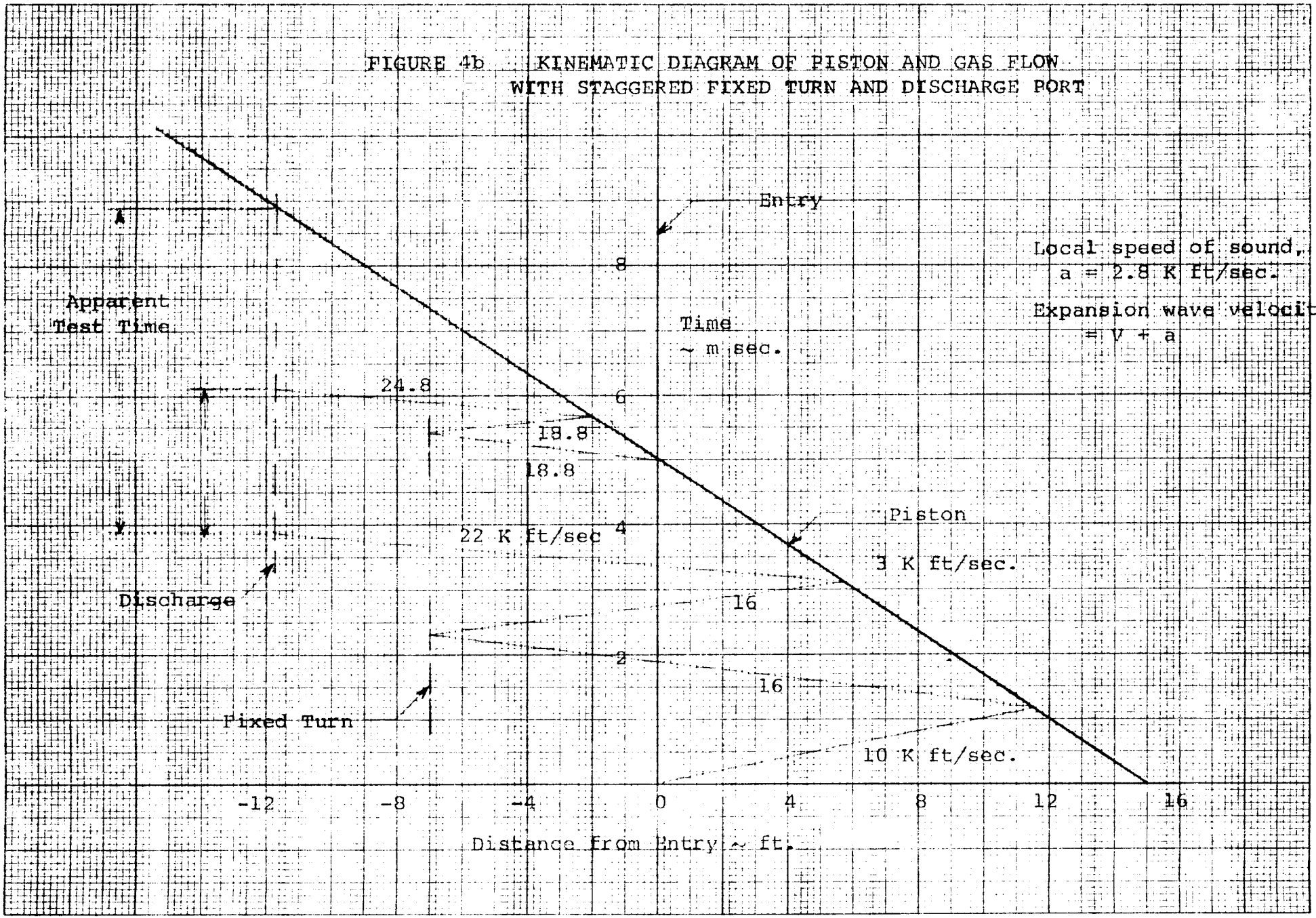

FIGURE 4c KINEMATIC DIAGRAM OF PISTON AND GAS FLOW WITH ENTRY, TURN, AND DISCHARGE IN ONE PLANE

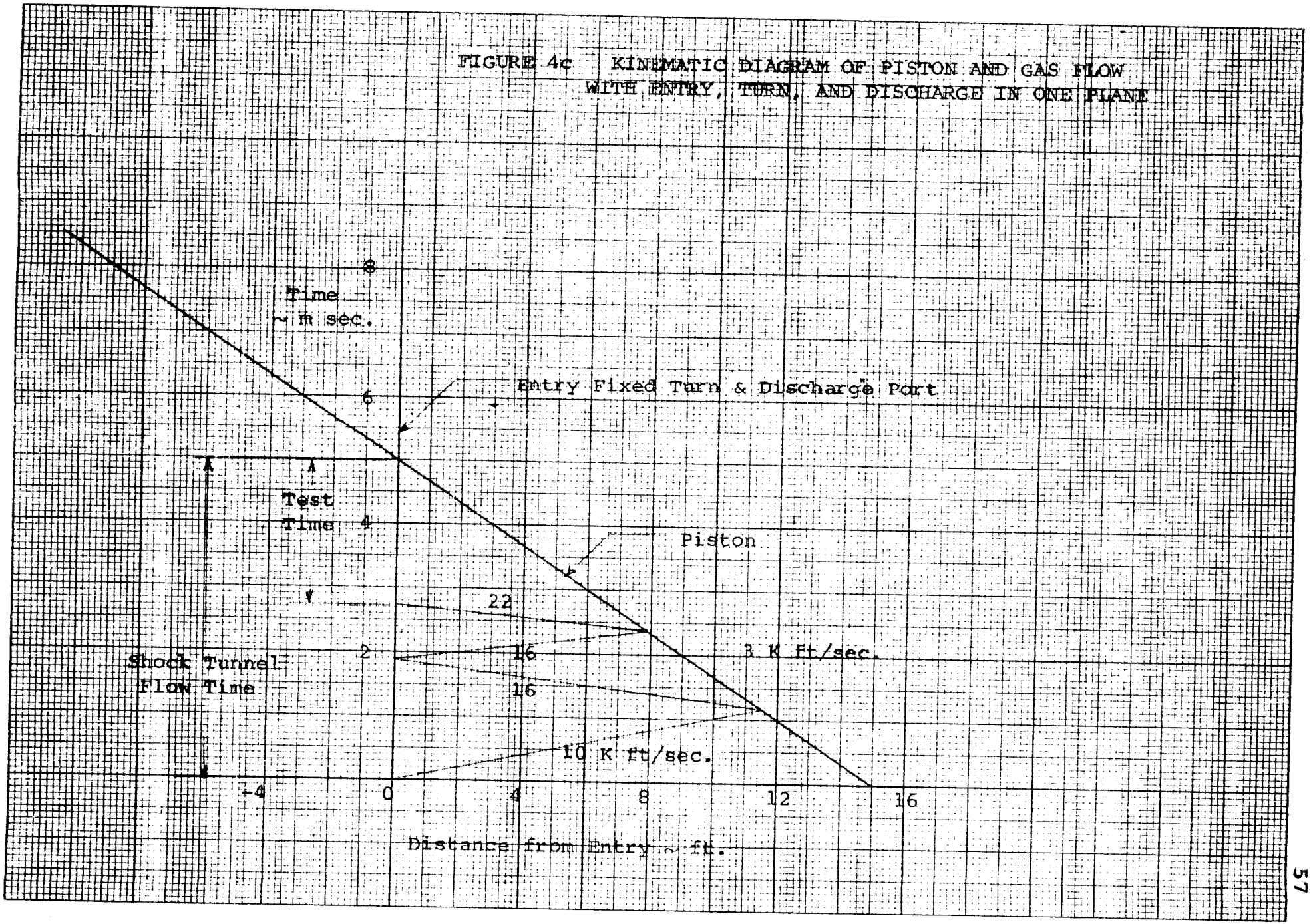

FIGURE 5

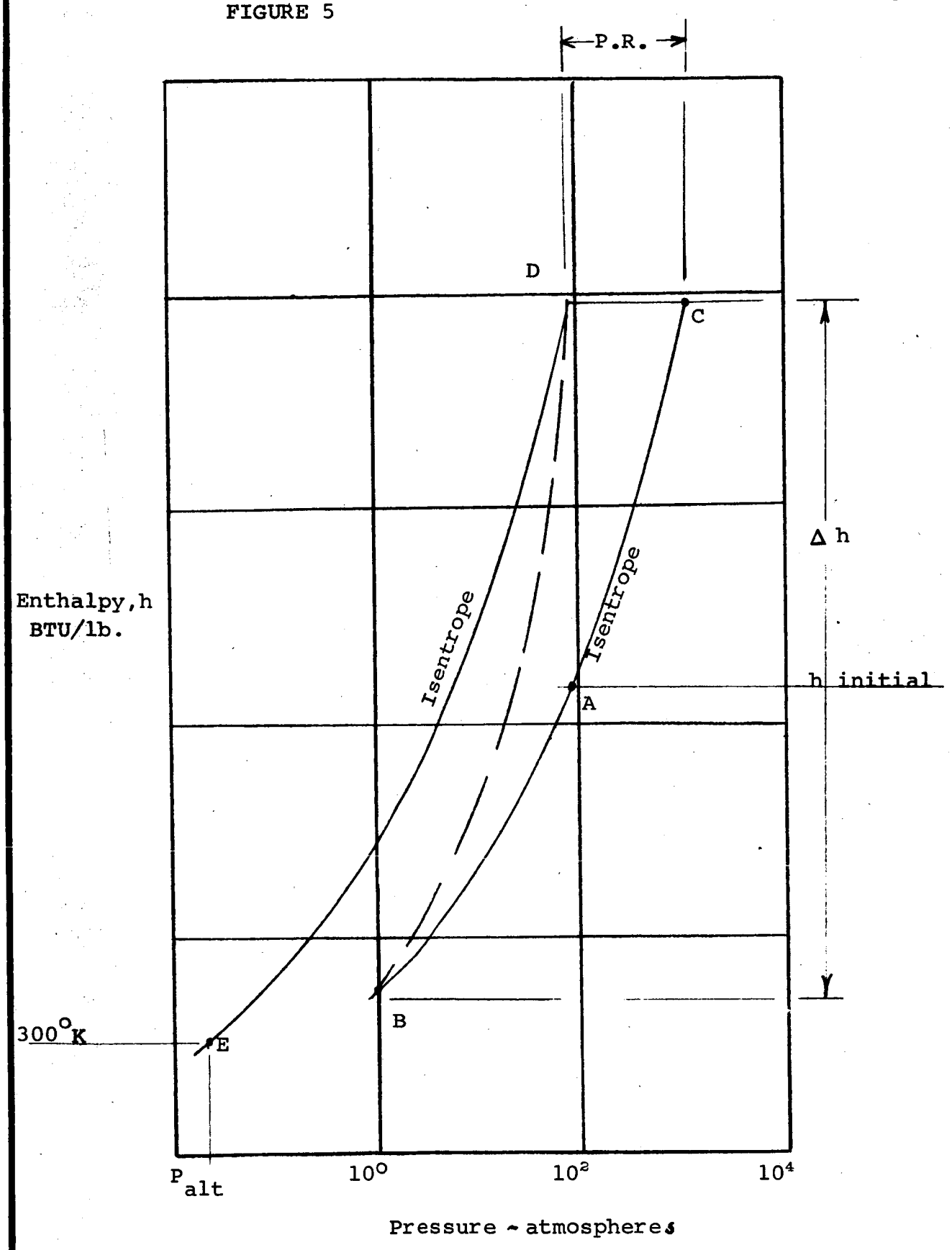
P.R.
D
C
Δ h
Enthalpy, h
BTU/lb.
Isentrope
Isentrope
h initial
A
B
300°K
E
P alt
10⁰
10²
10⁴
Pressure - atmospheres

FIGURE 6: Simulated Test Section Condition
Altitude vs Flow Velocity

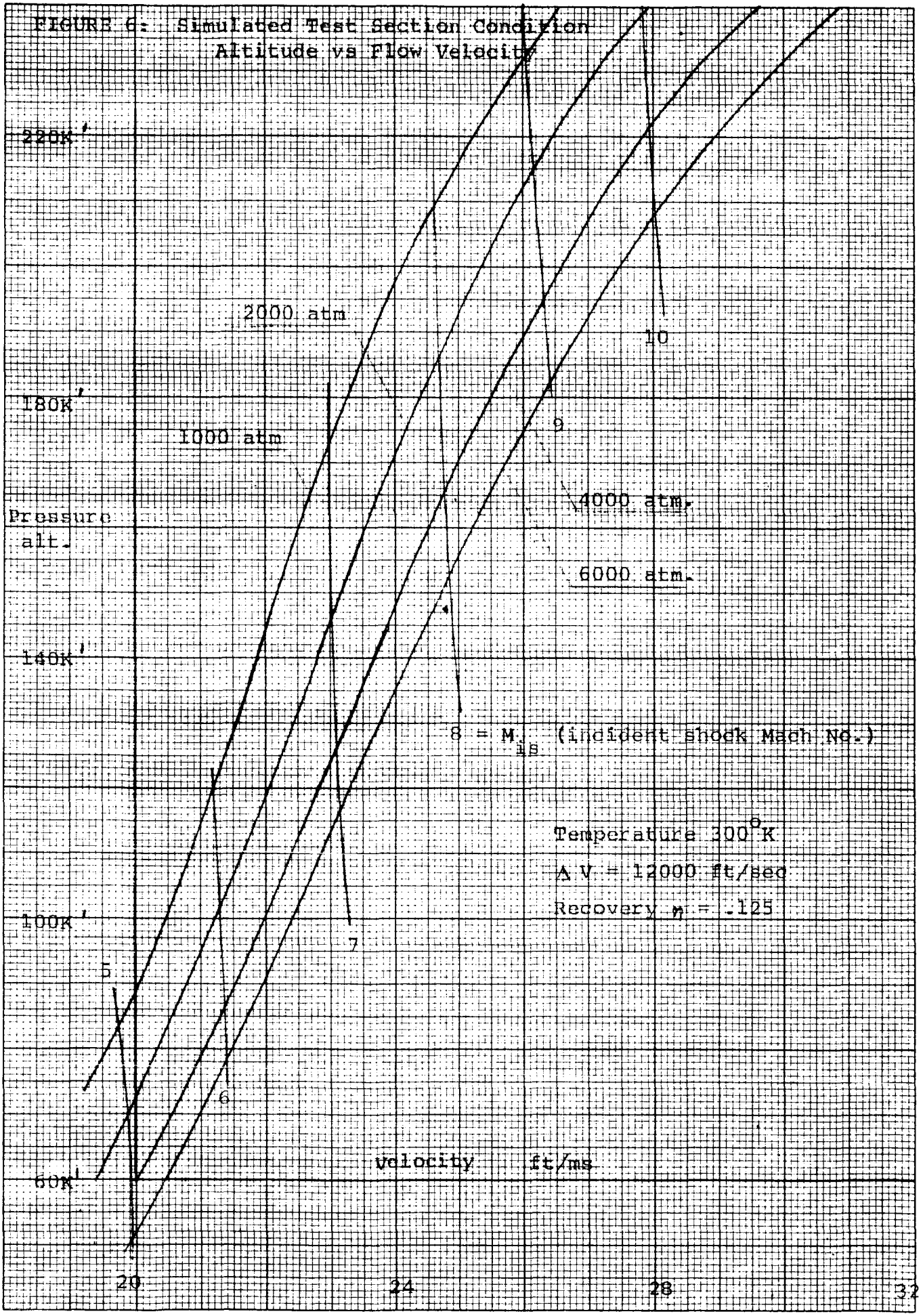

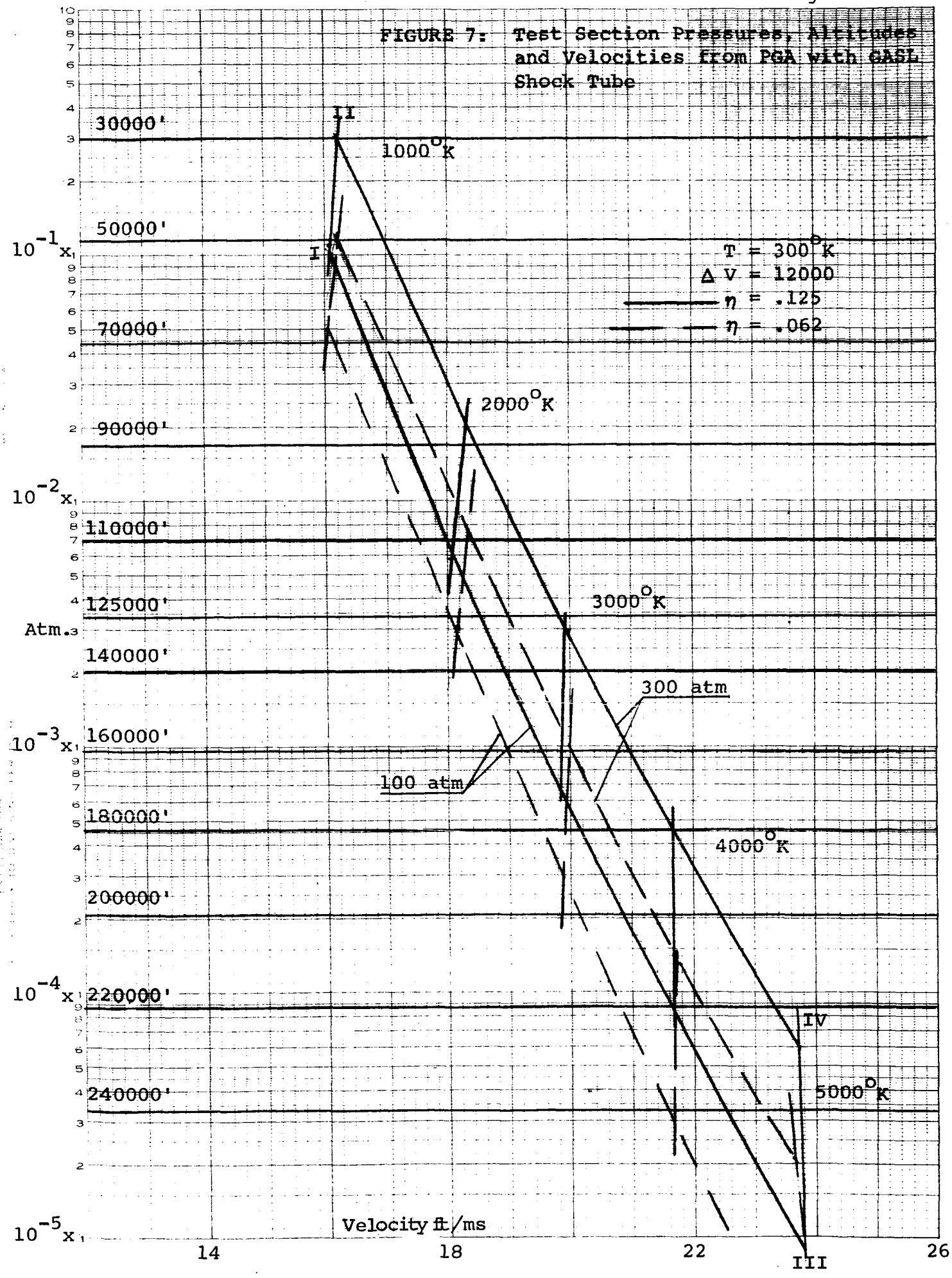

FIGURE 7: Test Section Pressures, Altitudes and Velocities from PGA with GASL Shock Tube

COMBUSTION CHAMBER

ACCELERATION C

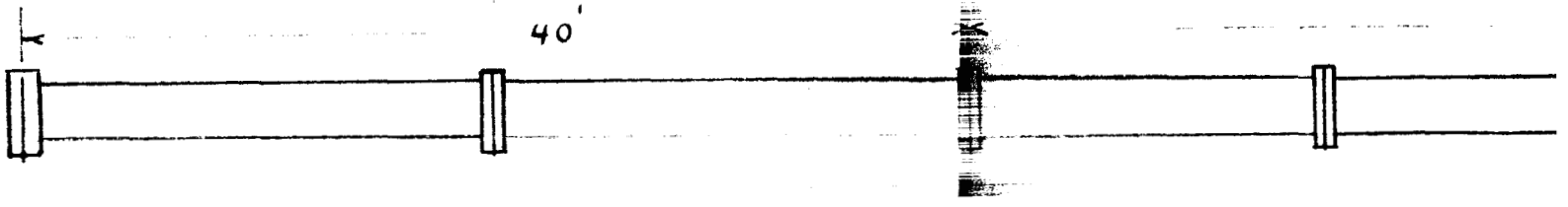

#1

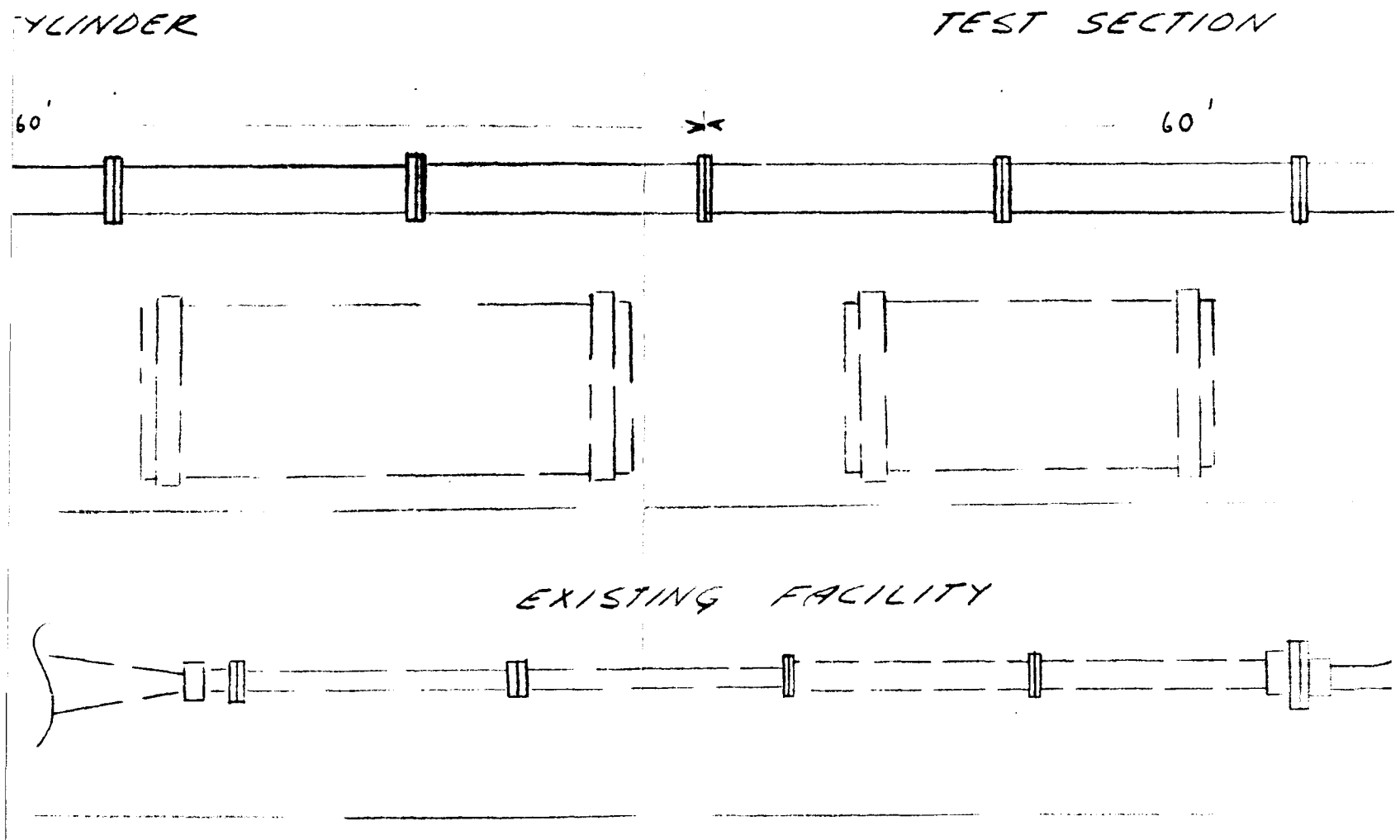
YCINDER
TEST SECTION
60'
60'
EXISTING FACILITY

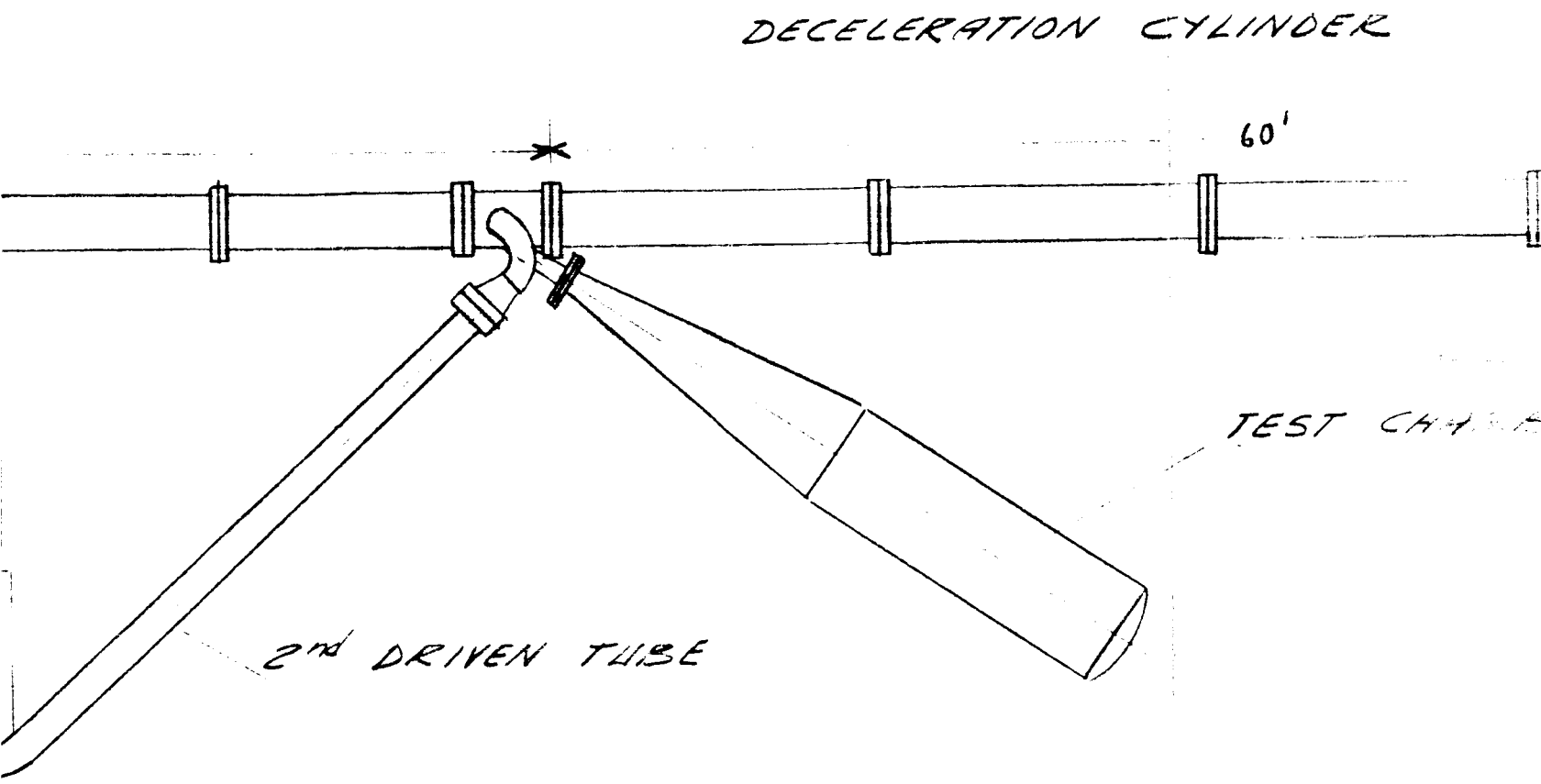

FIGURE 8

#3

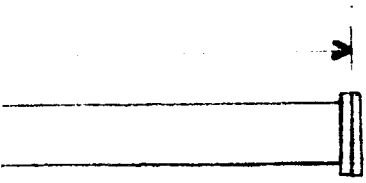

ER

CILITY LAYOUT

#4

FIGURE 9 - PISTON ACCELERATION TRAJECTORY

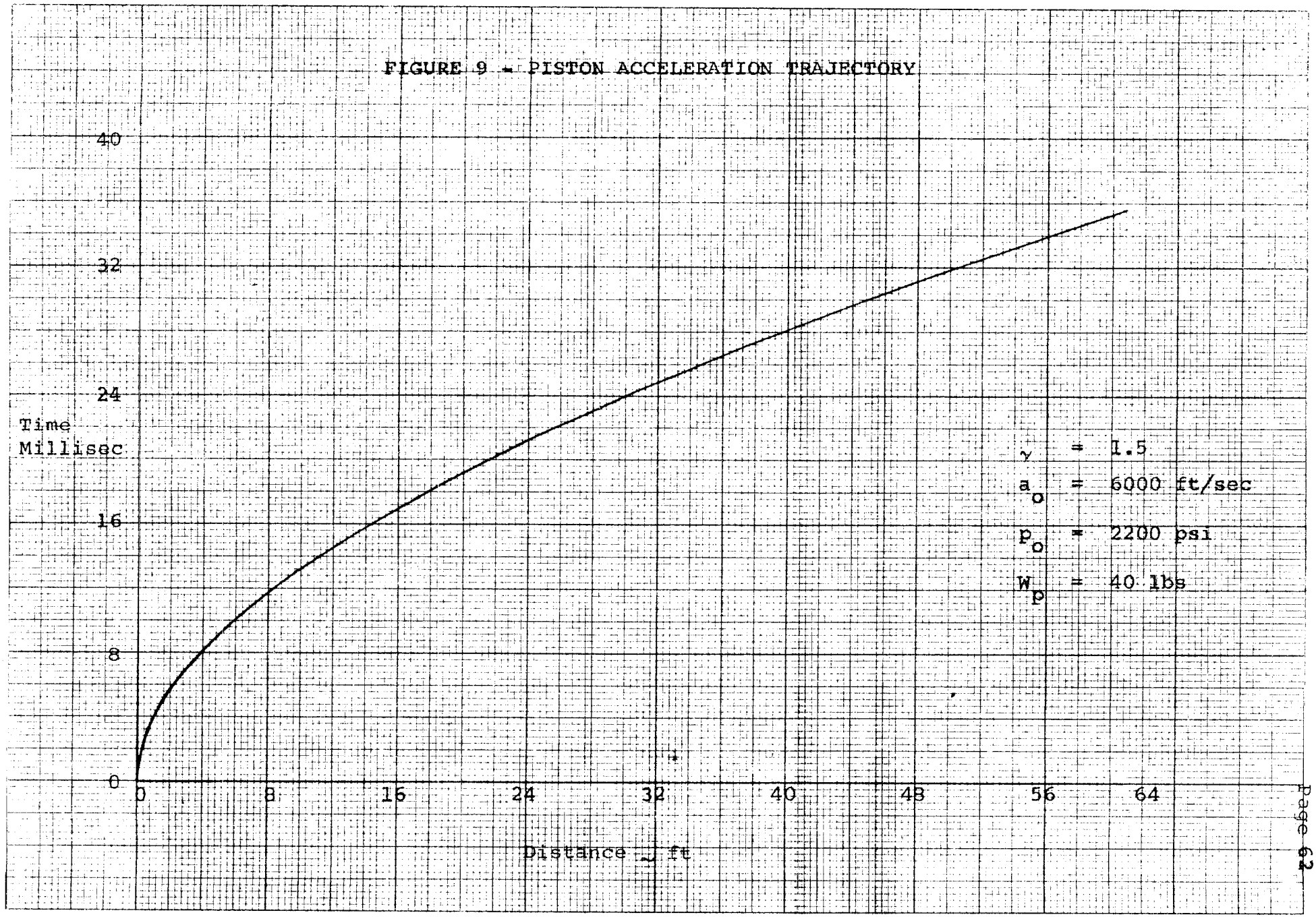

FIGURE 10 - PISTON DECELERATION TRAJECTORY
Distance - ft
0
10
20
30
40
50
60
50
40
30
20
10
0

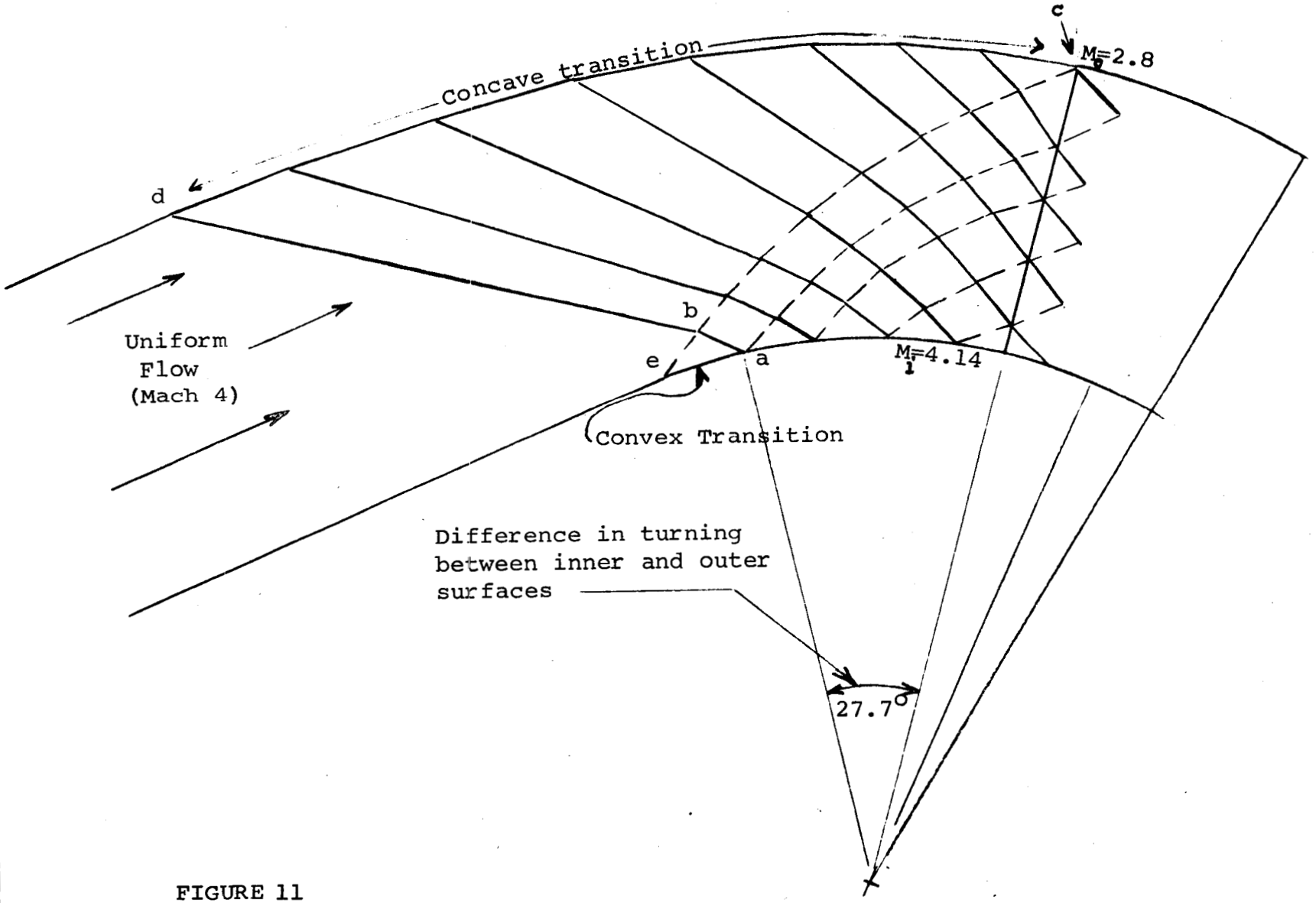
c
Concave transition
M_c=2.8
d
b
Uniform
Flow
(Mach 4)
e
a
M_1=4.14
Convex Transition
Difference in turning
between inner and outer
surfaces
27.7°

FIGURE 11

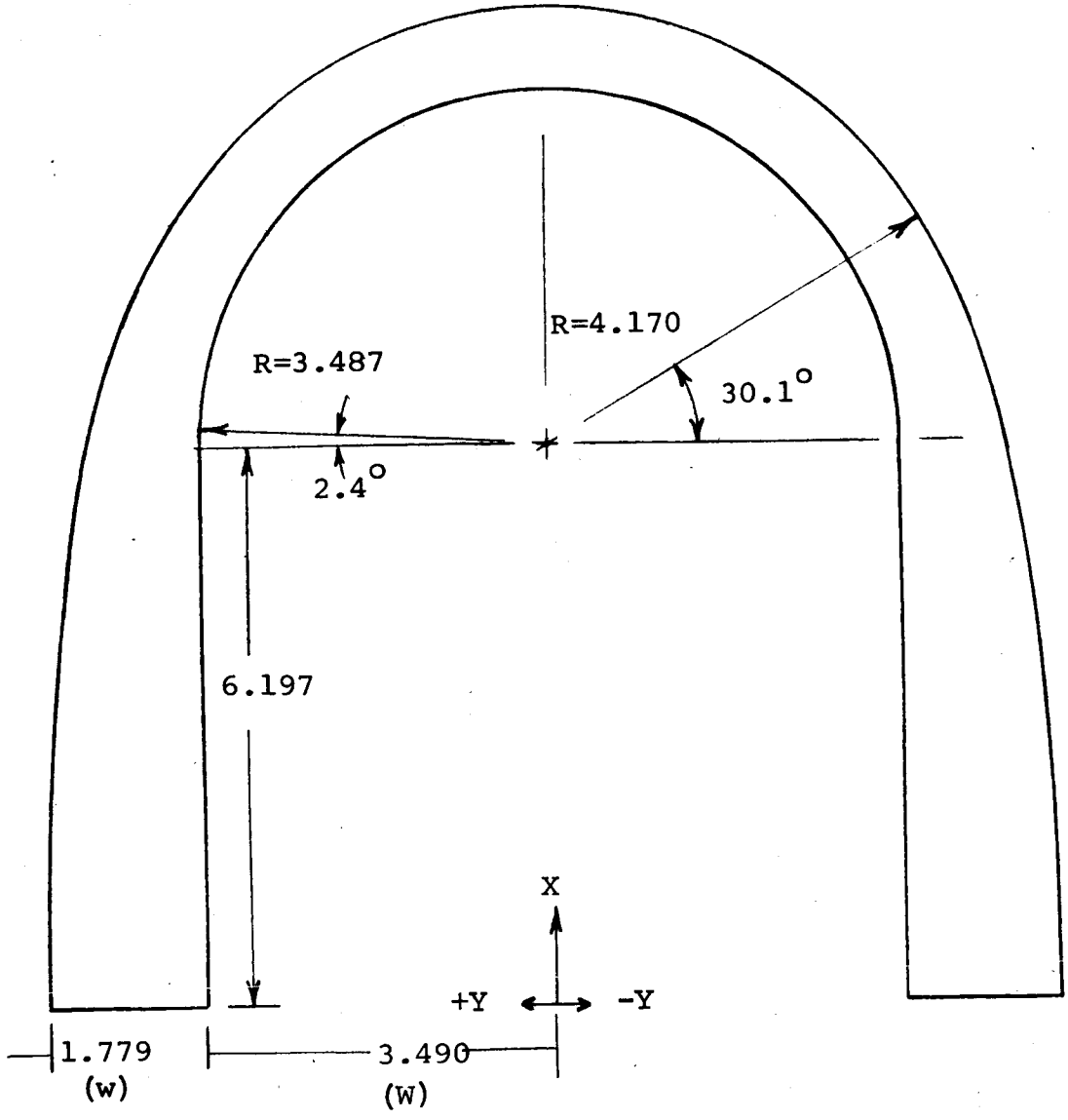

Figure 12. 180° Turning Passage

Figure 15 - Photograph of 180° Test Passage

Figure 14

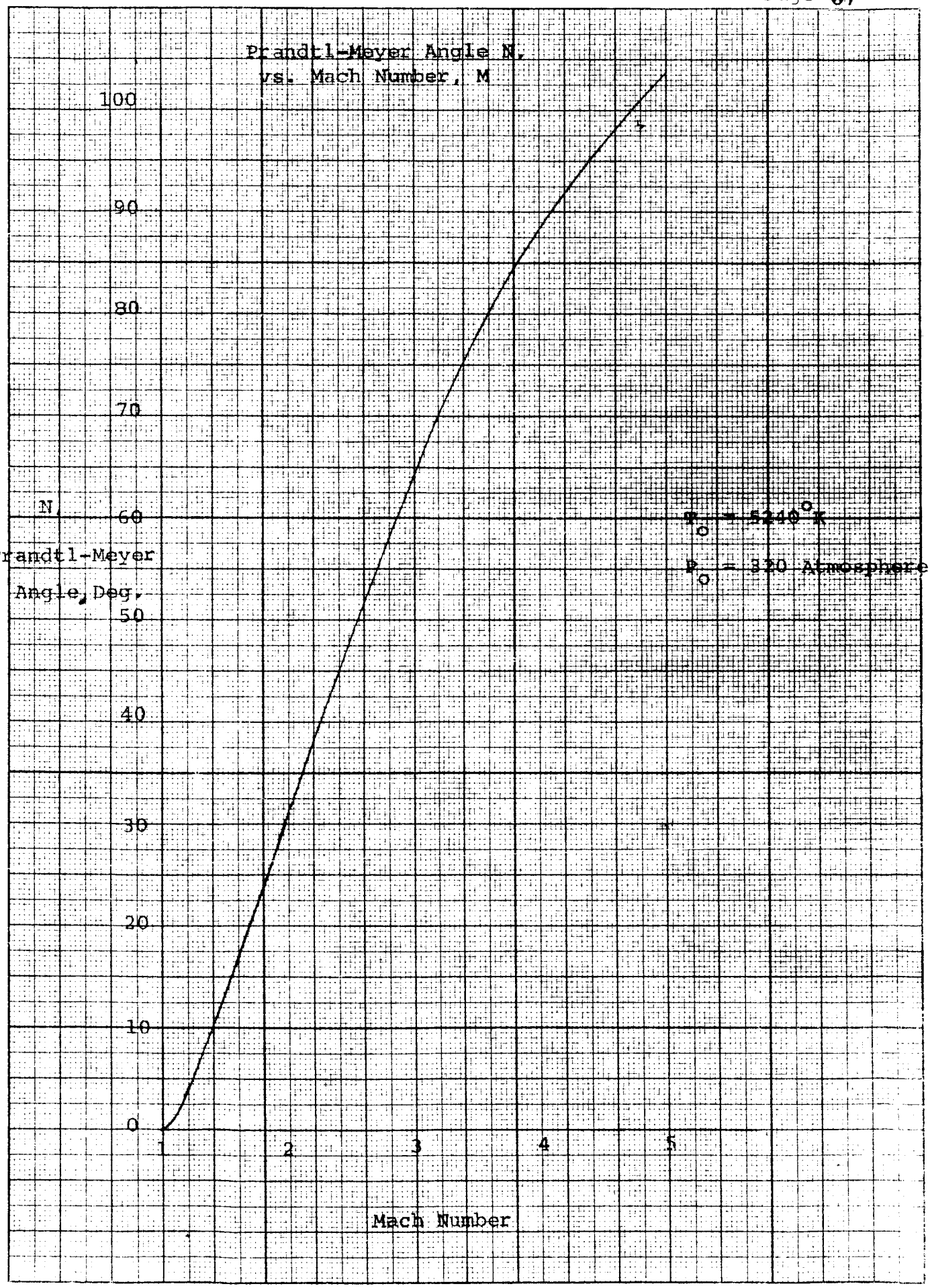
Prandtl-Meyer Angle N,
vs. Mach Number, M
100
90
80
70
N,
60
Prandtl-Meyer
Angle, Deg.
50
40
30
20
10
0
1
2
3
4
5
Mach Number
T_o = 5240°K
P_o = 320 Atmospheres

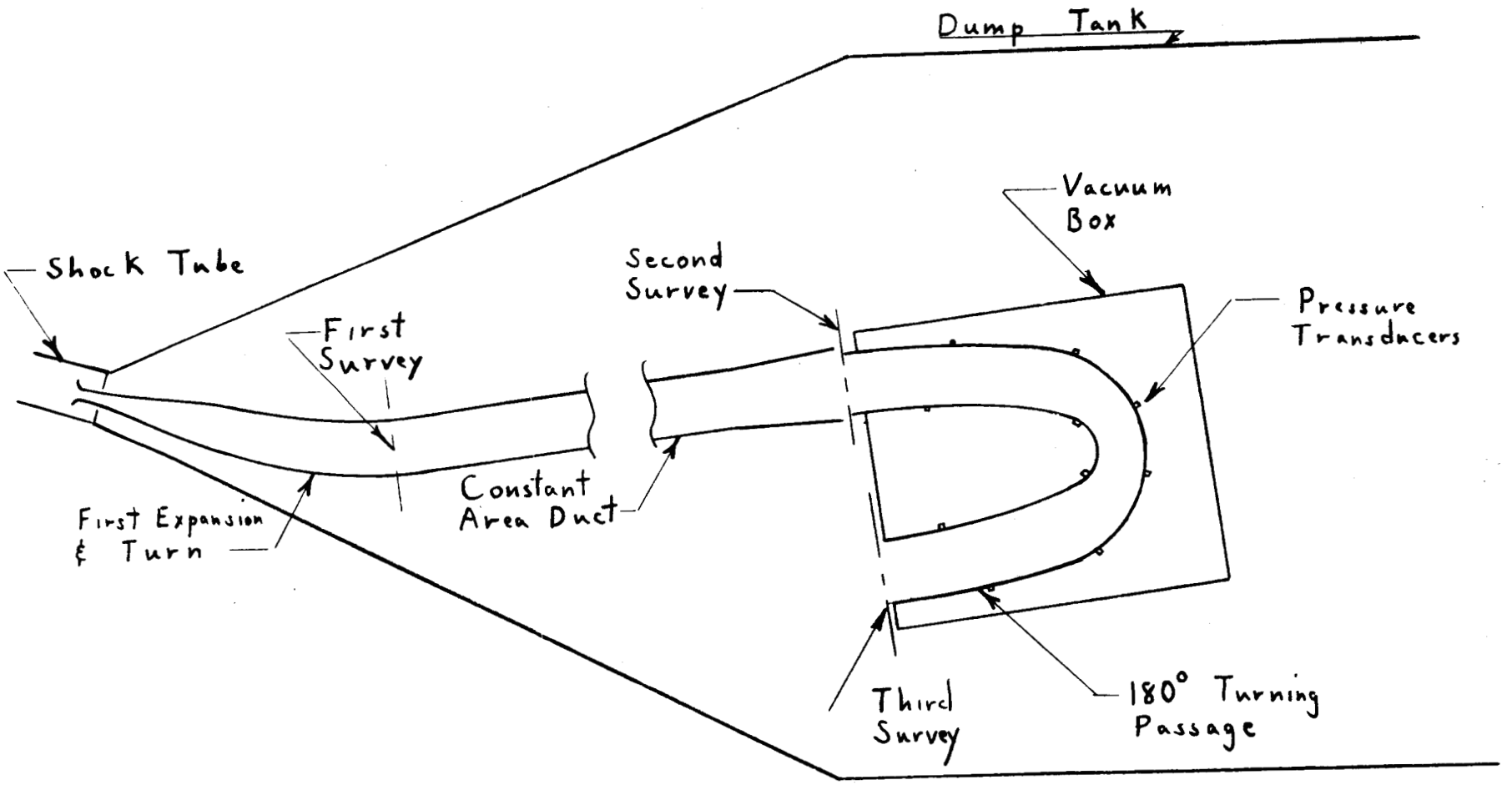

FIGURE 16. SCHEMATIC OF TEST RIG

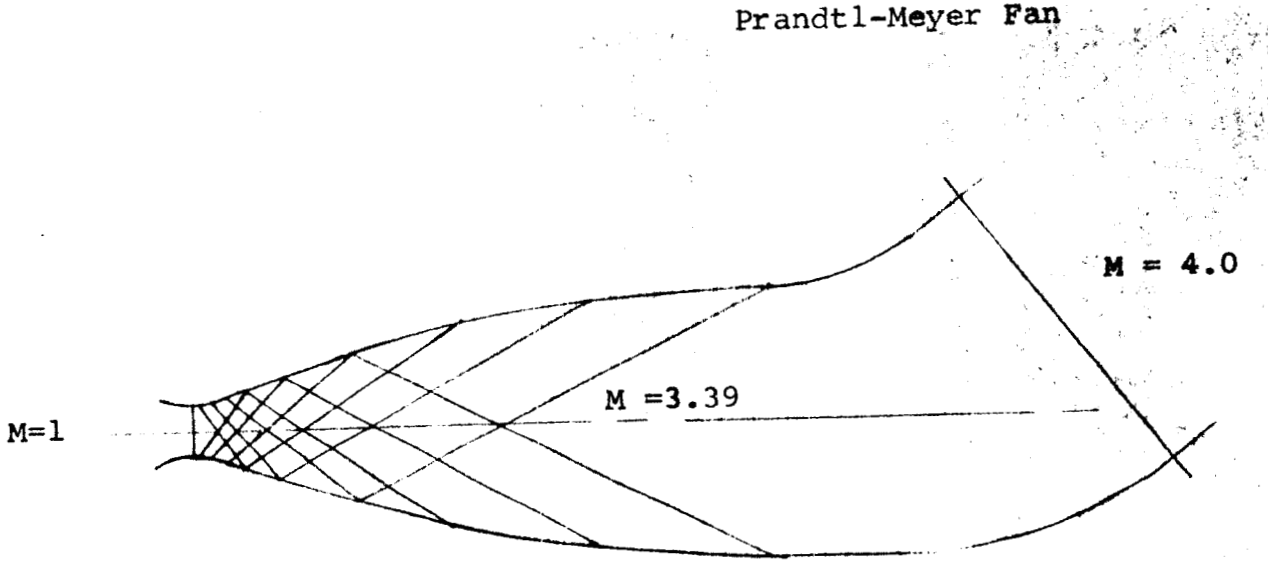

Figure 17 Characteristic System for First Turning Passage

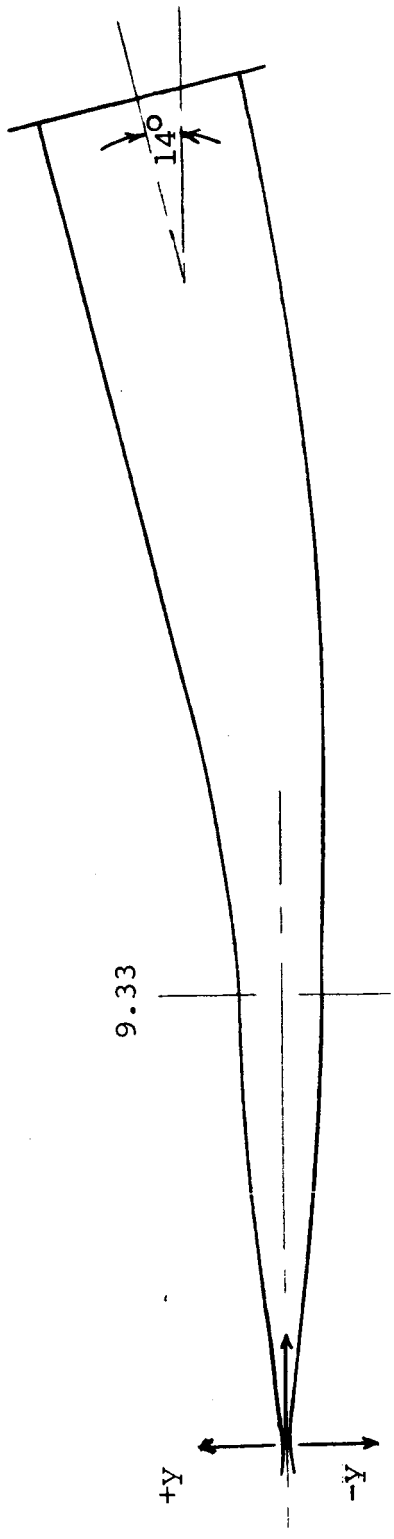

Figure 18 First Turning Passage

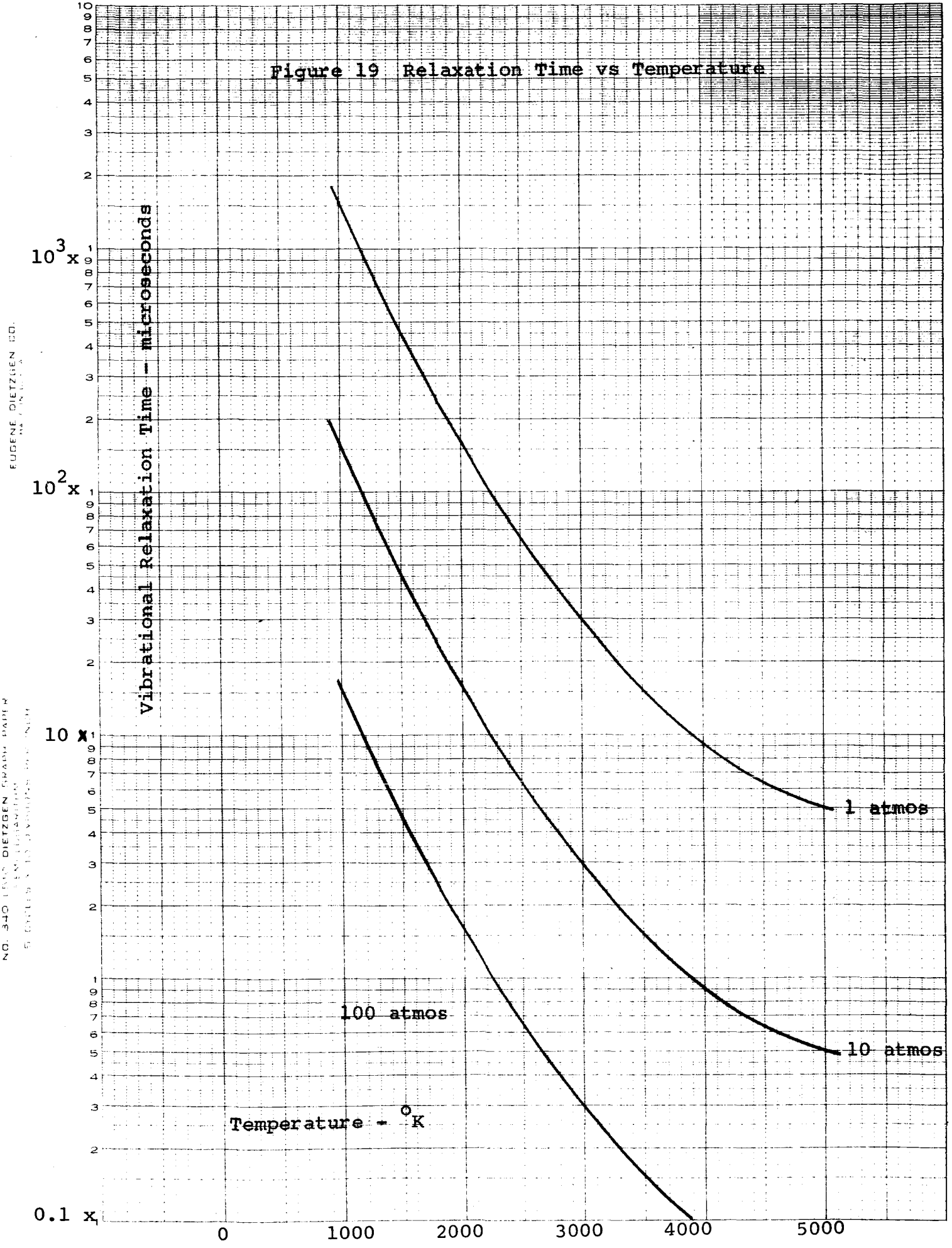
Figure 19 Relaxation Time vs Temperature
Vibrational Relaxation Time - microseconds
10^3 x
10^2 x
10 x
0.1 x
1 atmos
10 atmos
100 atmos
Temperature - °K
0
1000
2000
3000
4000
5000

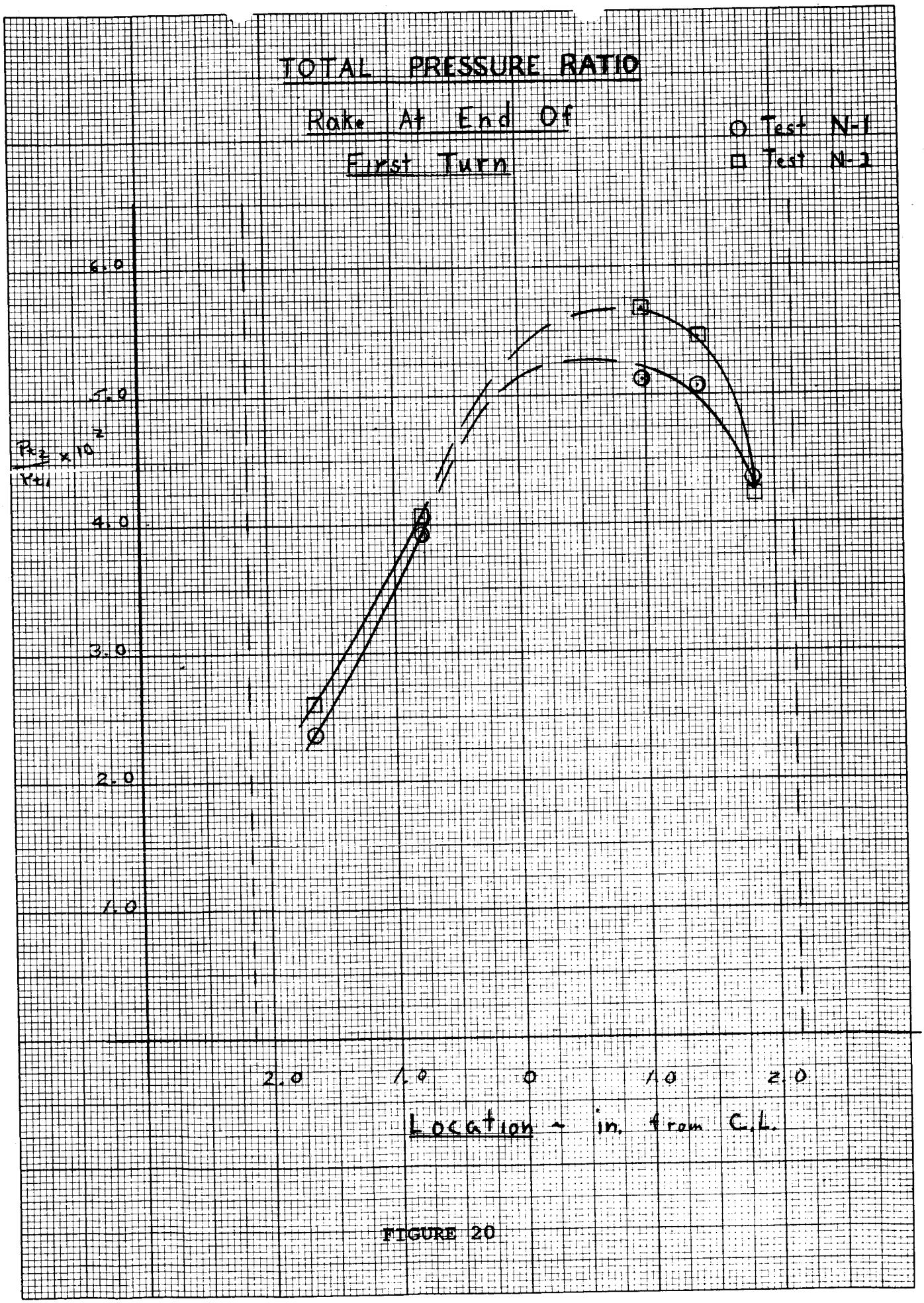

FIGURE 20

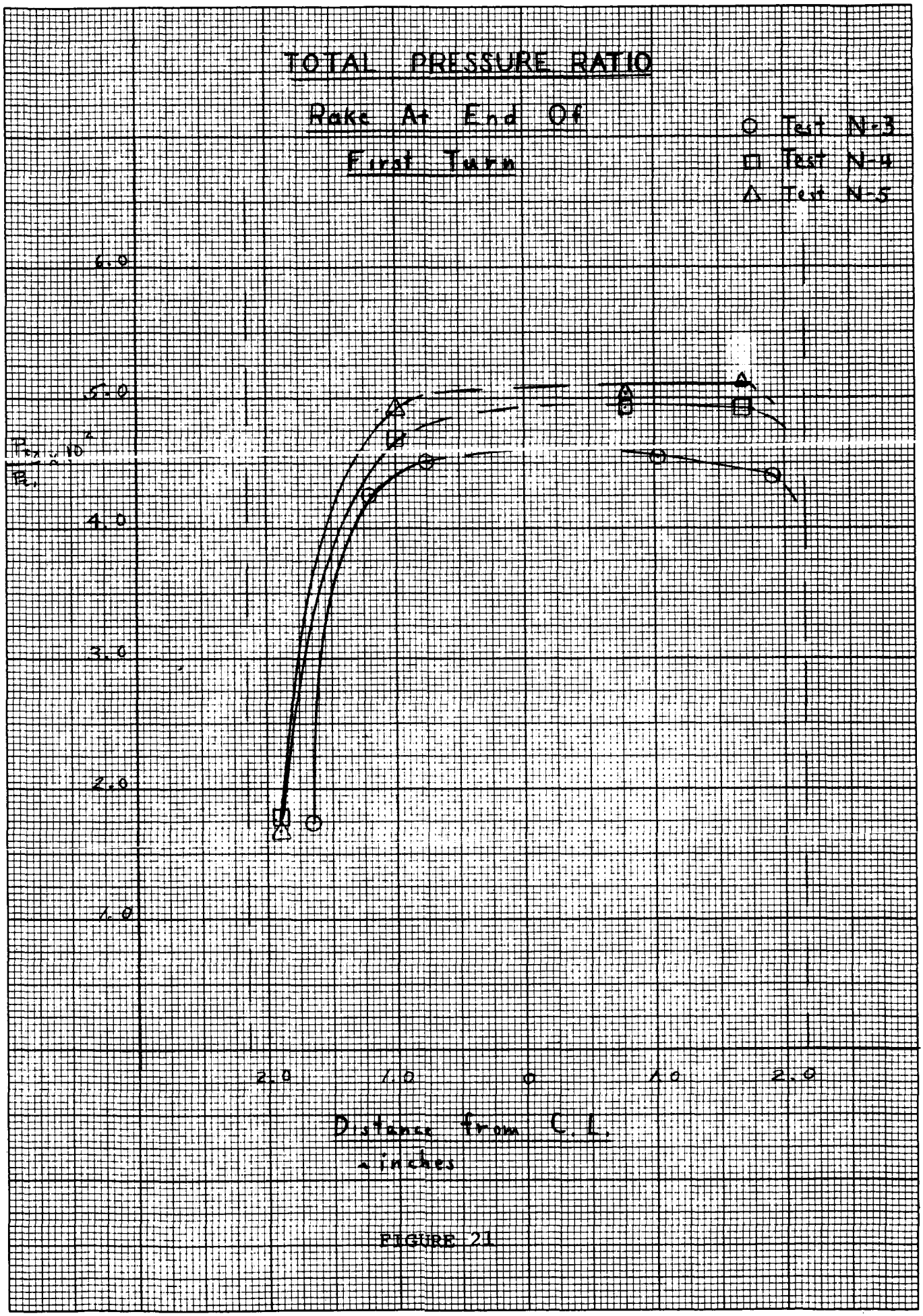

FIGURE 21

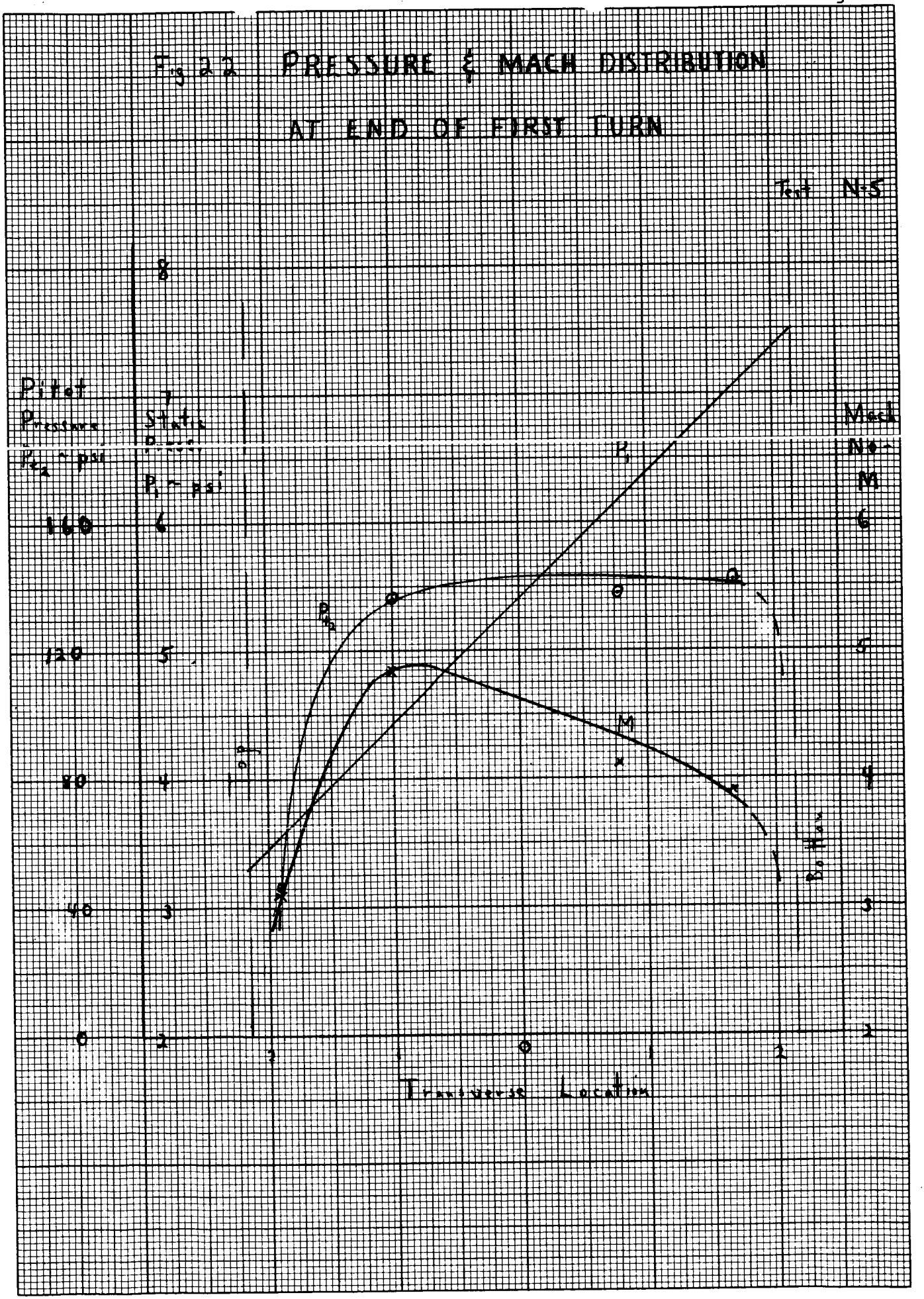

Fig 23. Pressure & Mach Distribution

At End of First Turn (with Jet)

Test N-7

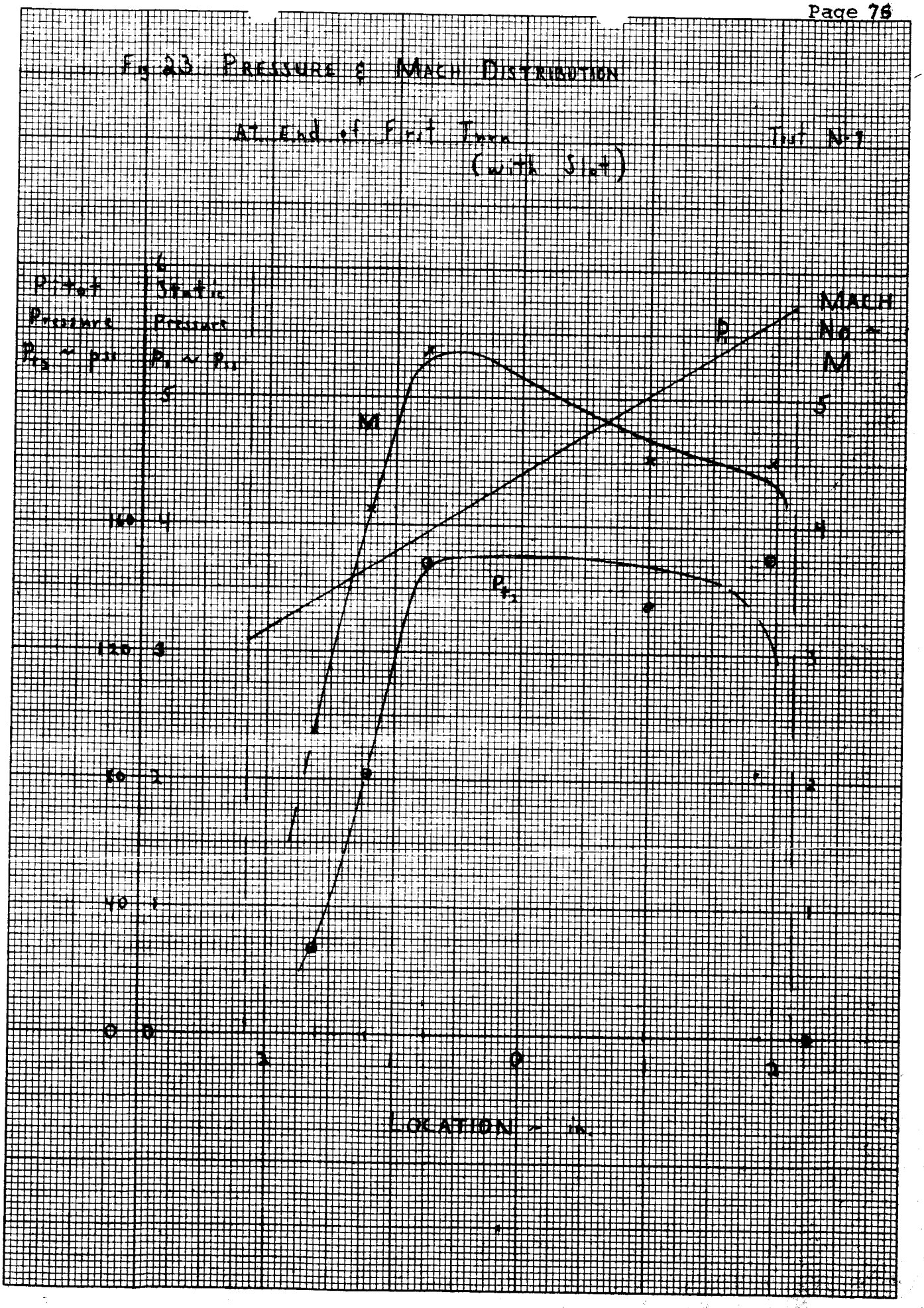

Fig. 24 MACH NUMBER & PRESSURE AT END OF FIRST TURN HOT TEST (N-11)

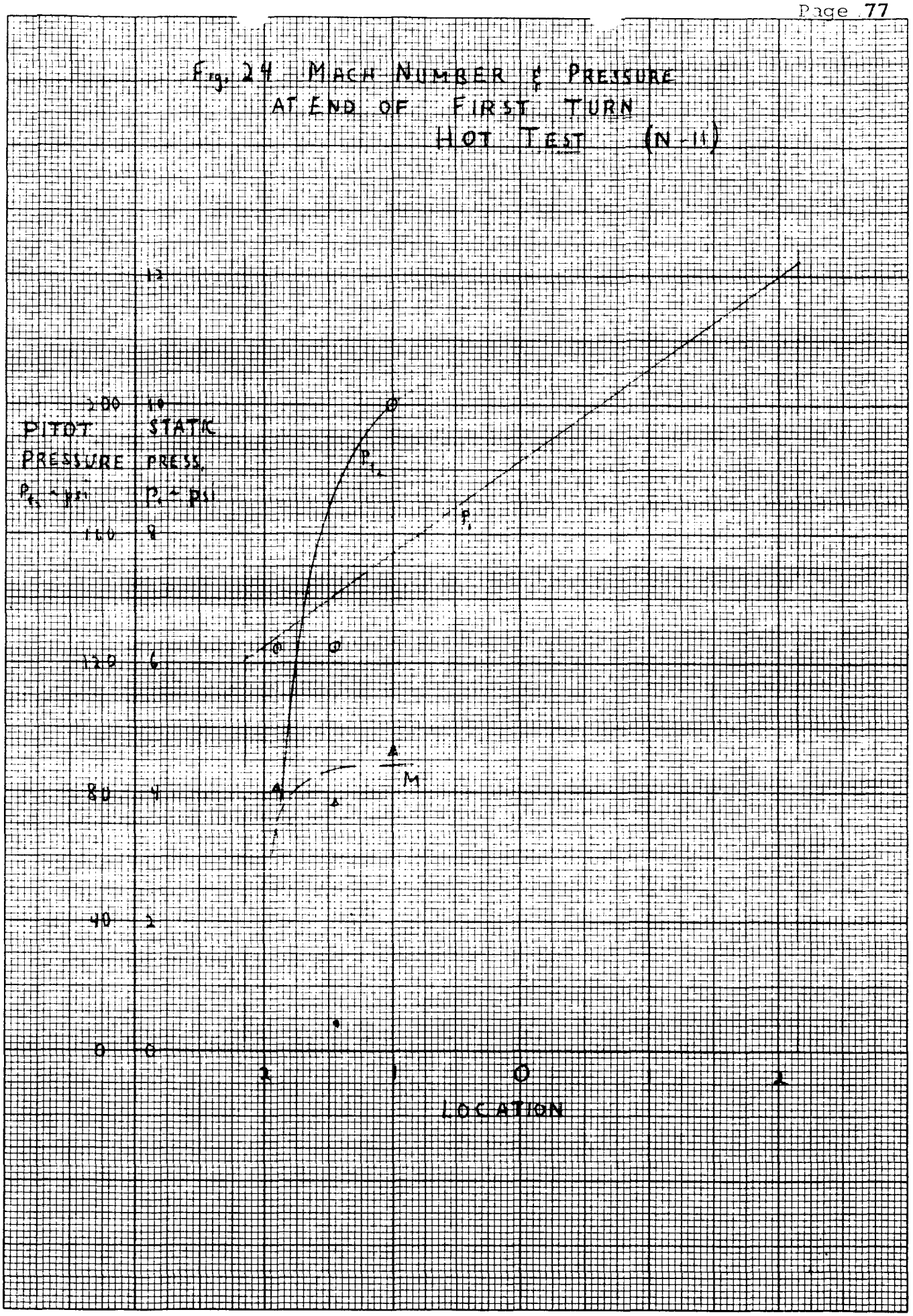

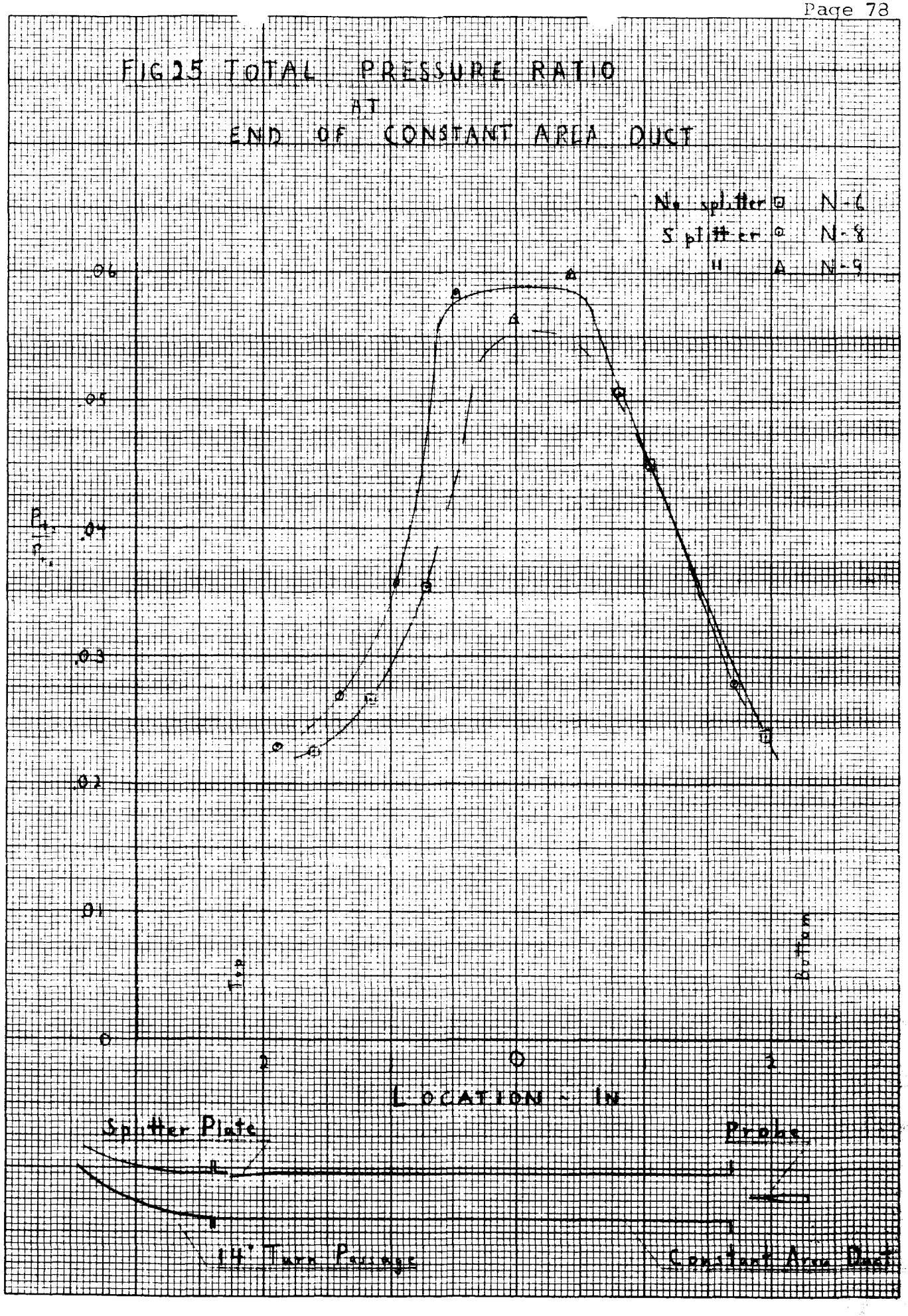
FIG 25 TOTAL PRESSURE RATIO
AT
END OF CONSTANT AREA DUCT
No splitter □ N-6
Splitter ○ N-8
" △ N-9
.06
.05
.04
.03
.02
.01
0
LOCATION - IN.
Splitter Plate
Probes
14° Turn Passage
Constant Area Duct

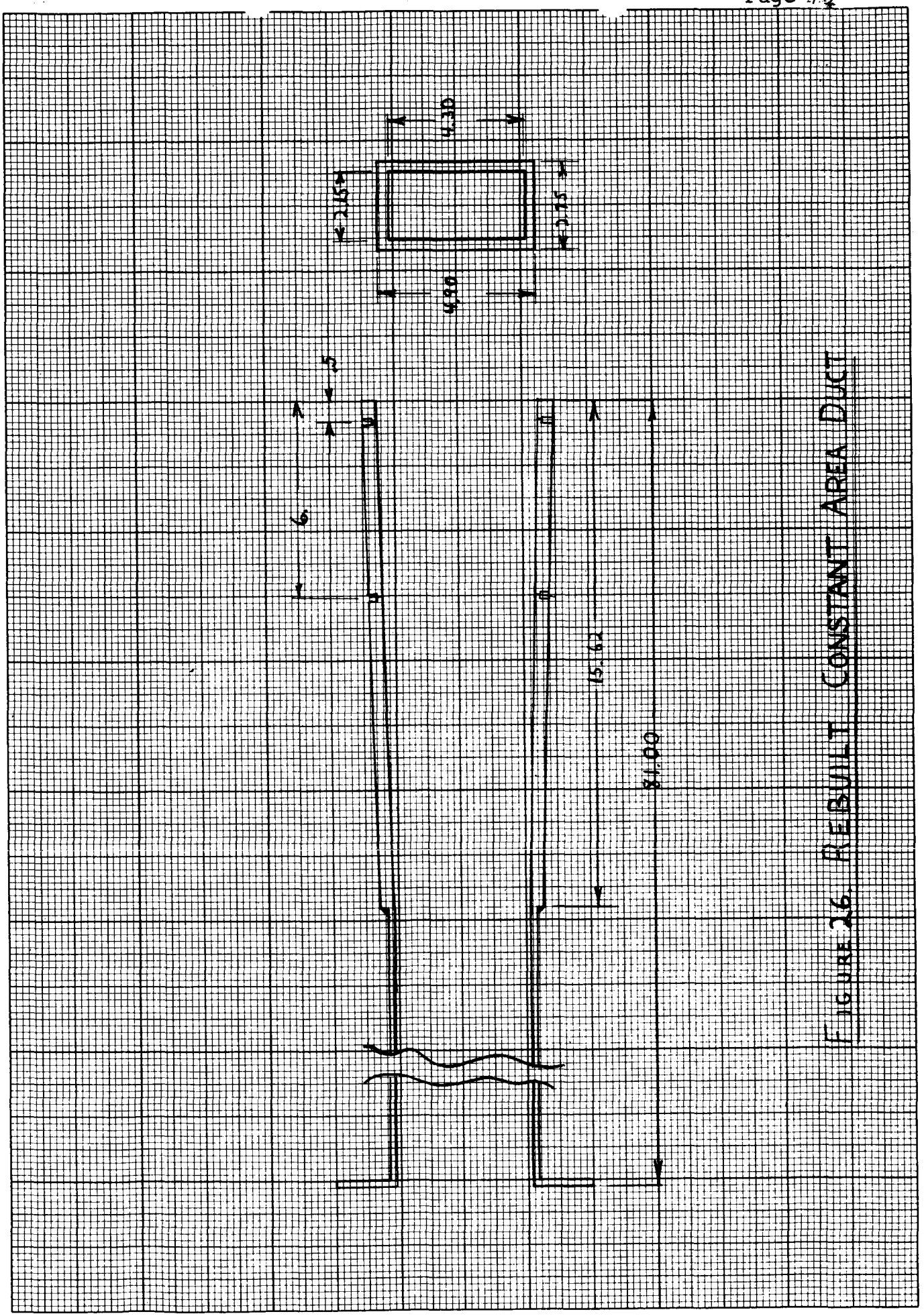

FIGURE 26. REBUILT CONSTANT AREA DUCT

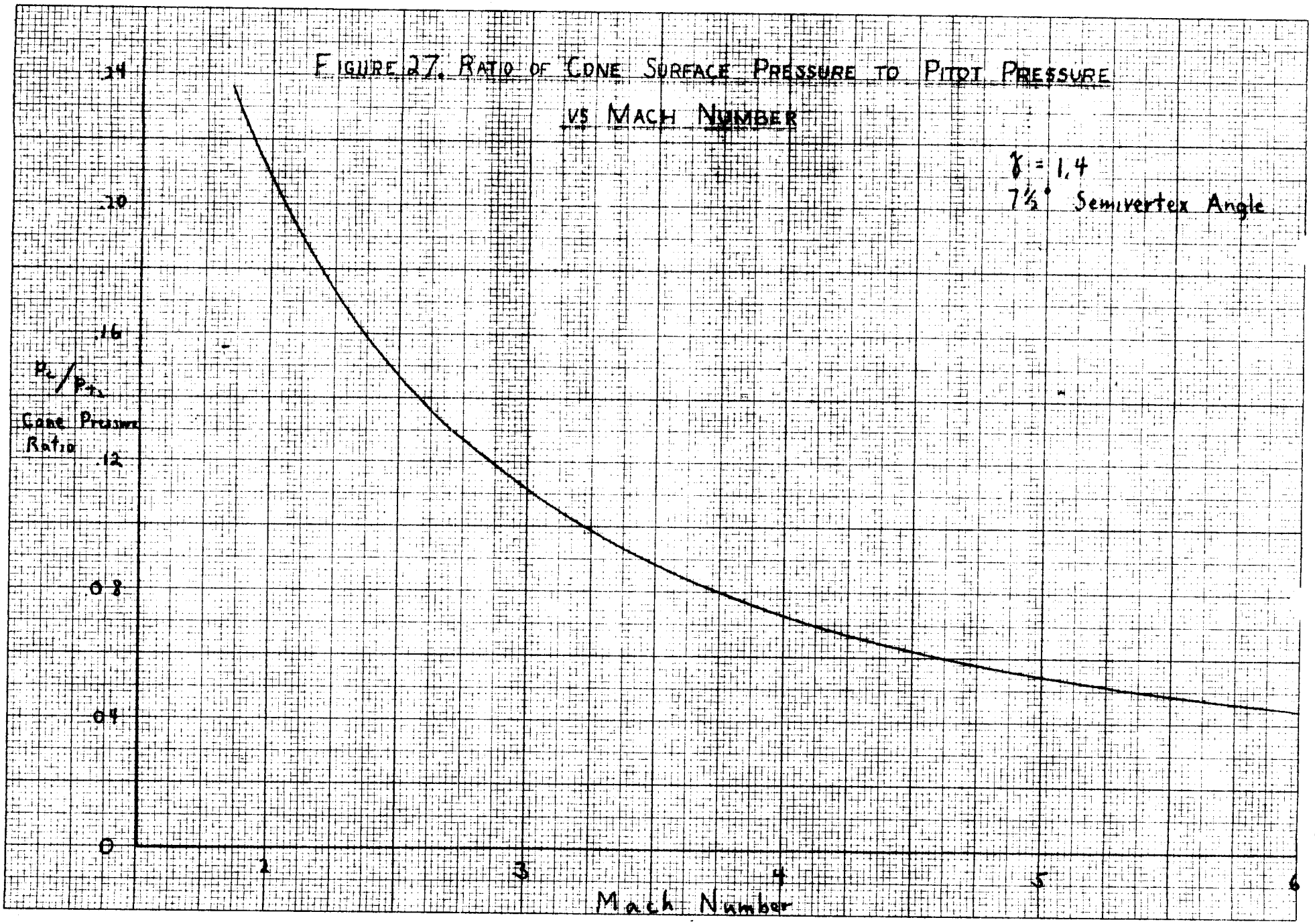

FIGURE 27. RATIO OF CONE SURFACE PRESSURE TO PITOT PRESSURE VS MACH NUMBER

FIGURE 28. STATIC PRESSURE RAKE

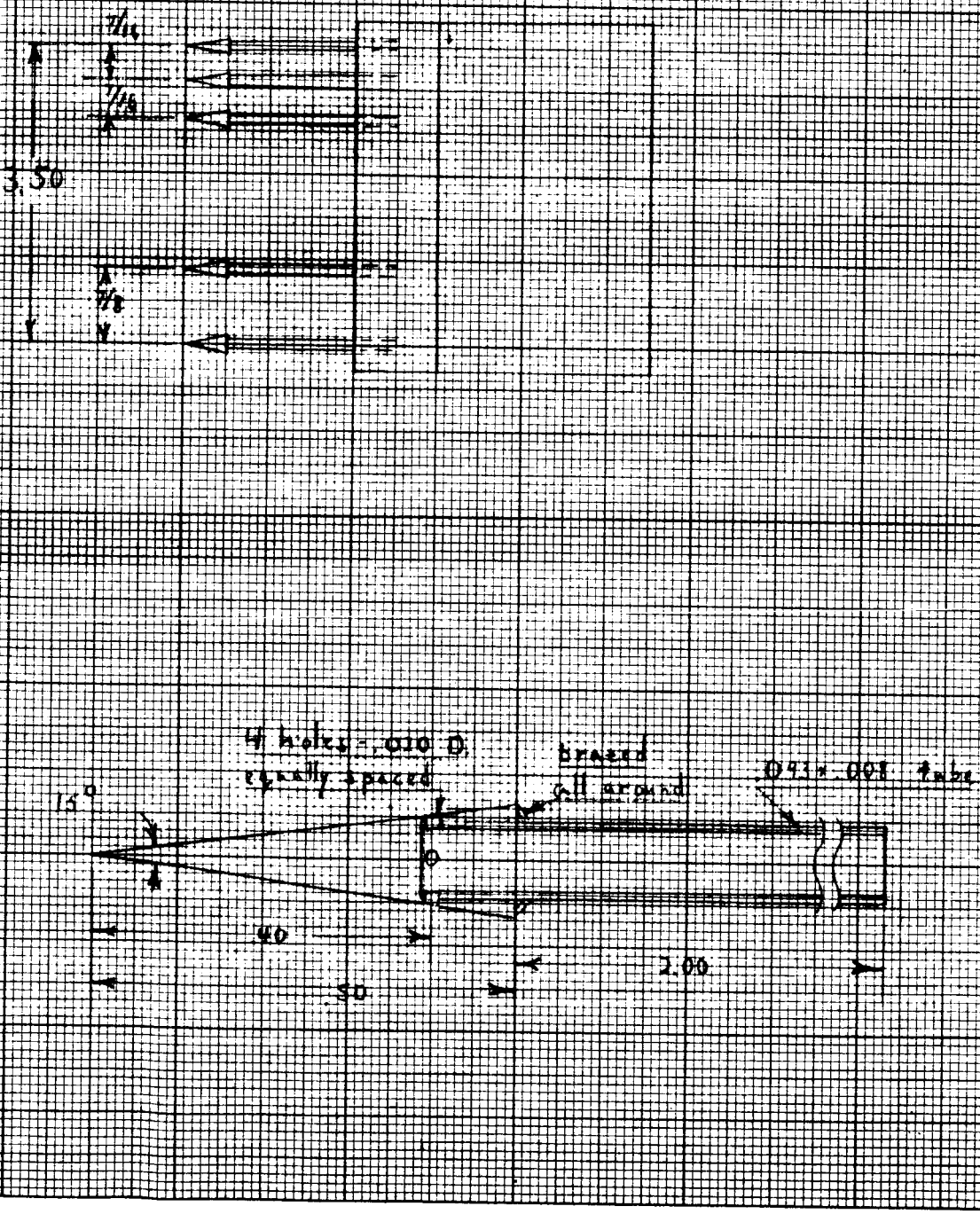

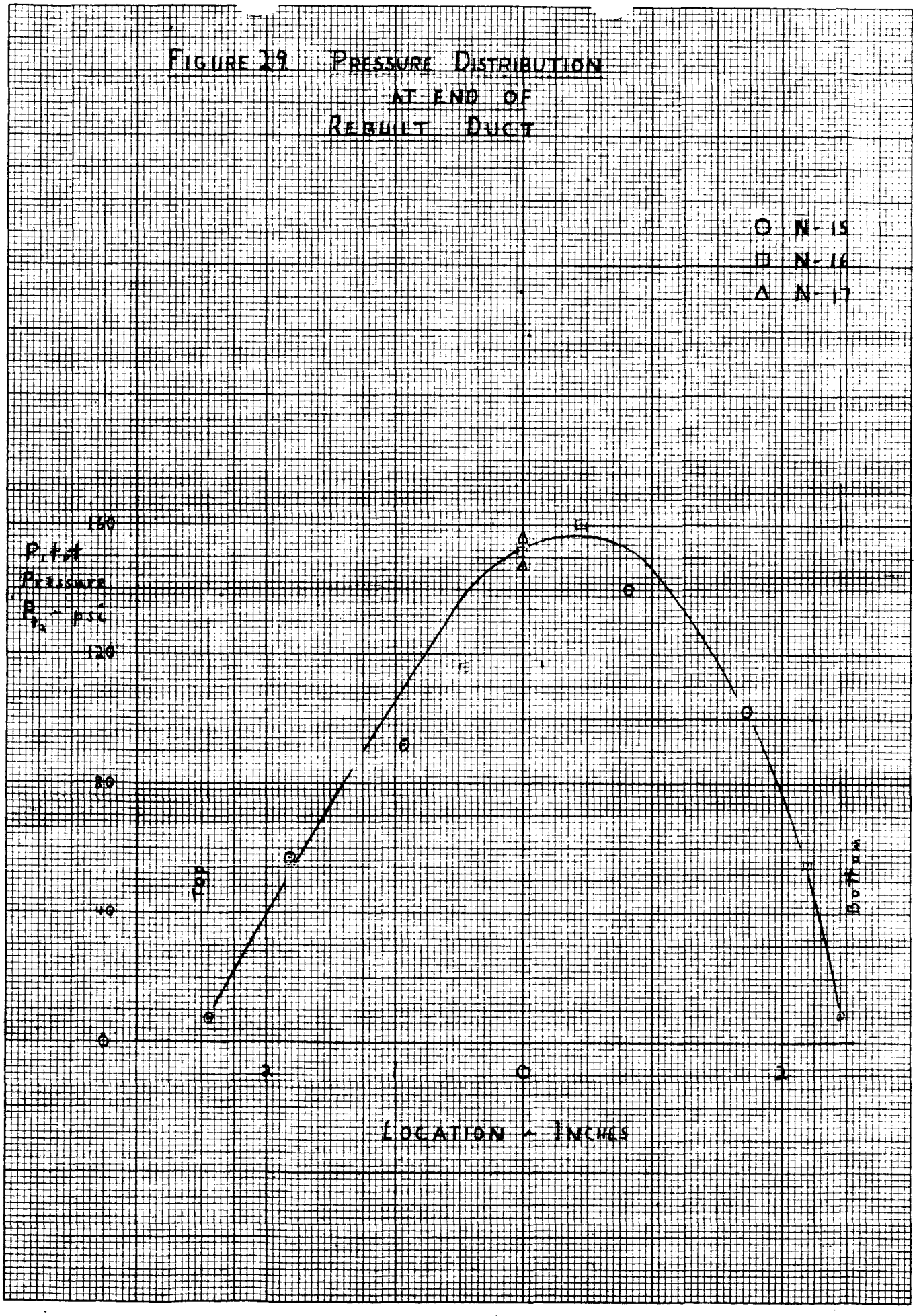
FIGURE 29. PRESSURE DISTRIBUTION AT END OF REBUILT DUCT
O N-15
□ N-16
Δ N-17
150
120
90
60
30
0
2
0
2
LOCATION - INCHES
Duct Wall

FIGURE 30. CONE PRESSURE DISTRIBUTION AT END OF CONSTANT AREA DUCT

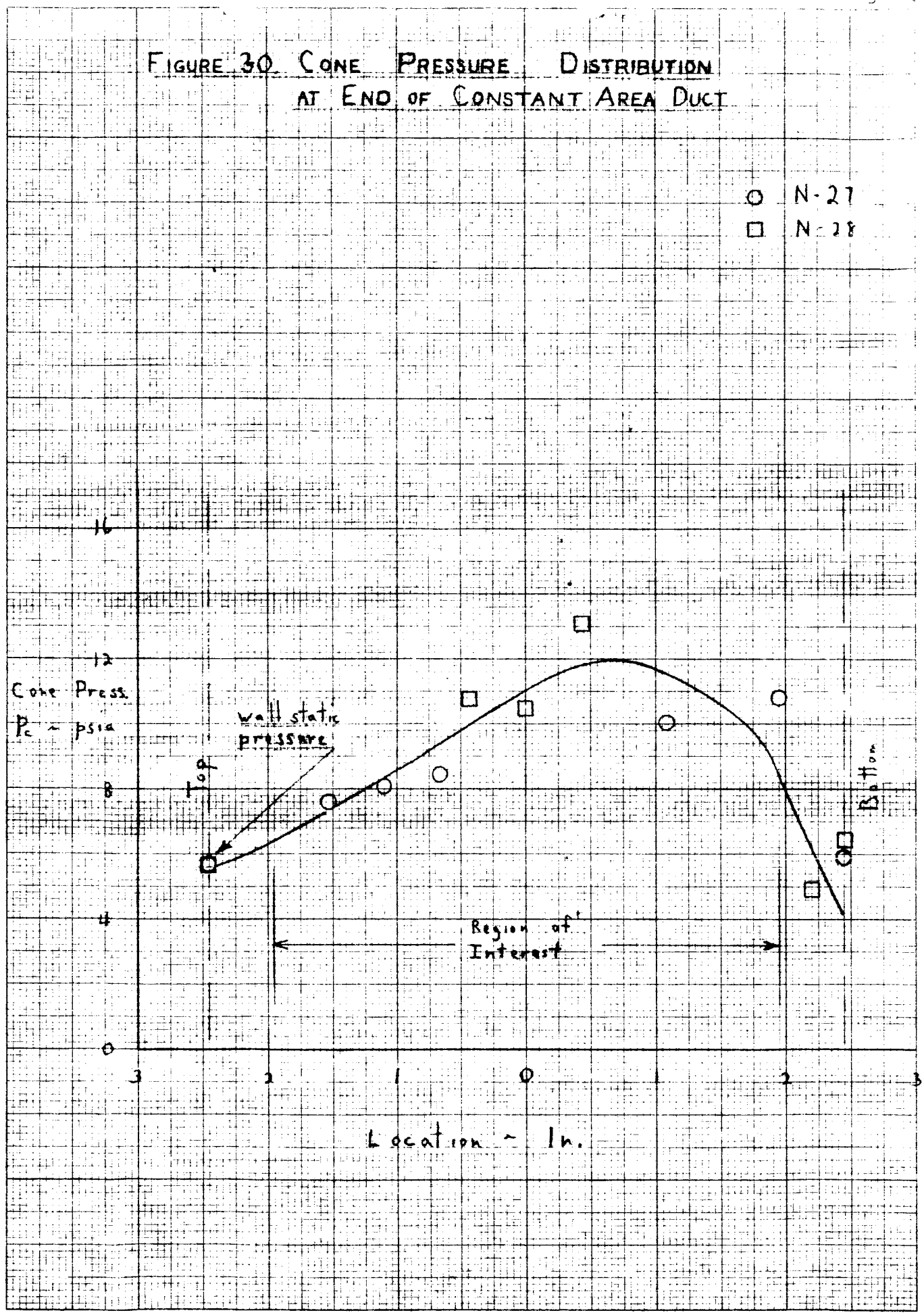

Figure 11. Mach Number & Stagnation Pressure at End of Constant Area Duct

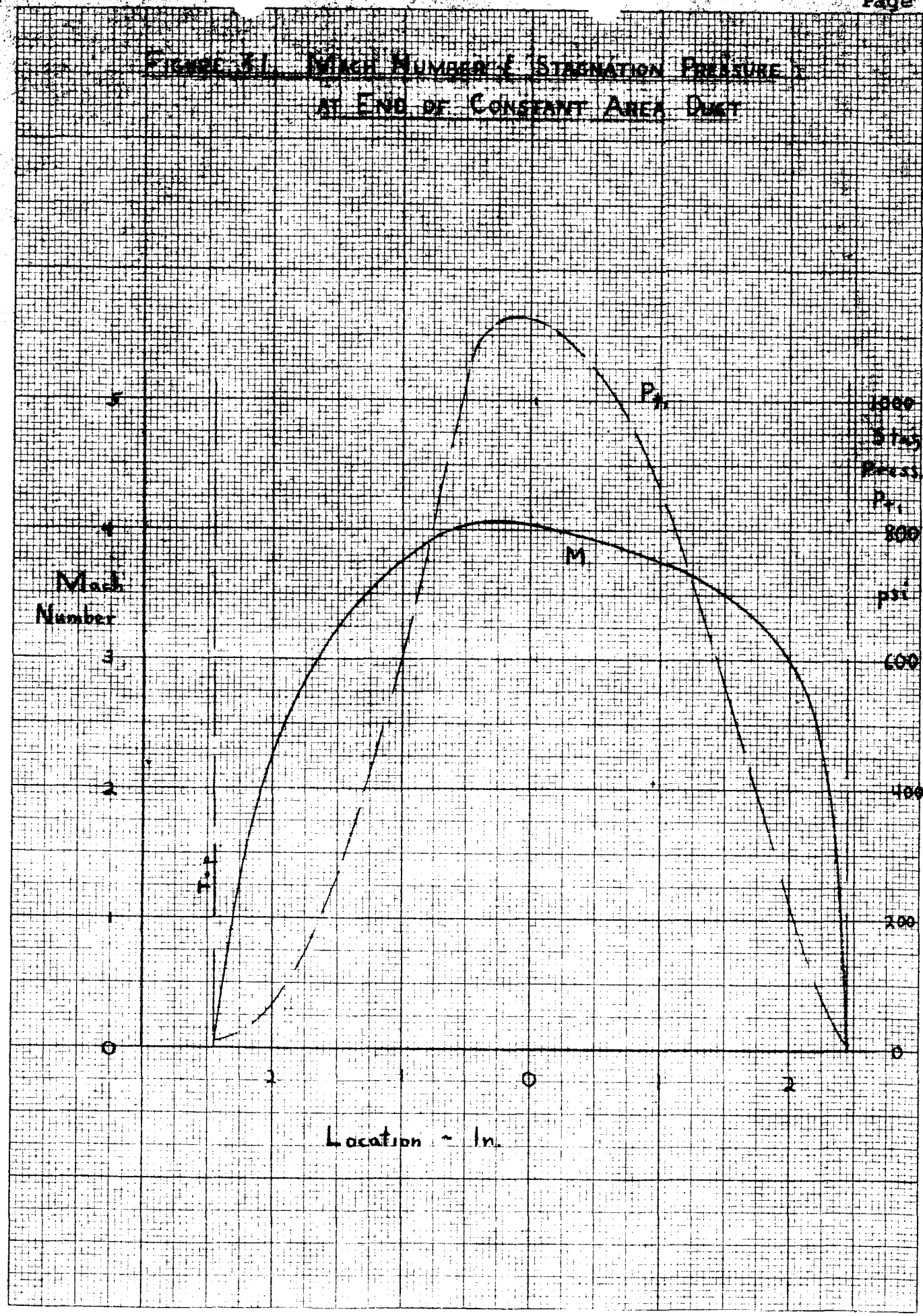

STATIC PRESSURE TRACE AT ENTRY TO 180° DUCT

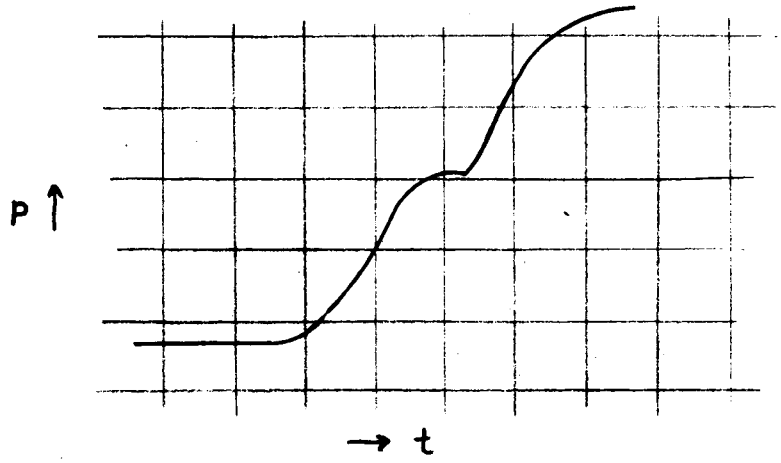

Trace at X on Figure 34

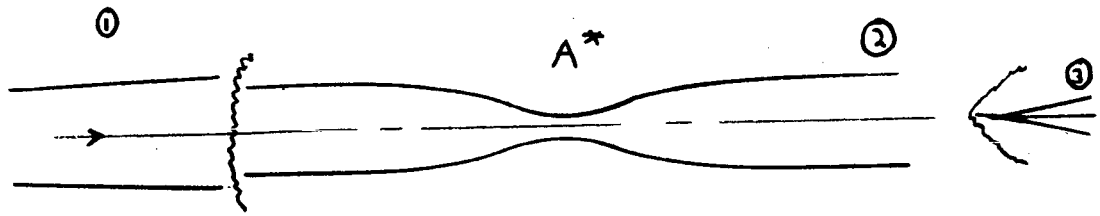

$M_1 \sim 4.6$

$P_{t_2} \sim 160$ psi (Test N-17)

$\frac{A_2}{A^*} \sim 2.5 \quad \therefore \quad M_2 \sim 2.45 \quad \therefore \quad \frac{P_{t_3}}{P_{t_2}} \sim .5$

FIGURE 32 UNSTARTED FLOW

FIGURE 33 PRESSURE DISTRIBUTION AT END OF 180° TURN PASSAGE

TEST N-18 ○
N-19 ✕

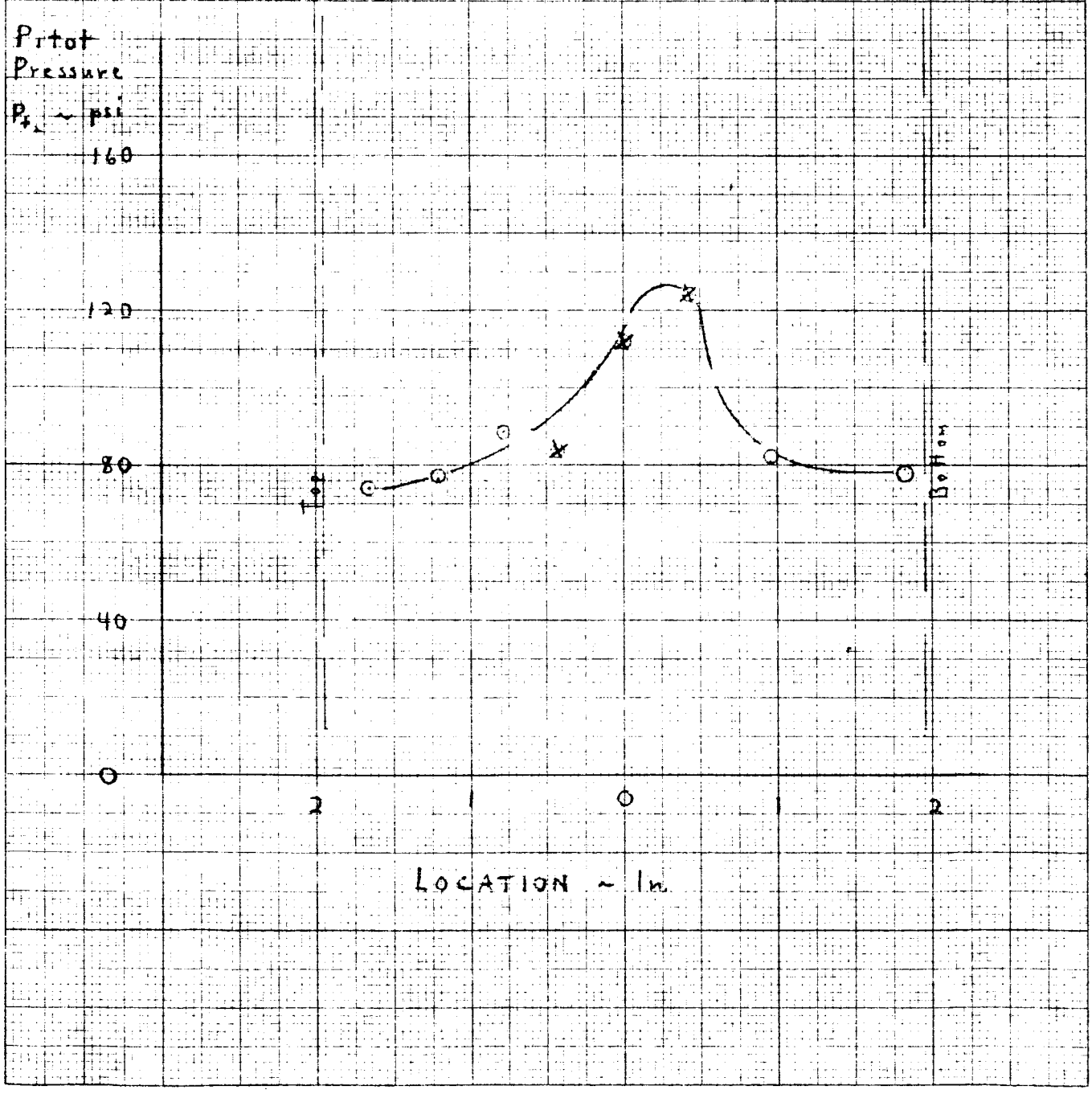

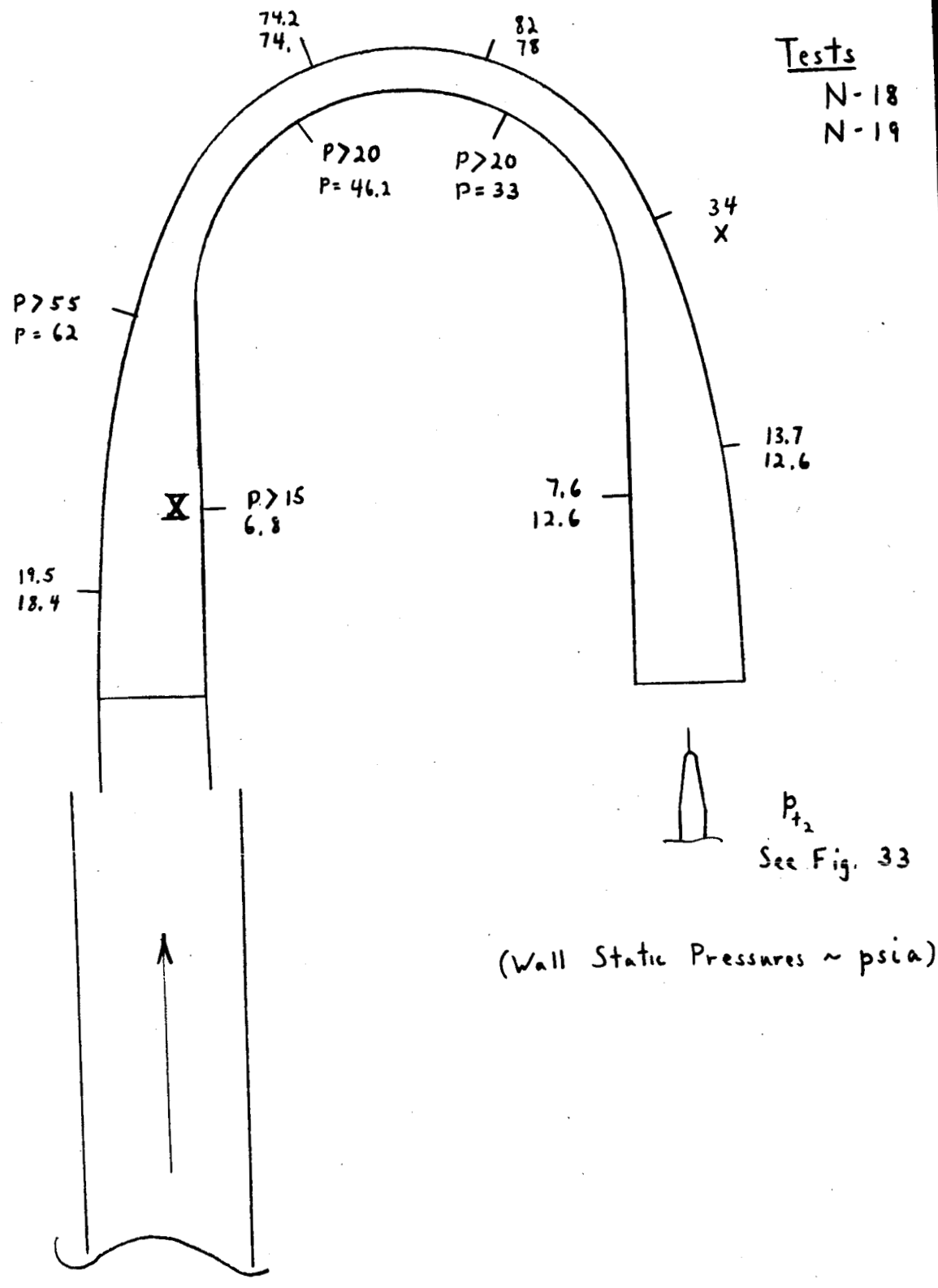

FIGURE 34. UNSTARTED DUCT PRESSURES

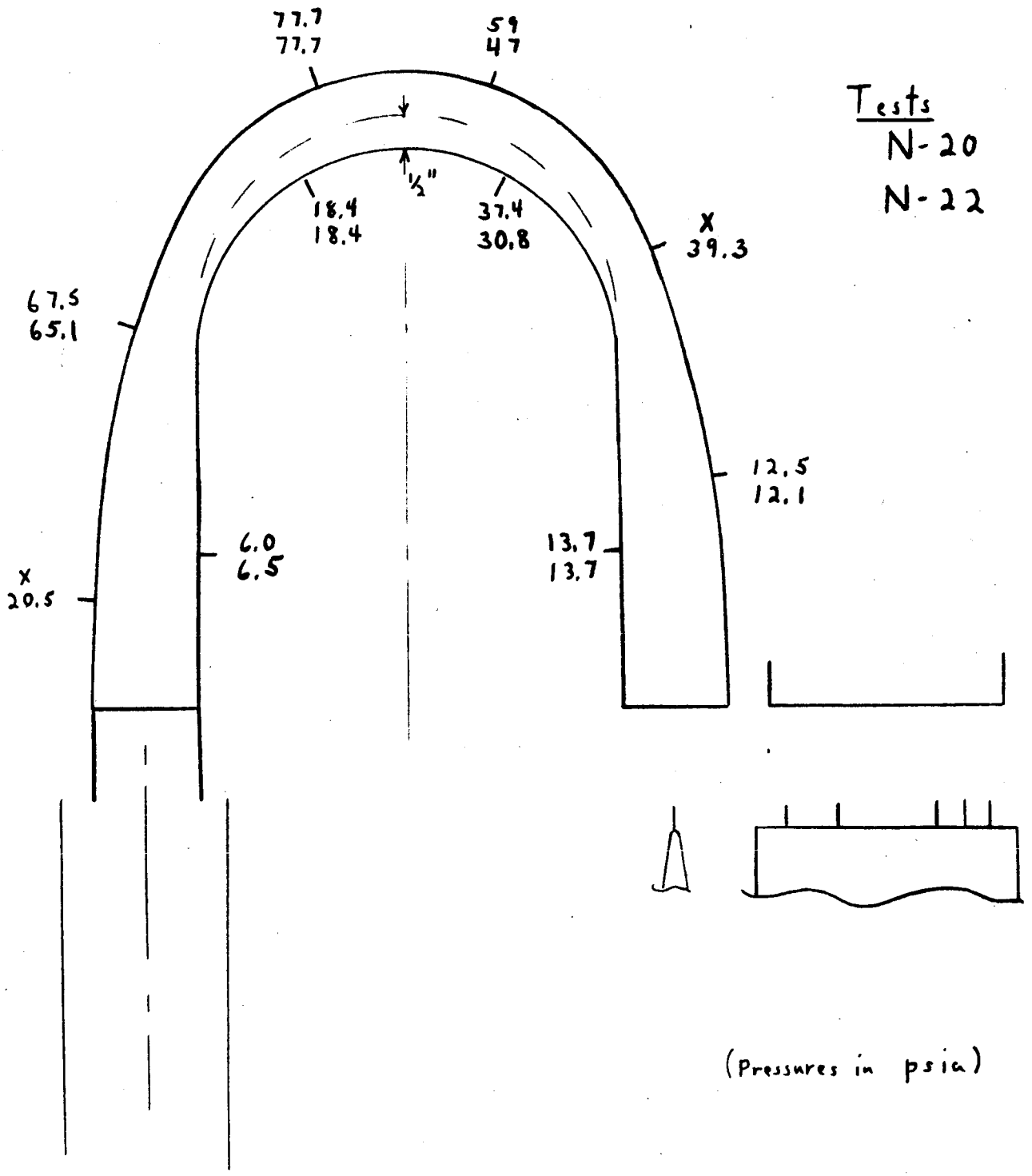

FIGURE 35. WALL STATIC PRESSURES

OPENED THROAT I

FIGURE 36 PRESSURE DISTRIBUTION AT END OF 180° TURN PASSAGE WITH OPENED THROAT T

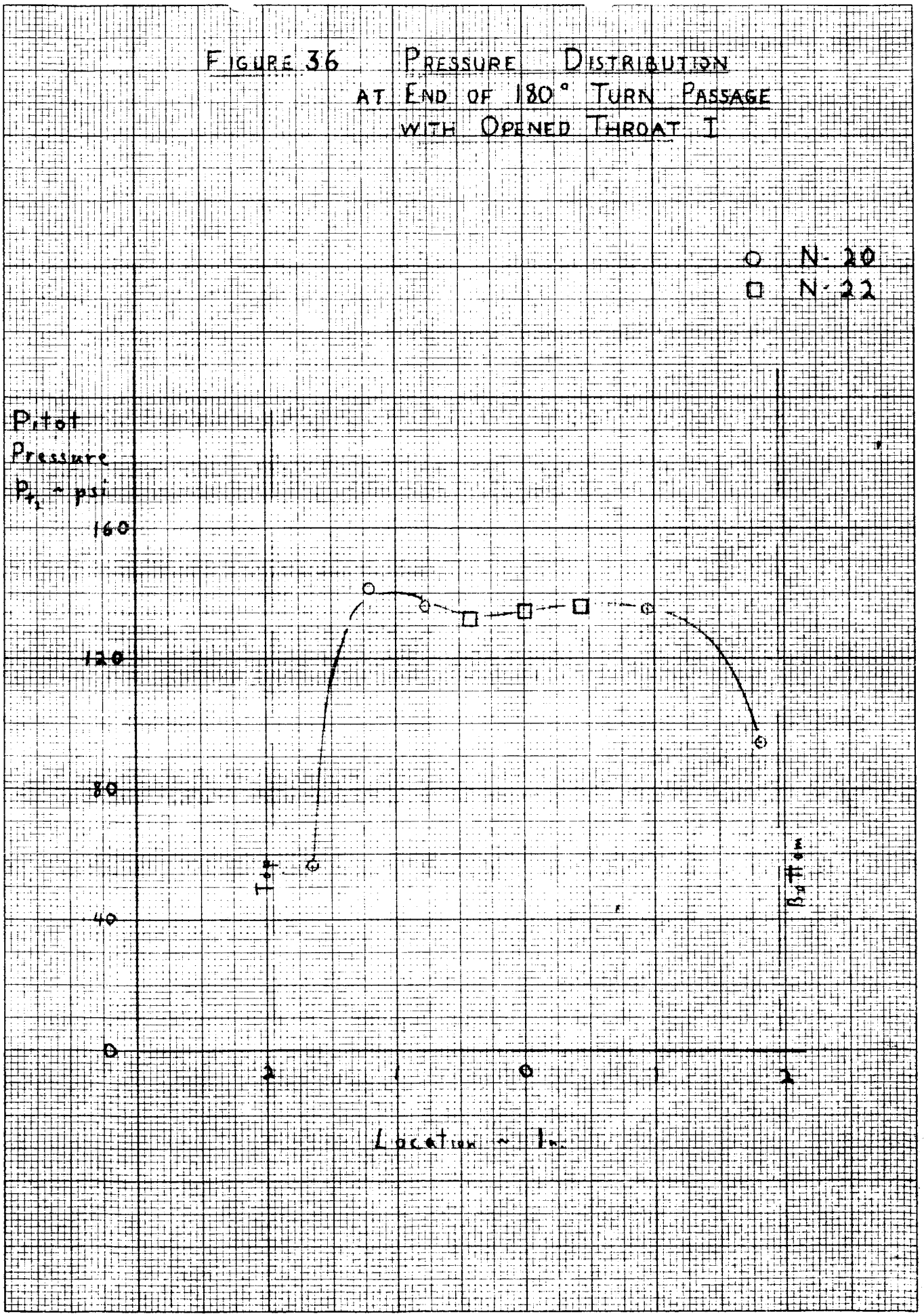

FIGURE 37 CONE PRESSURE DISTRIBUTION AT END OF 180° TURN PASSAGE WITH OPENED THROAT I

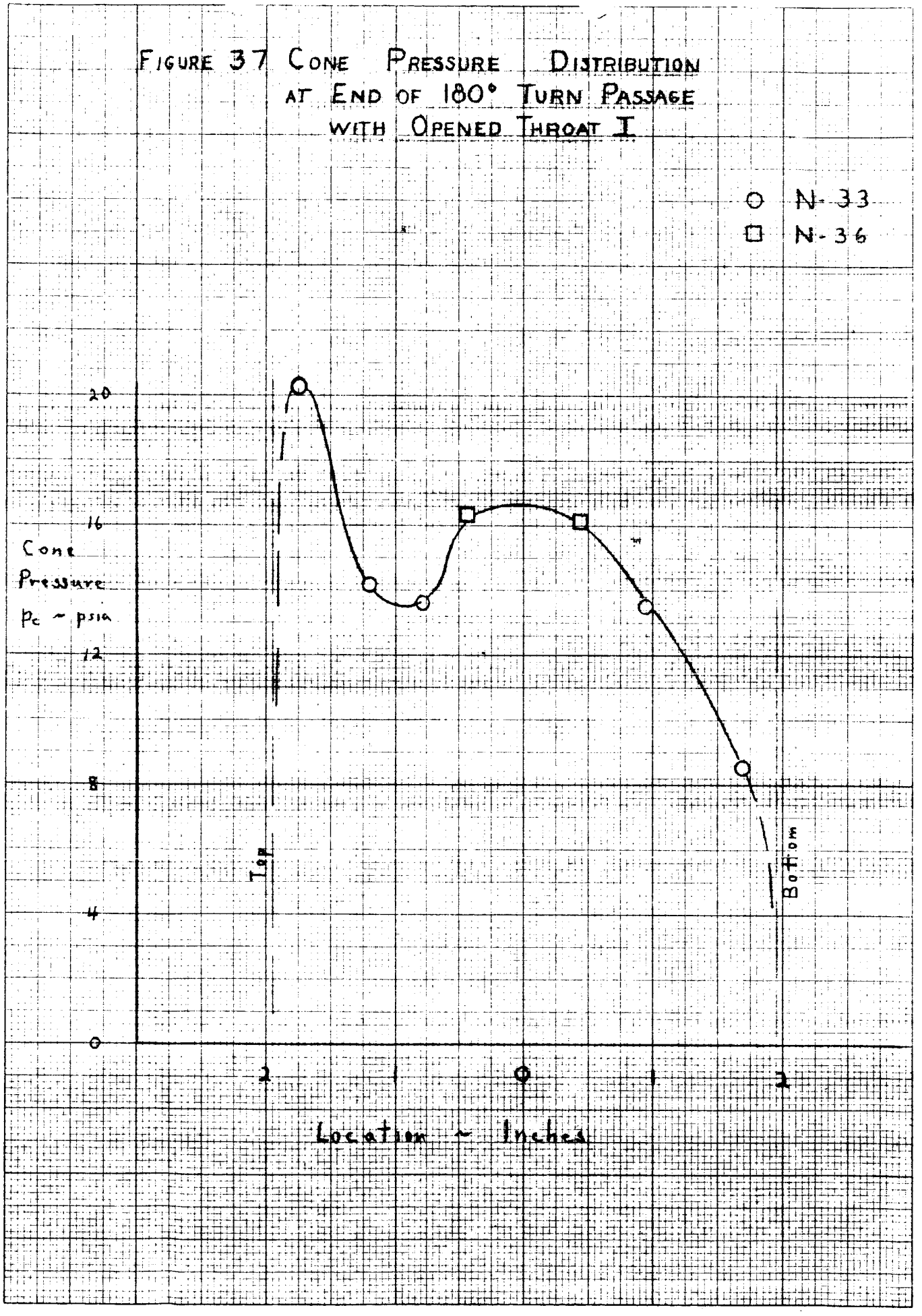

FIGURE 3.8. MACH NUMBER & STAGNATION PRESSURE AT END OF 180° TURN PASSAGE WITH OPENED THROAT I

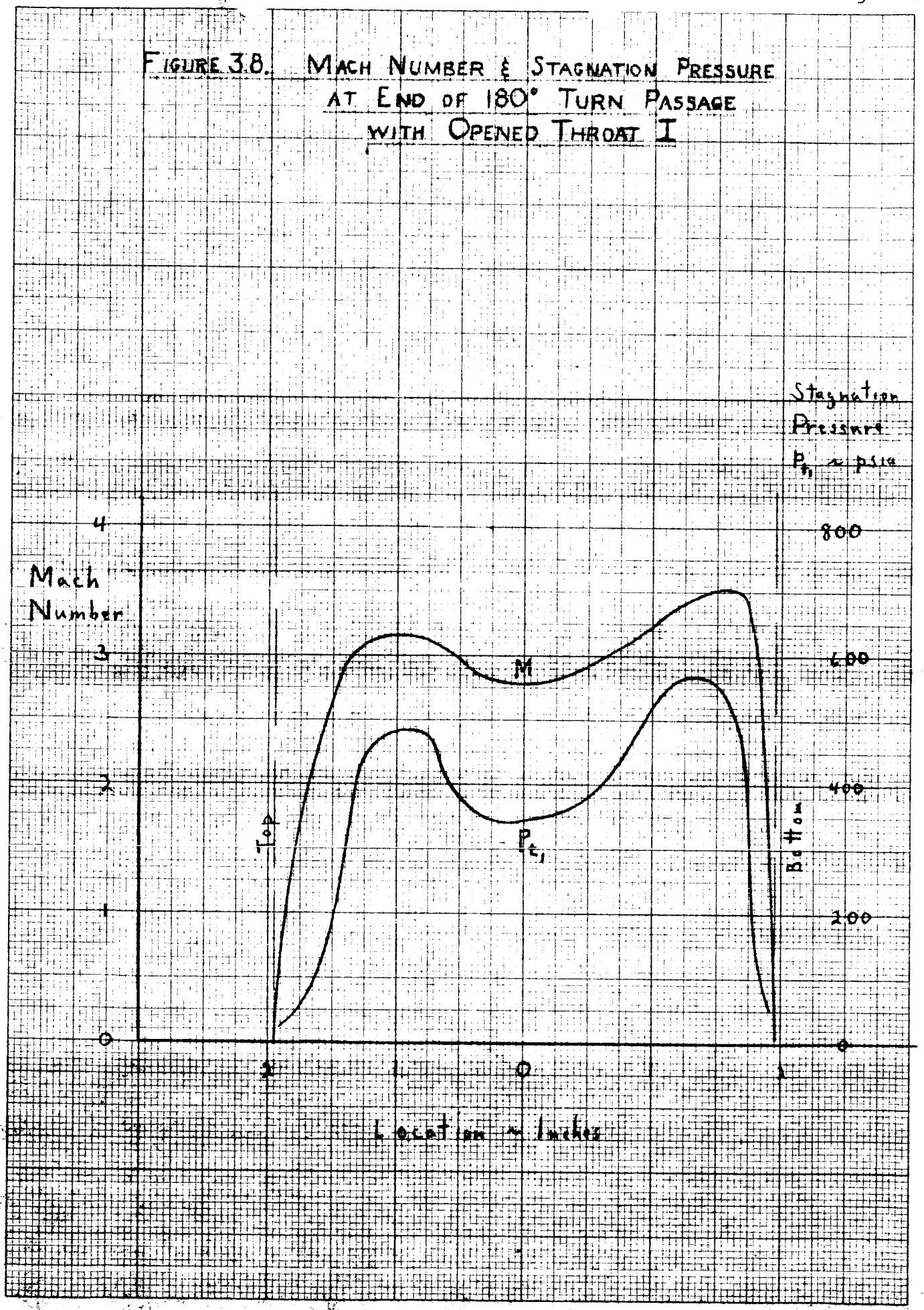

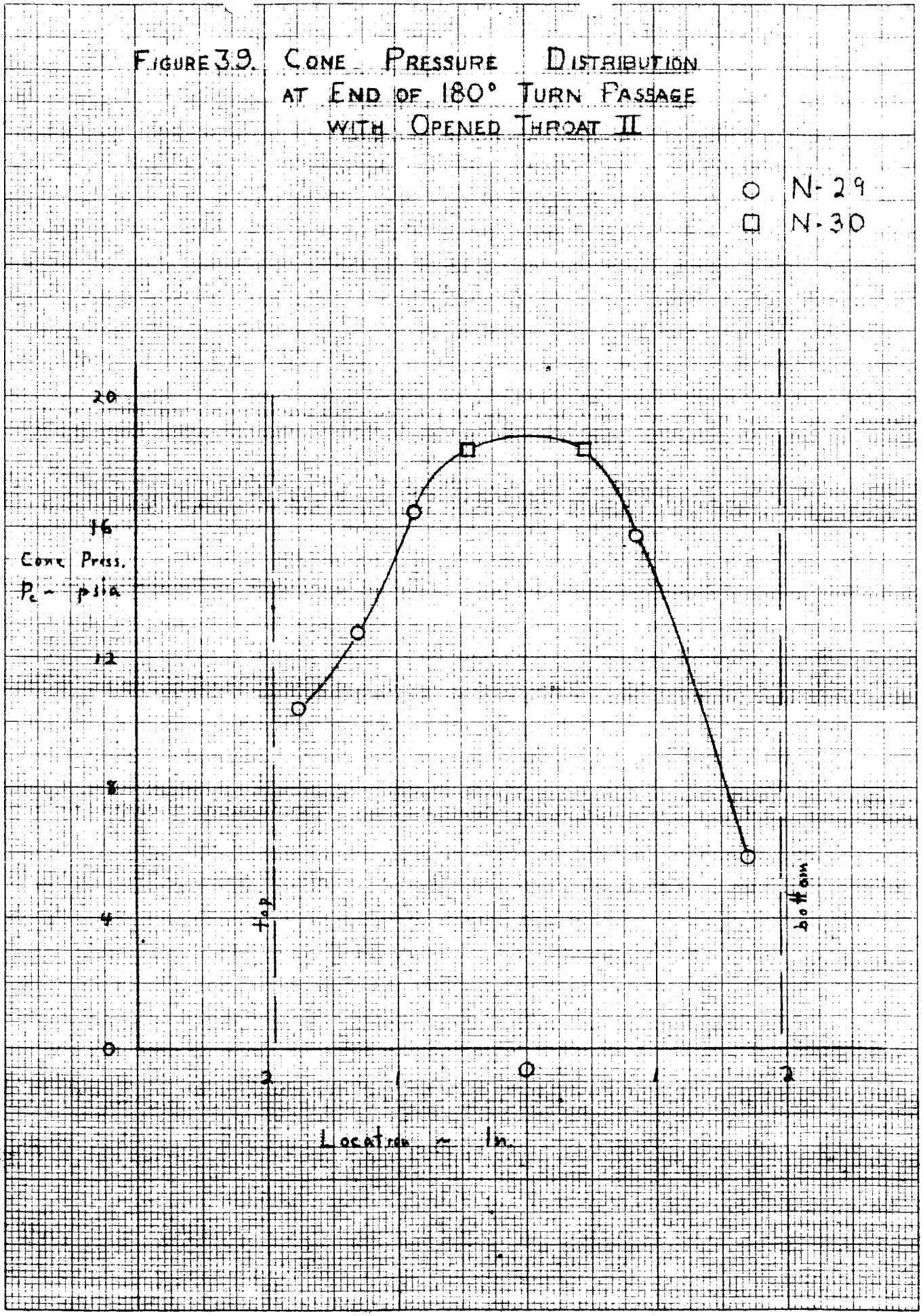
FIGURE 3.9. CONE PRESSURE DISTRIBUTION AT END OF 180° TURN PASSAGE WITH OPENED THROAT II
○ N-29
□ N-30
20
16
12
8
4
0
Cone Press.
P_c ~ psia
top
bottom
3
2
1
0
1
2
Location ~ In.

FIGURE 40. PRESSURE DISTRIBUTION AT END OF 180° TURN PASSAGE WITH OPENED THROAT II

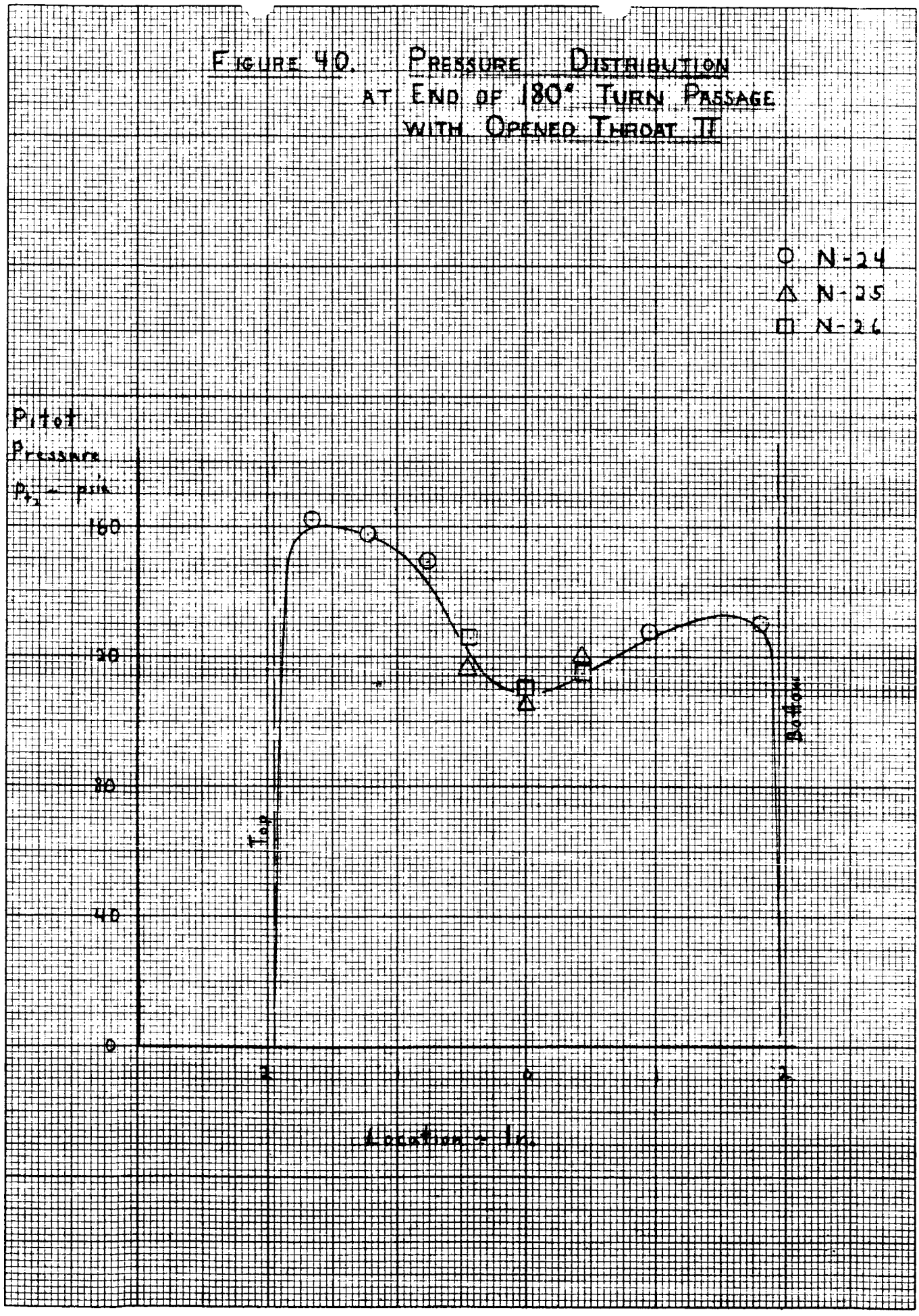

FIGURE 41. MACH NUMBER & STAGNATION PRESSURE AT END OF 180° TURN PASSAGE WITH OPENED THROAT II

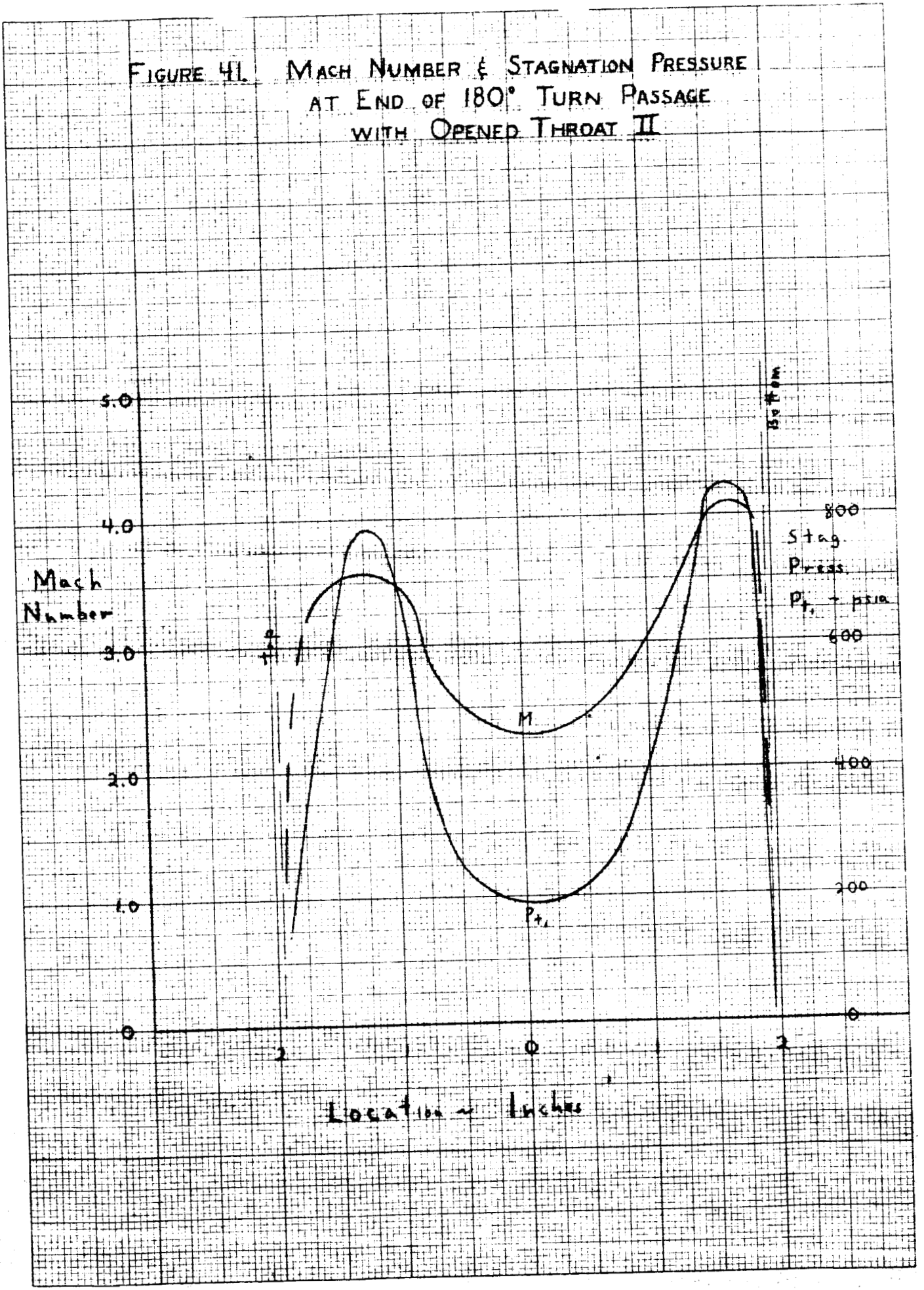

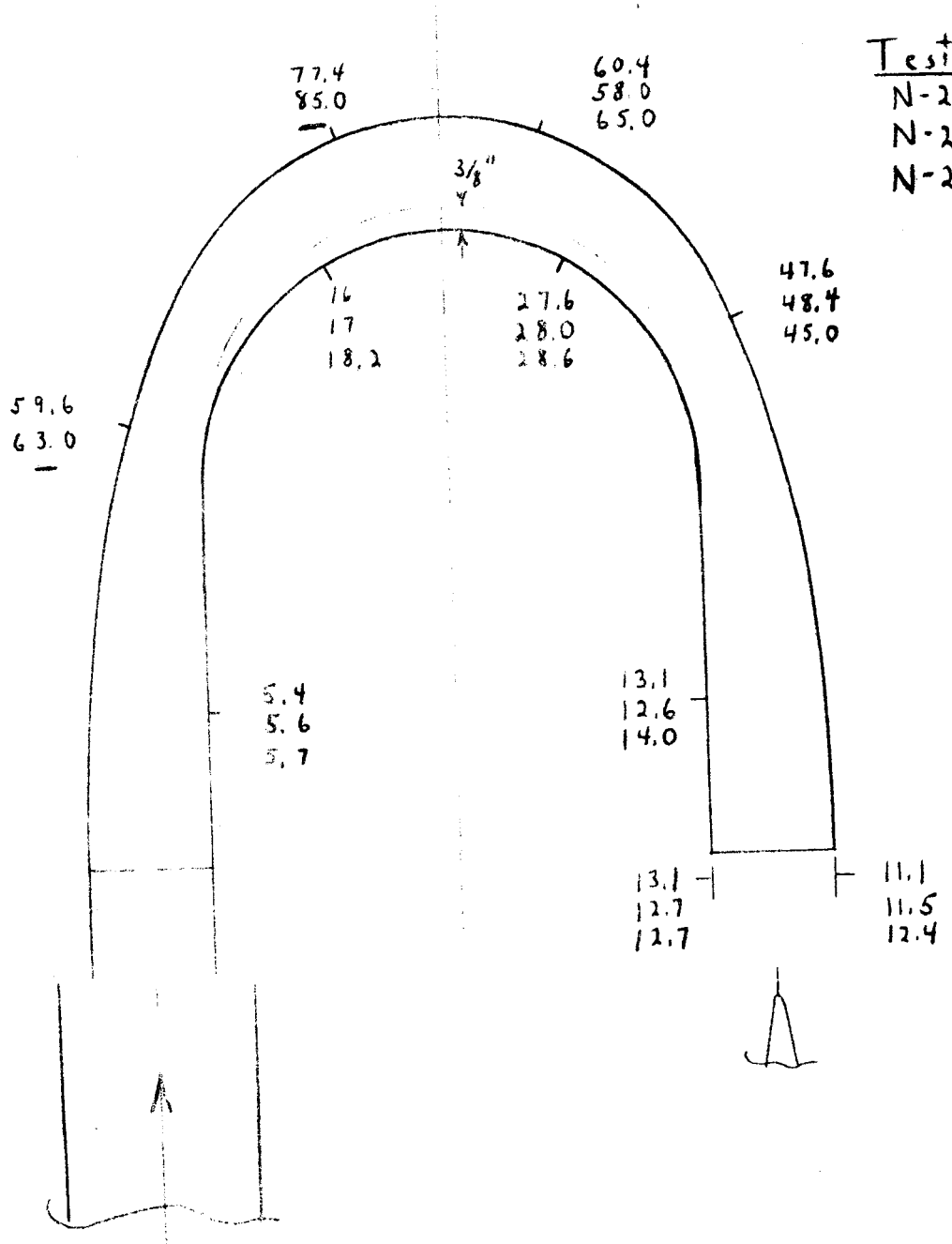

FIGURE 42.

WALL STATIC PRESSURES WITH OPENED THROAT II

(Pressure - psia)

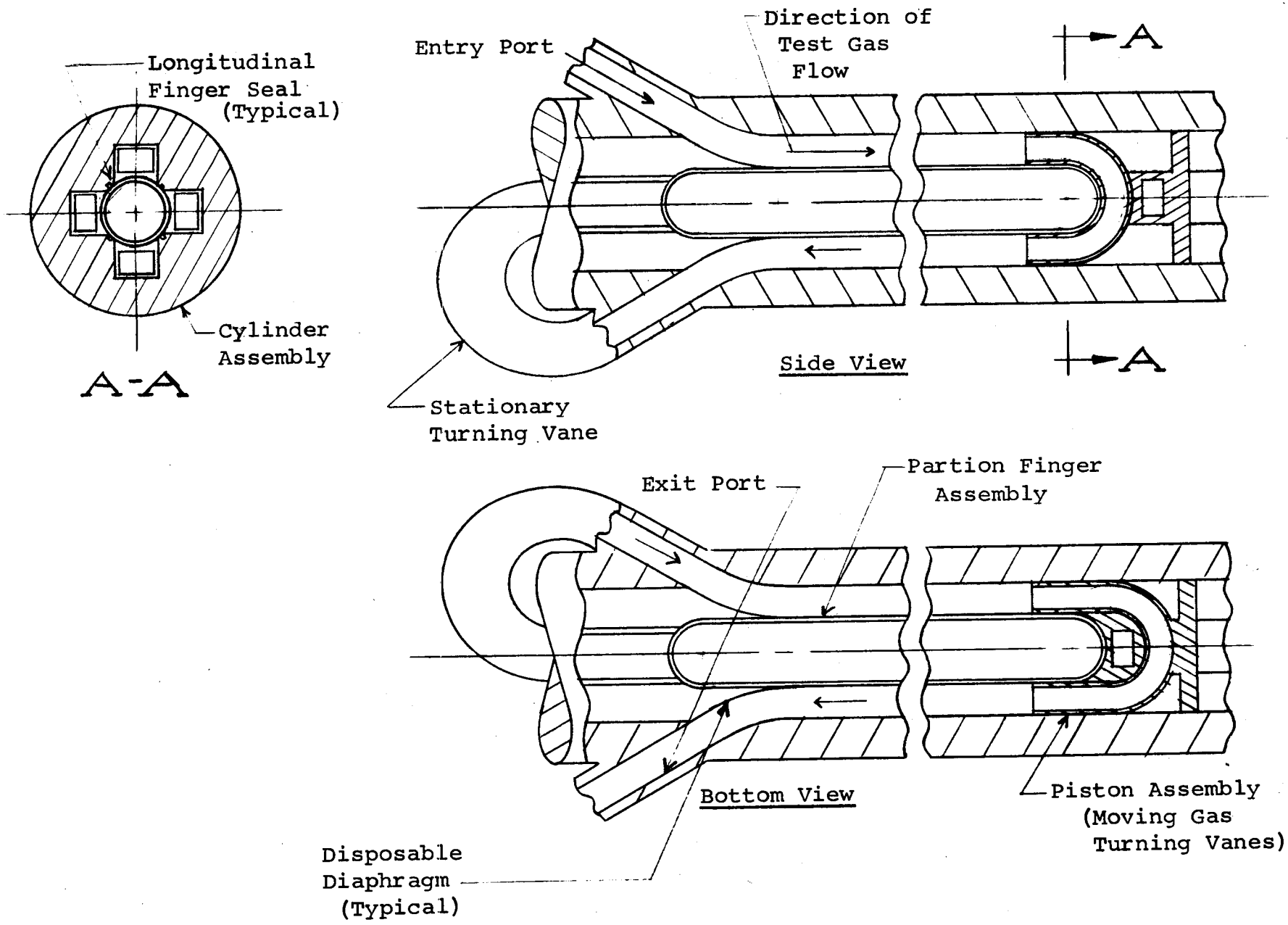

FIGURE 43 "PARTITION FINGER" APPROACH

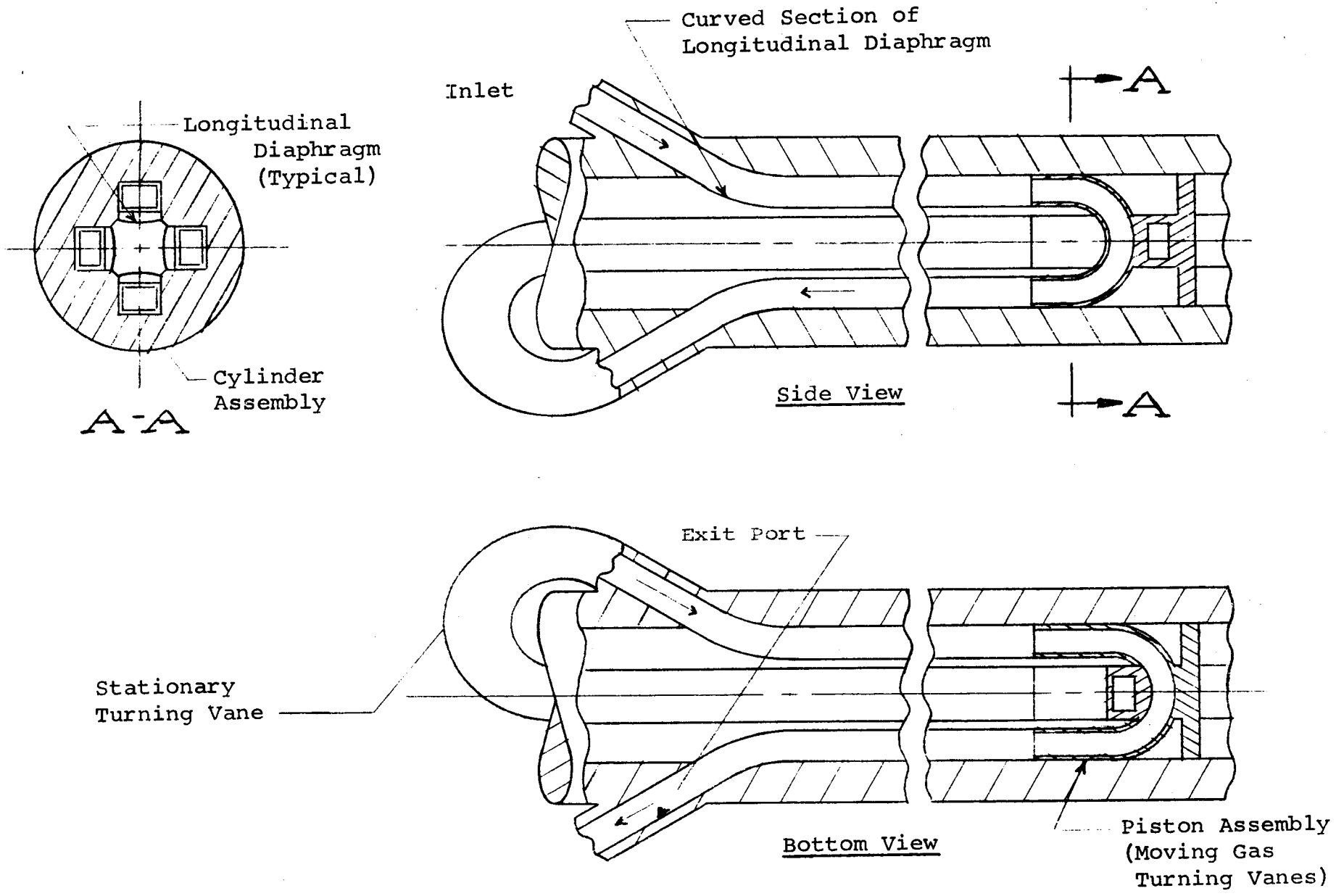

FIGURE 44 "LONGITUDINAL DIAPHRAGM" APPROACH

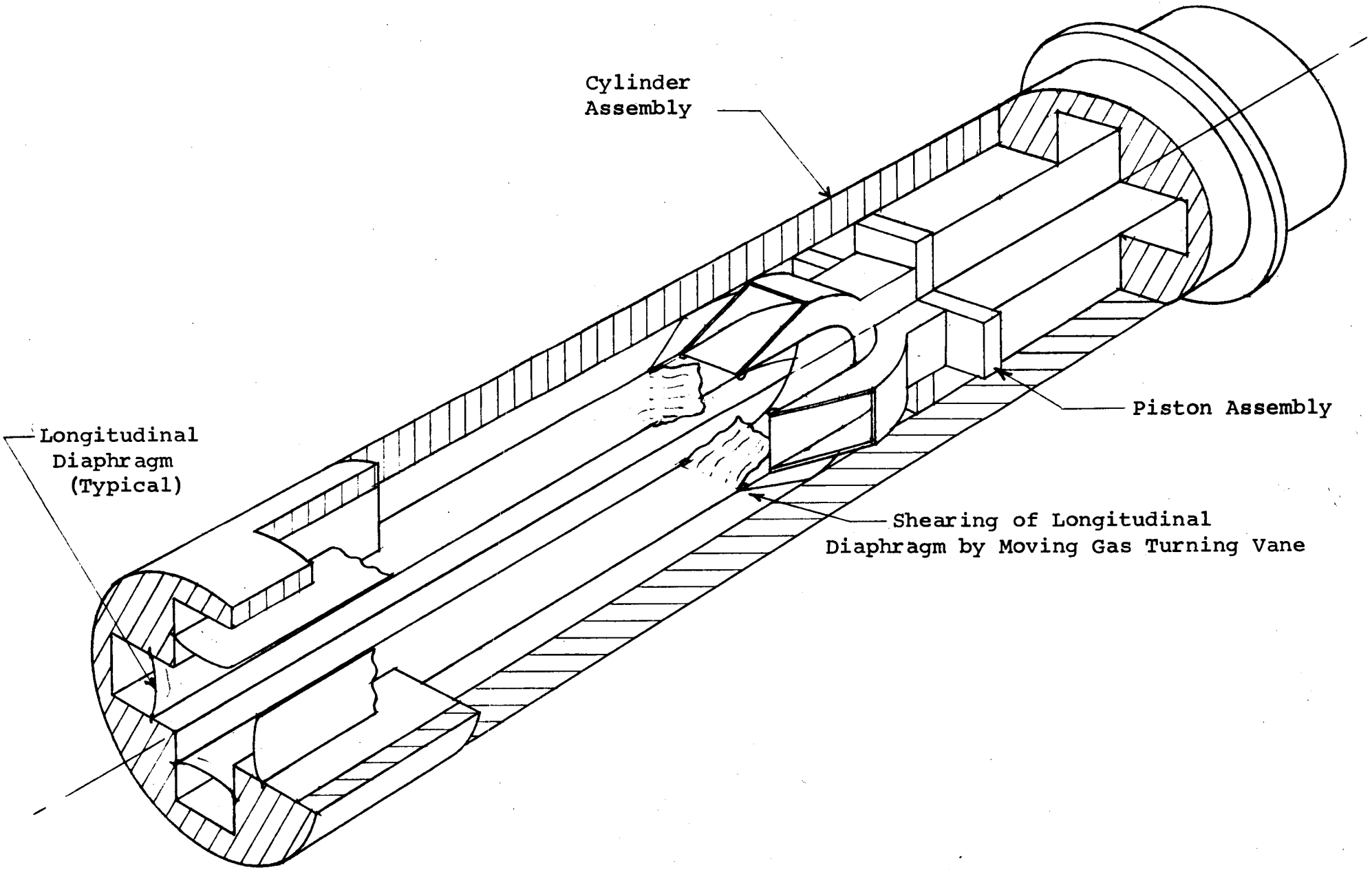

FIGURE 45. PISTON GAS ACCELERATOR

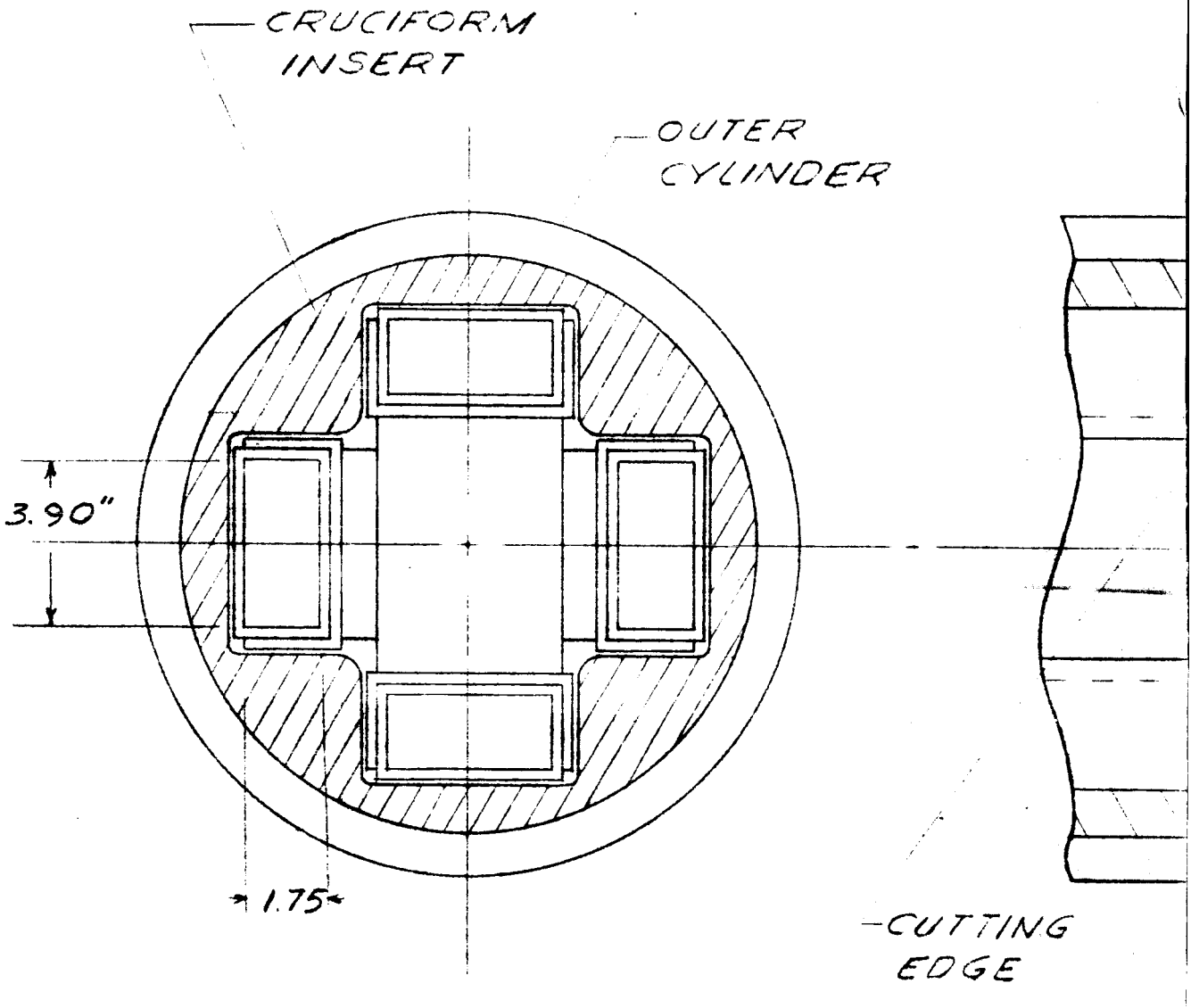
CRUCIFORM INSERT
OUTER CYLINDER
3.90"
1.75
CUTTING EDGE

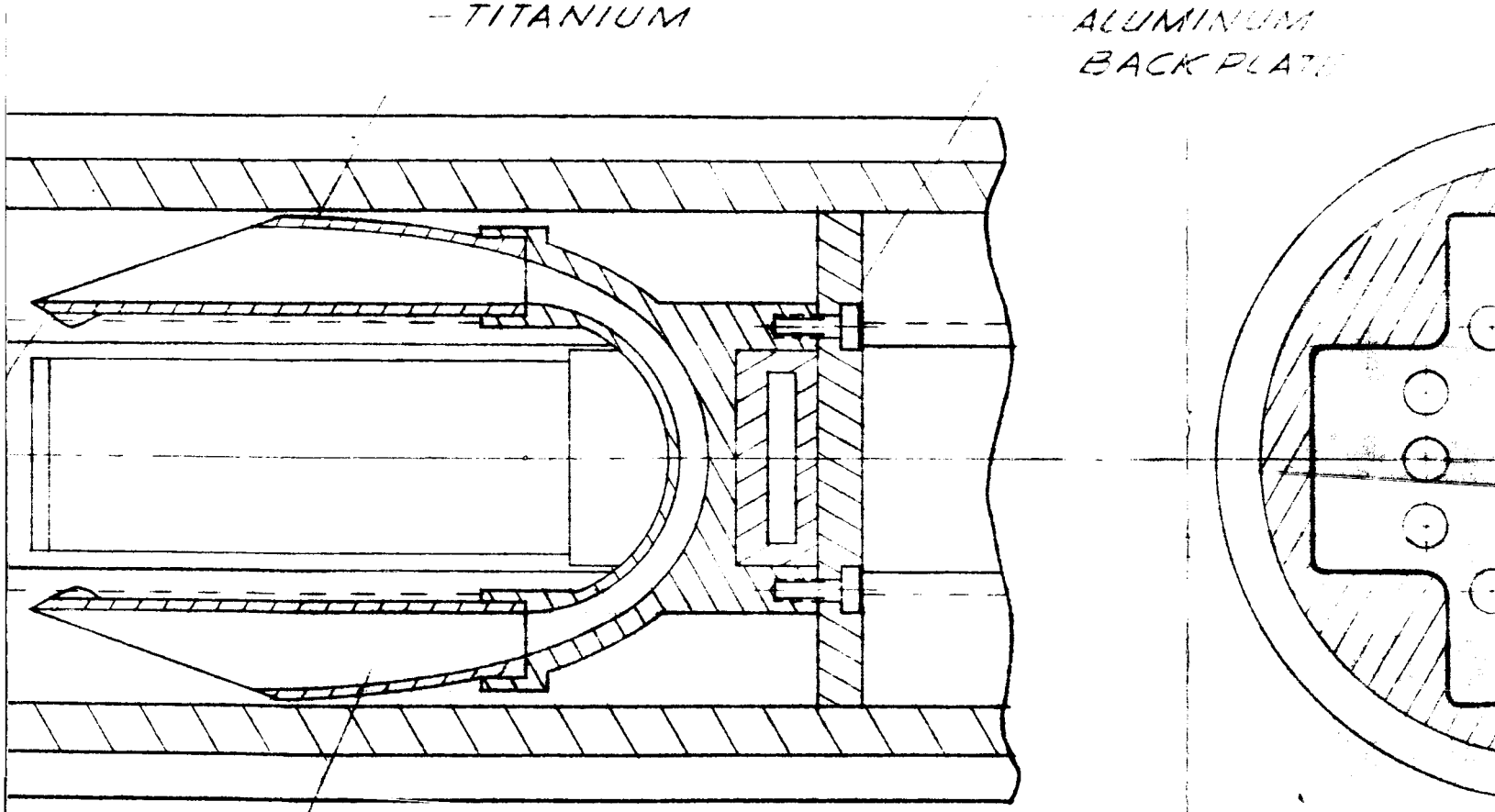
TITANIUM
ALUMINUM BACK PLATE
TURNING VANE PASSAGE (TYPICAL)

FIG. 46

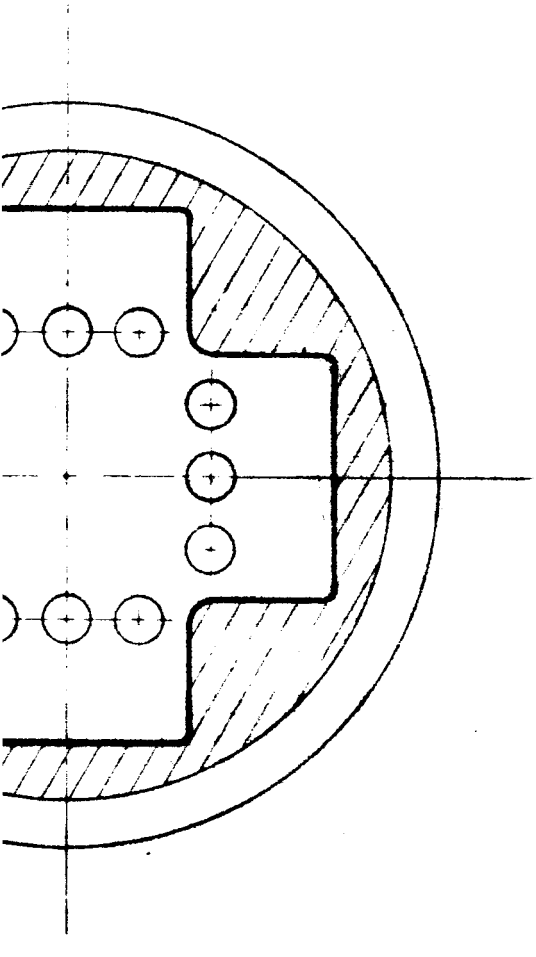

TON LAYOUT

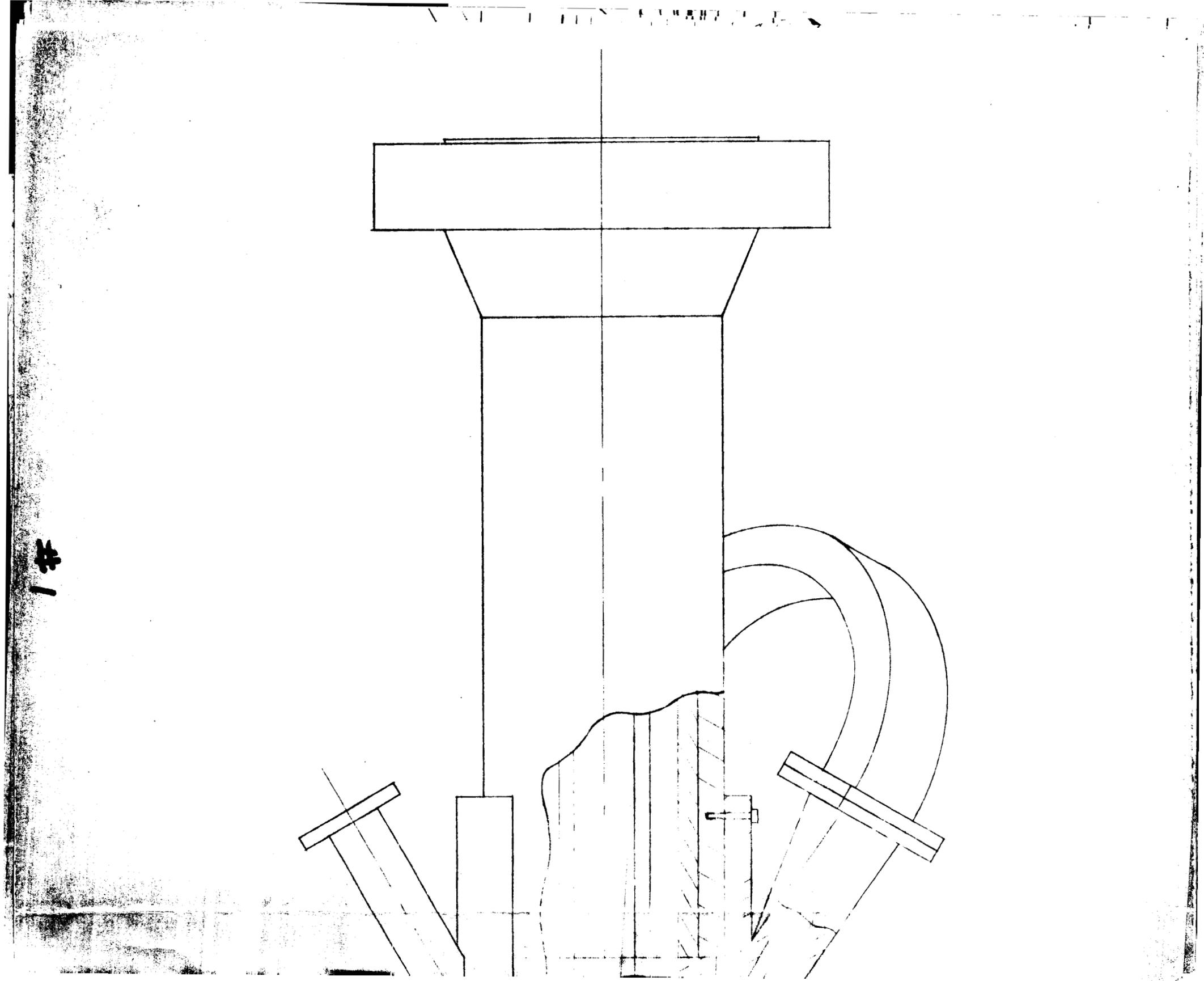

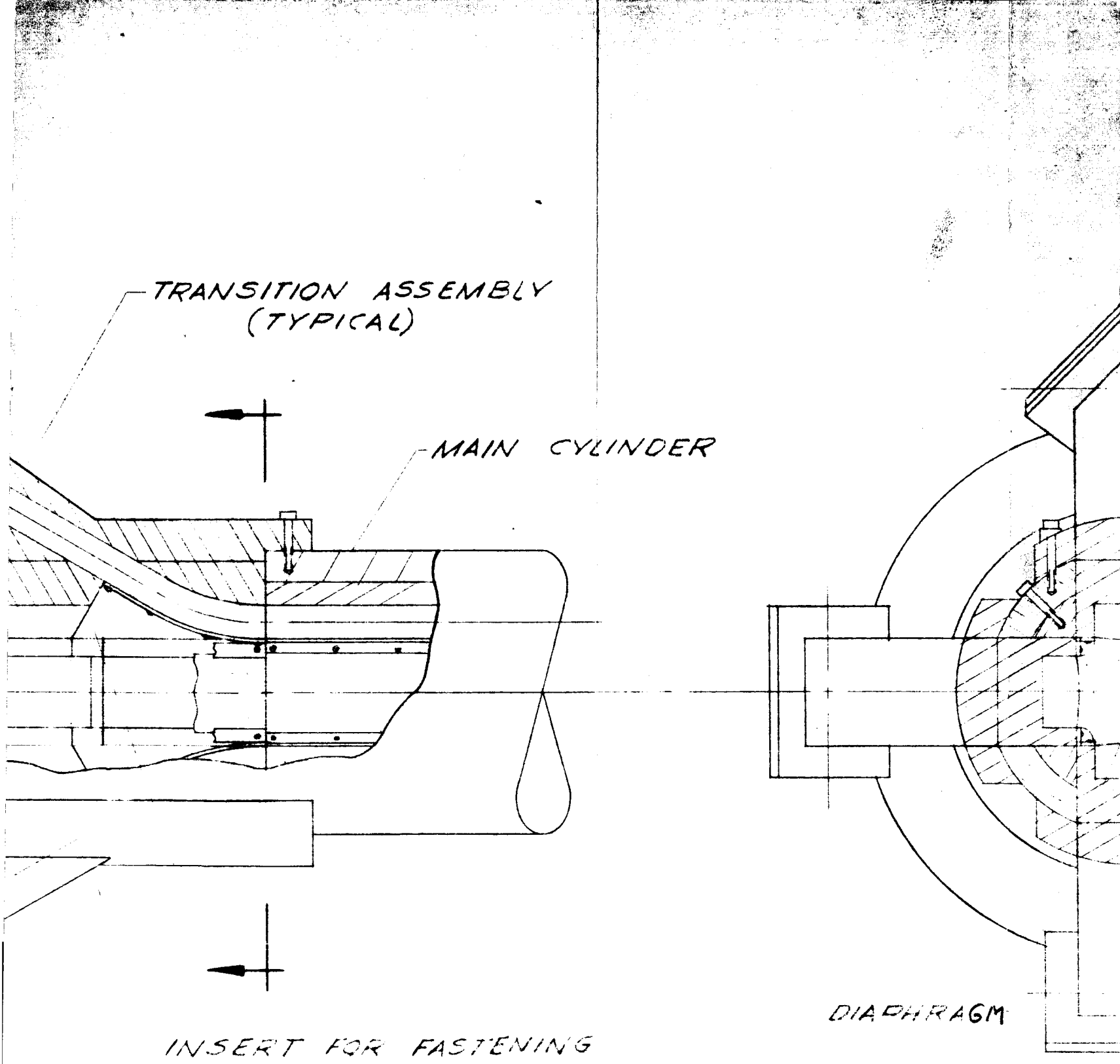

INSERT FOR FASTENING
CURVED DIAPHRAGM SECTION
IN PLACE.

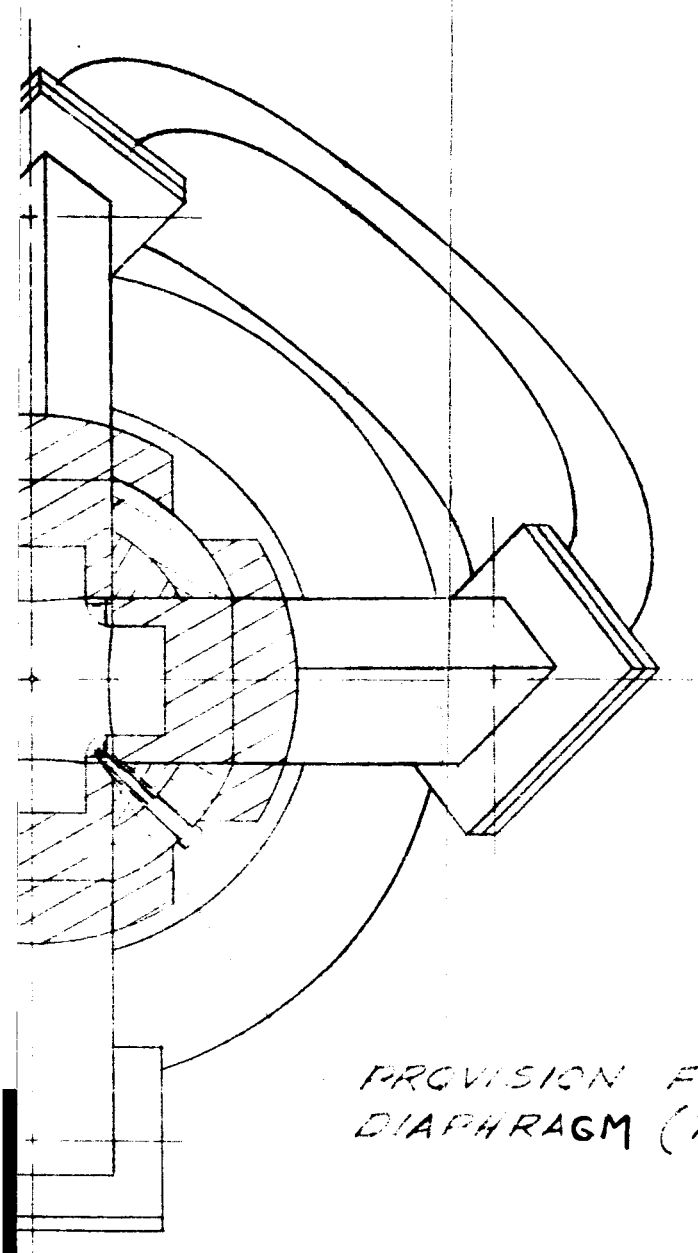

FIG. 47 LAYOUT OF CYLINDER AT THE STATIONARY TURNING VANE LOCATION

#3

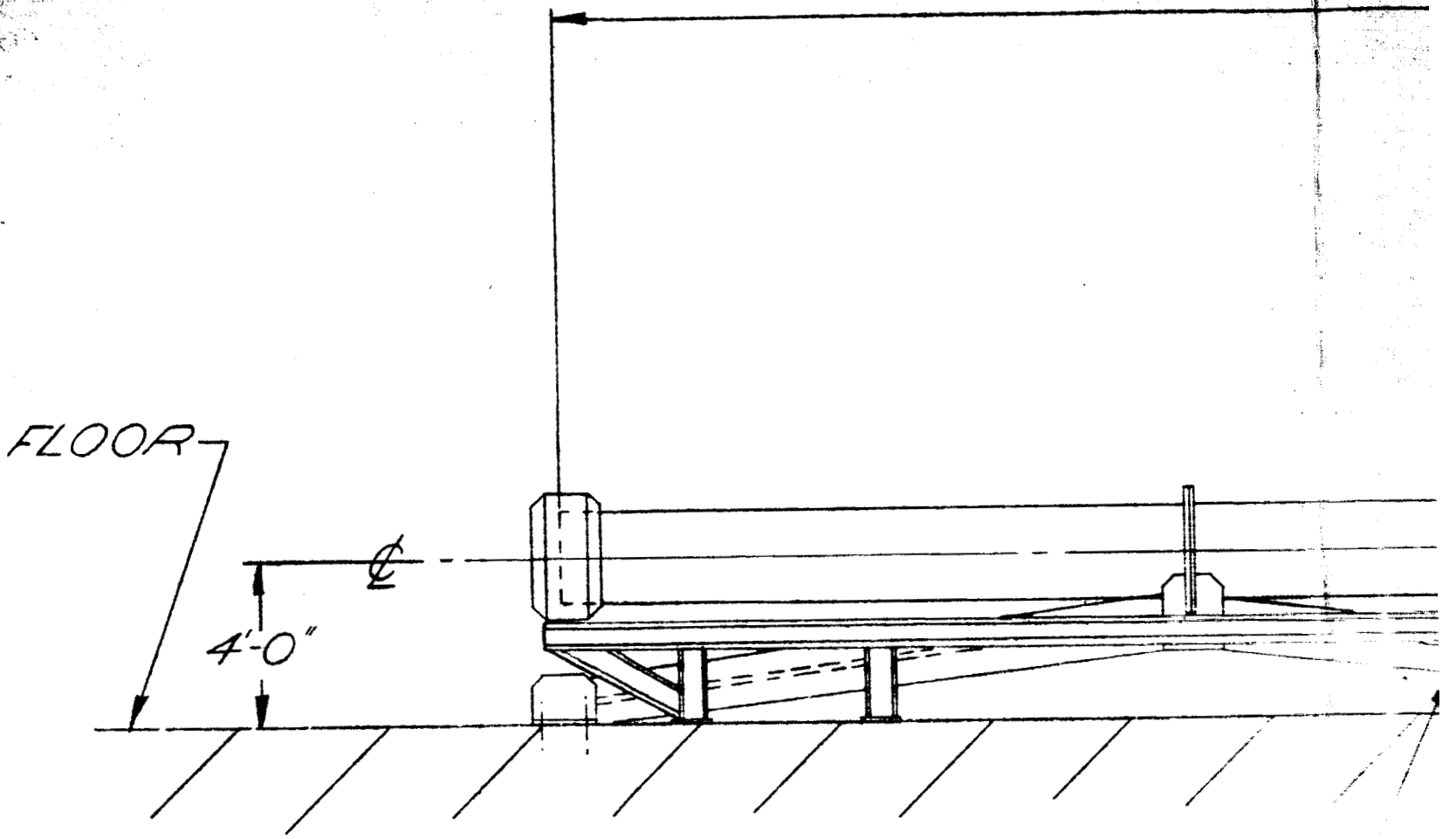
FLOOR
℄
4'-0"

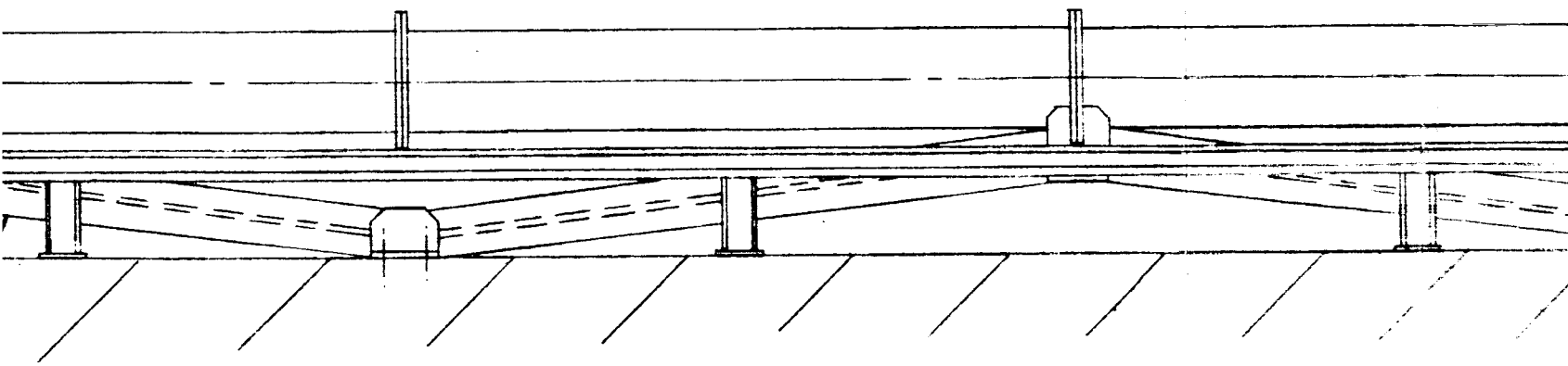

PUST LEGS

#2

220'-00"

112 SECTIONS @ 15

12 20

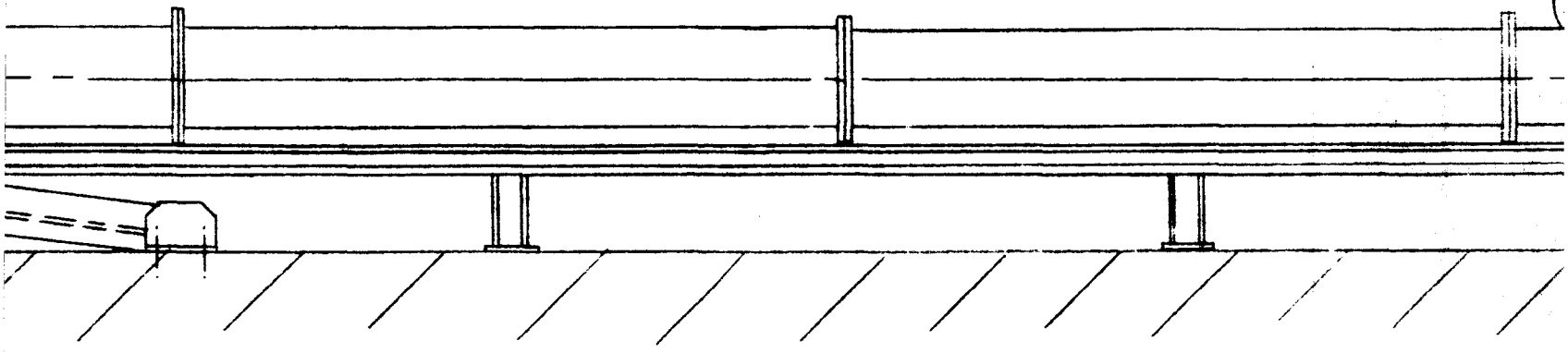

EL
S

#3

'EACH)
)

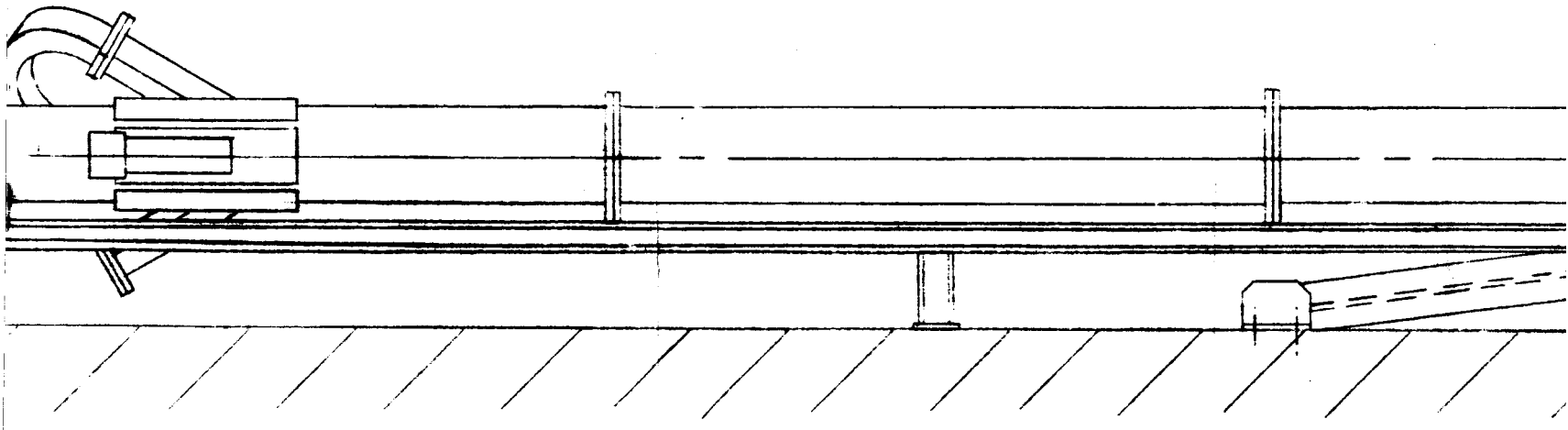

EVATION VIEW
CALE~$\frac{1}{4}$"=1'-0"

#4

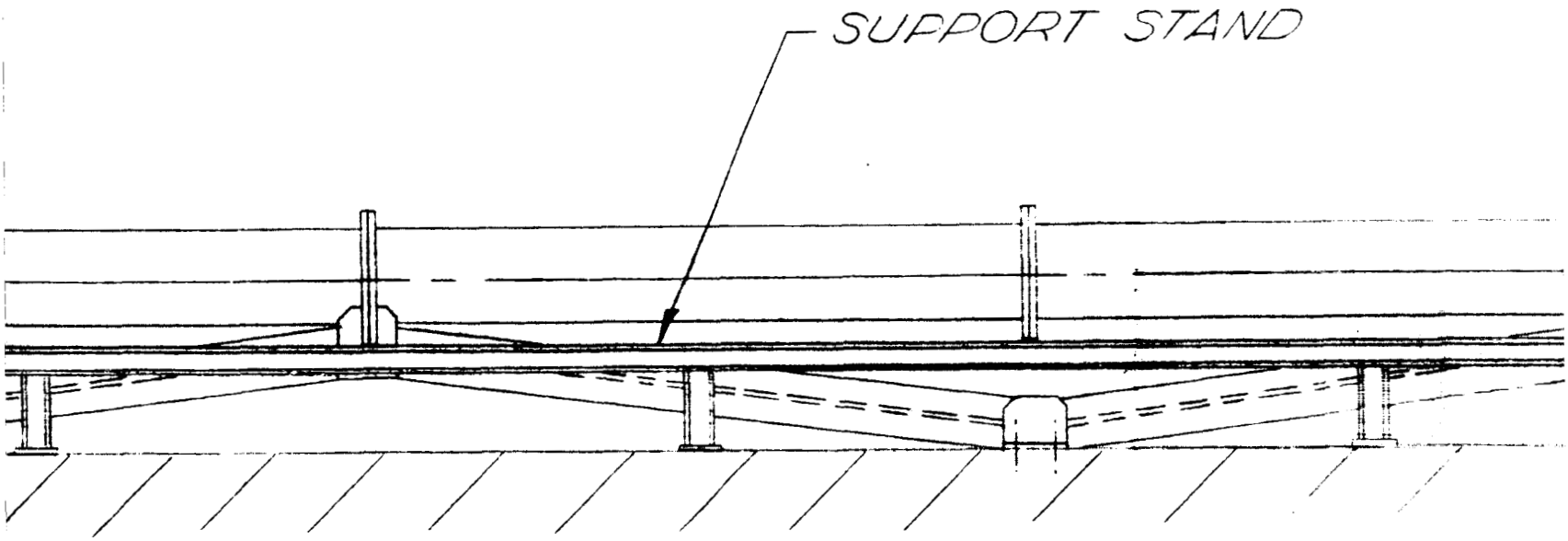

FIGURE 4

#5

Page 101

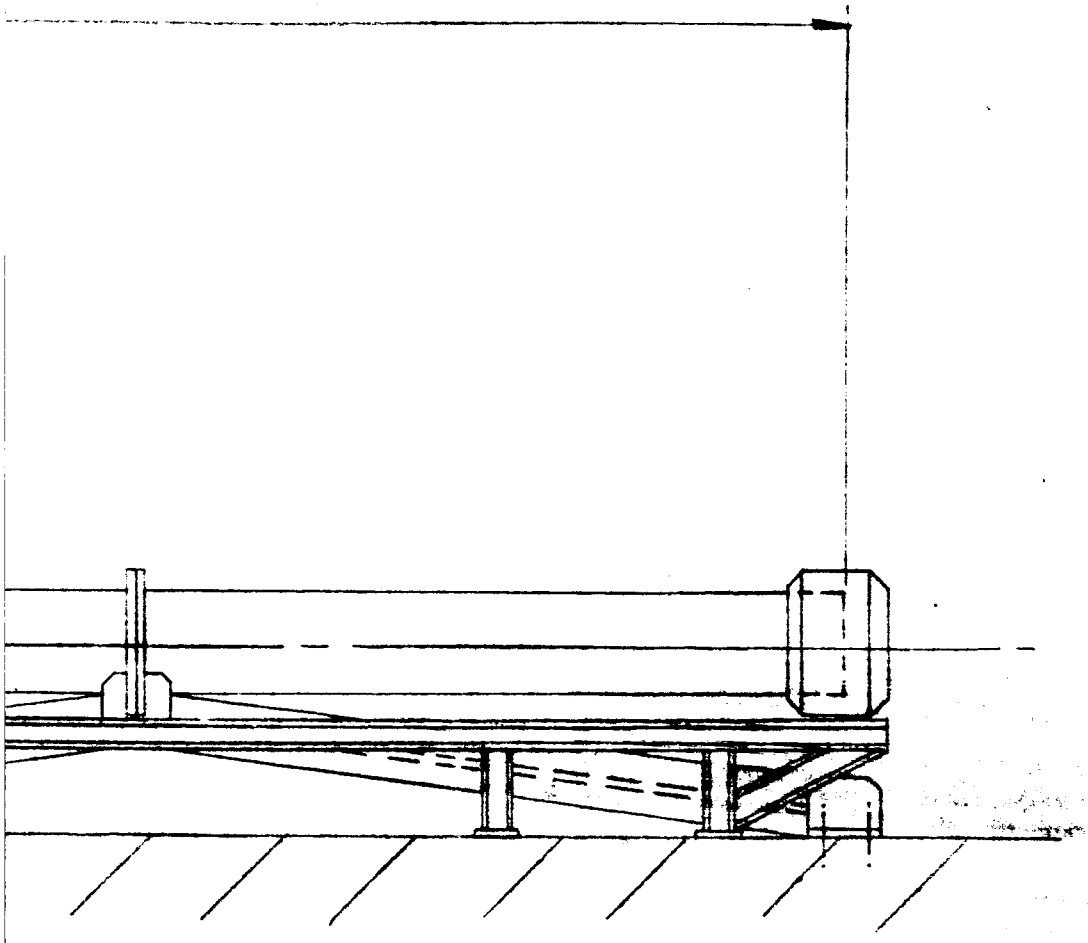

...ished in response to R.F.P. No. **UNSOLICITED**, shall not be disclosed outside the Government or be duplicated, ... any purpose other than ... proposal; provided that if a contract ... is awarded to this offeror in connection with ... the Government shall have ... right to duplicate, use or disclose this data to the extent provided ... This restriction does not limit the ... right to use information contained in such data if it is obtained from another source.

~TYPICAL CONFIGURATION